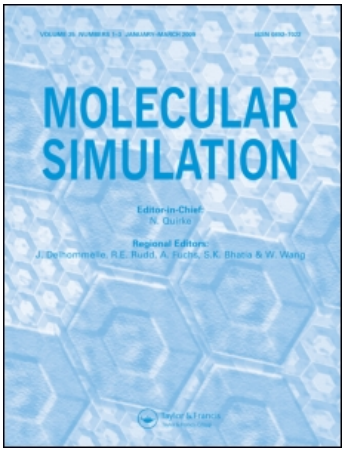

Molecular Simulation
Publication details, including instructions for authors and subscription information:
http://www.informaworld.com/smpp/title~content=t713644482

High Precision Canonical Ensemble Monte Carlo Simulations of Very Dilute, Primitive Z:Z and 2:1 Electrolytes and of Moderately Concentrated 1:1 Electrolyte Mixtures

Torben Smith Sørensen[a]
[a] Institute of Physical Chemistry and Center for Modelling, Nonlinear Systems Dynamics and Irreversible Thermodynamics. Technical University of Denmark, Lyngby, Denmark

To cite this Article Sørensen, Torben Smith(1993) 'High Precision Canonical Ensemble Monte Carlo Simulations of Very Dilute, Primitive Z:Z and 2:1 Electrolytes and of Moderately Concentrated 1:1 Electrolyte Mixtures', Molecular Simulation, 11: 1, 1 — 65
To link to this Article: DOI: 10.1080/08927029308022176
URL: http://dx.doi.org/10.1080/08927029308022176

Molecular Simulation, 1993, Vol. 11, pp. 1–65
Reprints available directly from the publisher
Photocopying permitted by license only

HIGH PRECISION CANONICAL ENSEMBLE MONTE CARLO SIMULATIONS OF VERY DILUTE, PRIMITIVE Z:Z AND 2:1 ELECTROLYTES AND OF MODERATELY CONCENTRATED 1:1 ELECTROLYTE MIXTURES

TORBEN SMITH SØRENSEN

Institute of Physical Chemistry and Center for Modelling, Nonlinear Systems Dynamics and Irreversible Thermodynamics. Technical University of Denmark, Building 206, DK2800 Lyngby, Denmark.

Received September 1992, accepted December 1992

Long-run Canonical Ensemble Monte Carlo Simulations of highly dilute, primitive model z:z and 2:1 electrolytes and of moderately concentrated (1 mol/L) mixtures of 1:1 electrolytes have been performed for a wide range of the number of ions (N) in the simulation cell (up to N = 1728). The excess energy, the excess Helmholtz' free energy, the excess heat capacity and the single ion activity coefficients have been simulated directly. The proper way of extrapolating the data to the thermodynamic limit is emphasized. In particular, the importance of the previously found analytical correction of the Widom method for the deviation from electroneutrality is stressed. The methodology presented opens up for the possible use of ≫ fast Monte Carlo ≪ simulations of e.g. single ion activity coefficients using systems with only a small number of ions. The Poirier formula - based on the exponential integral - for the mean ionic activity coefficients for the restricted primitive case (same ionic radii) seems to be confirmed for z:z and 2:1 electrolytes in highly dilute as well as moderately concentrated solutions. The ≫ negative deviations ≪ from the limiting law predicted at high dilution by the Poirier formula are found also by MC simulations. In mixtures of moderately concentrated 1:1 electrolytes, the Harned rule of linearity in the salt fraction was found valid for the mean ionic excess chemical potentials as well as for the single ion excess chemical potentials, the excess energy and the excess heat capacity at constant volume. The MSA theory gives a quite good approximation of the values. The radial distribution functions are also found by direct simulations and closely examined. In all cases investigated - except for high valency z:z electrolytes - the electric contributions to the potentials of mean force between the ions are very closely given by the electric potential of the linear Debye-Hückel theory. This is the content of the DHX model. Small deviations from the DHX potentials of mean force occur mainly between ions of the same sign and at large separations between the ions. At high Bjerrum parameters, formation of linear triplets perturbs the RDF's, however.

KEY WORDS: Primitive electrolytes, thermodynamic limit, Debye-Hückel, DHX, MSA, SPB, Poirier formula, Harned linearity, ion triplets.

INTRODUCTION

In a series of papers [1-14] our laboratory has made Monte Carlo simulations of the thermodynamic properties of charged hard spheres ≫ dissolved ≪ in an infinite dielectric continuum or in pores of finite size (primitive model electrolytes). In contrast to the pioneering work in the field of Card and Valleau [15] and many other

studies, the aim has been to focus more on the most dilute regime - where the electrostatic interactions are most dominant.

The first of our studies [1-3] made it increasingly clear, that the difficulties in this regime were *legio*, especially that one has to work with many more ions in the simulation cell (N) and with longer runs, in order to approach the thermodynamic limit and in order to get reliable radial distribution functions. For the first time, the test particle method of Widom [16-17] was used to simulate *directly* the *single ion* activity coefficients [4, 5, 7]. The N-dependence of such simulations was extraordinarily strong (leading term of order $N^{-1/3}$), but an analytical correction formula was found [8, 11] which made possible an *a posteriori* correction of the Widom simulation values for the deviation from electroneutrality introduced by the test particle.

To perform the appropriate extrapolations to an infinite system ($N \to \infty$, N/V finite) for other simulated thermodynamic quantities like excess energy, excess Helmholtz free energy and excess heat capacity showed up to be more complicated - the leading term being $N^{-2/3}$ and not N^{-1} as assumed by Card and Valleau - but finally a sensible calibration was made for the dilute regime which permitted extrapolation of canonical ensemble MC data to the thermodynamic limit with good precision - without having to resort to time consuming Ewald summation at each simulation step. A direct, numerical calculation of the error committed in the classical Debye-Hückel approximation was now possible for the first time [10-12].

The aims of the present paper are the following: 1) To give to the readership of *Molecular Simulation* a first hand account of the new methodology. 2) To study more closely extremely dilute z:z and 2:1 electrolytes by long run canonical ensemble MC simulation with Widom sampling included. 3) To compare with the Debye-Hückel (DH) and the DHX approximations as well as other approximations such as MSA(= (Mean Spherical Approximation), SPB(= Symmetric Poisson-Boltzmann) and Poirier's exponential integral expansion. 4) To make a careful study of the radial distribution functions - especially the long-tail properties, but also the structure close to contact at very high Bjerrum parameters. 5) To perform an improved analysis of a previously studied ternary ionic system (KCl/KF mixtures) in the moderately concentrated regime [6-7] in order to test the Harned linearity and in order to investigate if the concepts of Debye and Hückel - e.g. the Debye length ($1/\kappa$) - are still physically important in situations with $\kappa a \approx 1$ (a = mean contact distance).

In the appendix, the methodology and the nomenclature of the present presentation are summarized in order to facilitate the reading of the main text.

AN EXTREMELY DILUTE 2:2 ELECTROLYTE

It is well known, that 2:2 electrolytes exhibit strong non-Debye Hückel behaviour. Valleau, Cohen and Card [18] simulated such primitive electrolytes using canonical ensemble MC with minimum image (MI) energy cut-off, whereas van Megen and Snook [19] and Valleau and Cohen [20] used grand canonical ensemble + MI. Rogde and Hafskjold [21] used much longer Markov chains (8 million configs.) and canonical ensemble Ewald summation with the number of ions fixed to N = 216. The lowest concentration considered by the former authors was 0.01 mol/dm^3,

whereas the lowest concentration considered by Rogde and Hafskjold was 0.0001 mol/dm^3. All the above mentioned authors made simulations only of the excess energy.

In Reference [11] the Rogde-Hafskjold system with lowest concentration was reconsidered using canonical ensemble + MI and using N = 32, 36, 44, 64, 80, 100, 150, 216, 350, 512, 700, 1000, 1300 and 1728 particles in the central cell. The number of configurations was 8 million for each number of ions, except for N = 1728 where only 4 million configurations were tried. (A configuration is counted every time an ion was moved or attempted to be moved. The rejection rate is very low in such extremely dilute systems). In the present paper, an independent MC-run has been performed with N = 1728 and with 15 million configurations ($\approx 8680 \gg$ passes $\ll$ of each ion) in an attempt to validate the thermodynamic limiting values indicated earlier from extrapolations of simulations with different N-values. The main reason for the additional large-N simulation is to study carefully the long-tail radial distribution functions (RDF).

Thermodynamic Limit

The system simulated corresponds to a Bjerrum parameter B = 6.8116 and a dimensionless total concentration $\rho^* = 8.924 \cdot 10^{-6}$ and consequently a $\kappa a = 0.0276382$, where κ is the inverse Debye length and a the contact distance (ions of equal size). See the Appendix for further information.

Table 1 Long-run simulation (N = 1728, B = 6.8116, $\rho^* = 8.924 \cdot 10^{-6}$, 15.10^6 configurations).

Initial configurations rejected	$-E_{ex}/NkT$	$-\Delta F_{ex}/NkT$	$C_{V,ex}/Nk$	$-\ln\gamma_+$ *(PW)*	$-\ln\gamma_-$ *(PW)*
30,000	0.1266	0.09051	0.2391	0.08690	0.09320
60,000	0.1267	0.09052	0.2366	0.08664	0.09328
90,000	0.1267	0.09052	0.2355	0.08655	0.09332
120,000	0.1267	0.09052	0.2349	0.08636	0.09330
150,000	0.1268	0.09052	0.2350	0.08626	0.09336
Values adopted	0.1267	(0.09052)	0.235		0.089_8
	Corrected for electroneutrality deviation:				0.103_8
$N \to \infty$: (polynomial)	0.1262	–	0.238		0.103_4

Table 1 exhibits the results of the simulation and the effect of excluding from 30,000 to 150,000 of the initial configurations in the Markov chain, where it may not be in complete statistical equilibrium. This has very little effect on the dimensionless excess energy per E_{ex}/NkT, but some effect in the case of the excess heat capacity at constant volume $C_{V,ex}/Nk$ and the dimensionless, Plain Widom (PW) excess chemical potentials $\mu_+(ex)/kT = \ln\gamma_+$ and $\mu_-/kT = \ln\gamma_-$. The absolute value of the directly sampled electrostatic, Helmholtz' free energy $\Delta F_{ex}/NkT$ is too high. As stated already in Reference [1], the Metropolis sampling is not optimal for this quantity and is reliable only for small configurational energies (small N and/or small concentrations and/or small Bjerrum parameters, see the Appendix for further information). In Reference [11] it was found, that for the present system, the

Helmholtz free energy could be sampled and extrapolated to $N = \infty$ with some uncertainty from simulations with $N \leq 216$, when 8 million configurations were used.

The directly simulated quantities in Table 1 may be compared with another independent MC run for N = 1728, but with only 4 million configurations [11]. In that case, we found (with only the first 10,000 configurations. rejected): $E_{ex}/NkT = -0.1250$, $[\Delta F_{ex}/NkT = -0.08431]$, $C_{V,ex}/Nk = 0.1823$, $\ln\gamma_+(\mathrm{PW}) = -0.09583$ and $\ln\gamma_-(\mathrm{PW}) = -0.08986$. From the comparison it appears, that the spread in the sampled excess heat capacities (from energy fluctuations) is very large indeed at this high number of particles. (That the relative spread in $C_{V,ex}/Nk$ grows drastically with N is also apparent from Figure 9 in Reference [11]). Also, it is apparent that the difference between $\ln\gamma_+(\mathrm{PW})$ and $\ln\gamma_-(\mathrm{PW})$ is just statistical, and that it may take a *very* long run to make them closer together. The sampled value of E_{ex}/NkT seems reliable within 1-2% already after 4 million configurations. The plain Widom value for $\ln\gamma_\pm$ in Table 1 ($= -0.0898$) is corrected analytically for the deviation from electroneutrality (see Reference [11] and the Appendix). This is a considerable correction (13%). In contrast, the corrections due to the extrapolation to $N = \infty$ using the polynomials found earlier (see References [10-11] and the Appendix) are quite small due to the large number of particles used. The values in Table 1 for the single, long run simulation for N = 1728 may also be compared to the earlier $N \to \infty$ values obtained in Reference [11] from 8 million. configurations runs with many different values of N, see Table 2. Except for the electrostatic Helmholtz free energy, the values of the single, long N = 1728 run are all within the previously indicated uncertainty. So even if the uncertainties in the extrapolation plots (Figures 8-9 in Reference [11]) may seem drastical - especially at high N - the extrapolated mean values are quite good. Furthermore, the $-E_{ex}/NkT$ values may be compared to the one obtained by Rogde and Hafskjold [21] - using Ewald summation, N = 216 and 8 million configurations. It might seem, that the reward of using Ewald summation is very high, since the two figures are equal to 3 digits. However, already the relative uncertainty indicated by Rogde and Hafskjold (6%) shows the result to be quite uncertain. In Reference [11] a value almost the same (-0.128) was found for N = 216 *without* Ewald summation and the same number of configurations. This is a sheer happenstance, since e.g. at N = 700 a value of -0.135 was found (same number of configurations). This figure also deviates 6% from the estimated thermodynamic limit value. Ewald summation is by some researchers advocated in order to speed up the convergence to the $N = \infty$ limit, but the procedure is very time consuming and the arguments in favor of its use do not seem strong to me. In any case, this paper and our previous papers clearly show, that one can easily do without by extrapolating small N simulation data to the thermodynamic limit in an appropriate way (see for example Table 3).

To save time in the case of dilute systems, I shall therefore recommend another procedure. In Table 3 is shown the results of simulations with very few particles. In that case, the simulations are quite quickly performed even on a desk top computer. Using the extrapolation and correction procedures described earlier (and in the Appendix), good estimates are given for infinite systems. It is noteworthy, that all the values do not differ significantly from the values given in Table 2. They seem even to be more precise! This is so, since the uncertainty of the calculations with larger N-values is greater, when the same number of configurations is used, since

Table 2 Results for N-extrapolated MC runs with 8 million configurations and varying N. (B = 6.8116, $\rho^* = 8.924 \cdot 10^{-6}$).

Reference	$-E_{ex}/NkT$	$-\Delta F_{ex}/NkT$	$C_{V,ex}/Nk$	$-\ln y_{\pm}$ *(corr)*
Rogde and Hafskjold [21] (N = 216,Ewald)	0.127 ± 0.008	–	–	–
Sørensen [11]	0.127 ± 0.002	0.068 ± 0.006	0.248 ± 0.015	0.1043 ● 0.0009

Table 3 Calculating thermodynamic limit values from simulations with small N. Reference [11] (B = 6.8116, $\rho^* = 8.924 \cdot 10^{-6}$).

N	$-E_{ex}(\infty)/NkT$	$-\Delta F_{ex}(\infty)/NkT$	$C_{V,ex}(\infty)/Nk$	$-\ln y \pm$ *(corr,∞)*
32a	0.1228 [0.1344]	0.06661 [0.08483]	0.2417 [0.2058]	0.1042 [0.06103]
32b	0.1273 [0.1393]	0.06714 [0.08551]	0.2729 [0.2323]	0.1037 [0.06052]
36	0.1246 [0.1353]	0.06680 [0.08371]	0.2477 [0.2135]	0.1037 [0.06170]
44	0.1268 [0.1361]	0.06716 [0.08204]	0.2627 [0.2307]	0.1033 [0.06317]
64	0.1263 [0.1331]	0.06717 [0.07873]	0.2453 [0.2218]	0.1032 [0.06732]
80	0.1232 [0.1287]	0.06645 [0.07629]	0.2317 [0.2125]	0.1048 [0.07051]
Mean	0.1252 ± 0.0008	0.06689 ± 0.00013	0.2503 ± 0.0067	0.1038 ± 0.0003

The direct simulation values in square brackets. All simulations 8 million configurations (32a and 32b independent simulations). The values $\ln y_{\pm}$ (corr,∞) have first been corrected to electroneutrality and then extrapolated to N = ∞.

the number of ≫ passes ≪ decreases. Thus, the value of large N simulations mostly lies in a greater quality of the RDF's, see later.

Radial Distribution Functions (RDF)

The main purpose of simulations with large N at extreme dilution is to obtain reliable simulations of the RDF's as far out in the ≫ tails ≪ as possible. It should be noticed, that for N = 1728 at $\rho^* = 8.924 \cdot 10^{-6}$ the side length of the MC simulation box is L ≈ 578.5 (measured in contact distances a). We have $\kappa a = 0.0276382$ so the Debye length measured in contact distances is $1/(\kappa a) \approx 36.18$. The energy cut-off is at ≈ L/2 = 289.3 which is ≈ 8.0 times the Debye length. It is probably quite safe to sample the RDF's out to separations equal to $t_{max} = 120$. The volume of the t_{max} sphere is only 3.7% of the volume of the total simulation box with 1728 ions. Thus, in the average only 65 ions are inside the sphere, if the distribution were uniform. This is not much, but the statistics is made as an average over all 1728 ions - each in the center of its own MI box. In the following, t is r/a and all RDF's are sampled in 60 spherical shells of equal thickness (Δt) dividing the distance from 1 and t_{max}.

Figure 1 shows the sampled values of the RDF's $g_{+-}(t)$ and $g_A(t) \equiv g_{++}(t) = g_{--}(t)$ in the form of the dimensionless potentials of mean forces $W_{+-}(t) \equiv -\ln g_{+-}(t)$ and $W_A(t) \equiv -\ln g_A(t)$ multiplied with t (to remove the spherical singularity at $t = 0$). These quantities are plotted against $\exp(-\kappa at)$.

With correlation coefficient 1.000 the following regression is found:

$$t \cdot W_{+-}(t) = 0.056 - 6.686 \exp(-\kappa at) \quad (1)$$

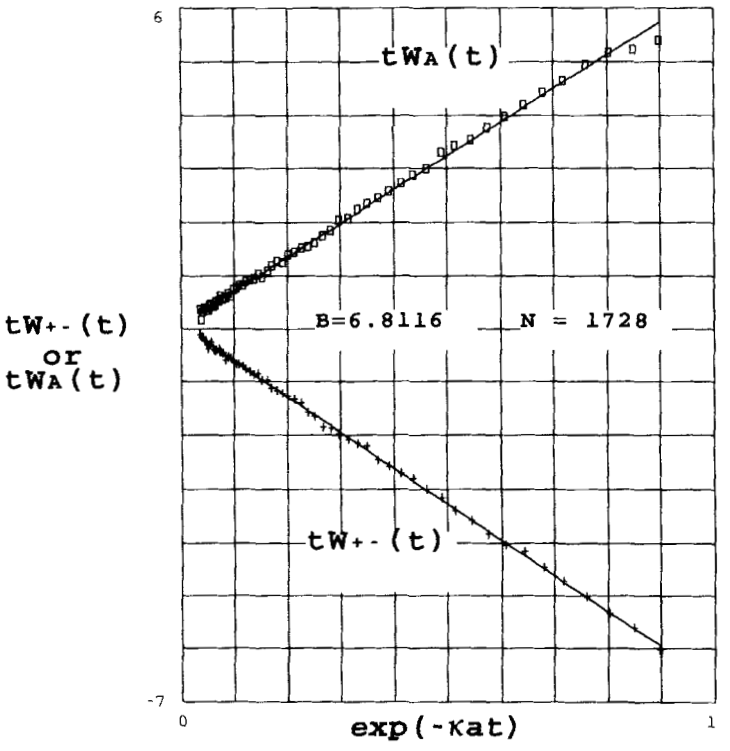

Figure 1 The RDF's $g_{+-}(t)$ and $g_A(t)$ for the 2:2 electrolyte with B = 6.8116, $\rho^* = 8.924.10^{-6}$ and N = 1728. The ordinates are $t \cdot W_{+-}(t)$ or $t \cdot W_A(t)$, where $t \equiv r/a$ and $W(t)$ are the dimensionless potentials of mean forces $\equiv -\ln g(t)$. The subscript A stands for interactions between ions of like charges. (+ + and − − are pooled together, since the cations and anions have the same size). The abscissa is $\exp(-\kappa at)$. The regression lines are given by equations (1) and (3). The values of t run from 4 to 120 with $\Delta t = 2$. The first point for t = 2 is omitted due to large deviation (discretisation error too great close to contact).

The slope is close to B = 6.8116 and indeed the approximation

$$t \cdot W_{+-}(t) \approx -6.8116 \exp(-\kappa at) \tag{2}$$

is almost as good as (1), see later. (The value centered in t = 2 is deviating quite strongly and is omitted. This is due to the fact that $\Delta t = 2$ is a very thick shell close to contact, where drastical variations in $g_{+-}(t)$ take place). Similarly, we find the regression

$$t \cdot W_A(t) = 0.100 + 6.284 \cdot \exp(-\kappa at) \tag{3}$$

with a correlation coefficient of 0.999 with only t = 2 omitted. Again, the expression

$$t \cdot W_A(t) \approx +6.8116 \cdot \exp(-\kappa at) \tag{4}$$

is also an approximation, but not so good as (2) for $t \cdot W_{+-}(t)$.

The approximations (2) and (4) correspond to the so-called ≫ exponential model ≪ (EXP), where the limiting ≫ Debye-Hückel ≪ electrostatic potential multiplied with the proper charges is identified with the potential of mean force. Ramanathan and Woodbury have shown from the BBGKY hierarchy [22], that the EXP is the leading term model with an error in the RDF's within $O([\kappa\lambda_B]^2 h_{ij})$ outside the hard core for *symmetrical* electrolytes. The λ_B is the Bjerrum length (= B/a) and $h_{ij}(t)$ is the correlation function $g_{ij}(t) - 1$ between ions of types i and j. This is in contrast to dilute plasmas and asymmetric electrolytes, where the error is of $O(\kappa\lambda_B h_{ij})$ for large separations.

If one takes as potential of mean force the full expression for the electrostatic potential from the (linear) Debye-Hückel theory (where the charge distribution has been normalized), one obtains the so-called DHX-model:

$$t \cdot W_{+-}(t) \approx -B \exp(\kappa a)\exp(-\kappa a t)/[1 + \kappa a] \tag{5a}$$

$$t \cdot W_A(t) \approx +B \exp(\kappa a)\exp(-\kappa a t)/[1 + \kappa a] \tag{5b}$$

In the present case, where $\exp(\kappa a)/[1 + \kappa a] = 1.000375 \approx 1$, the DHX model is practically identical to EXP, but for somewhat higher values of κa, the DHX is slightly better than EXP. A very careful analysis of the thermodynamic consistency of the DHX model comparing different routes of calculation and comparison with MC data and HNC data has been performed in References [10–11] for 1:1 electrolytes with B = 1, 1.546, 1.681 and B = 2. It was found, that the DHX model yields excellent fits of the RDF's close to contact and up to quite large separations and quite good values of the thermodynamic parameters up to $\kappa a \approx 0.3$ (where $\exp(\kappa a)/[1 + \kappa a] = 1.0384$). Even for the presently treated dilute 2:2 electrolyte, the DHX is able to explain the deviation found in the MC excess heat capacity from the Debye-Hückel value of *ca.* 450%! (see Reference [11], Figure 10).

In Figures 2–3, we show for a system with N = 1000 and 8 million configurations, but still B = 6.8116 and $\rho^* = 8.924 \cdot 10^{-6}$, the properties of the sampled RDF's more close to contact. It is seen, that the values calculated from (1) and (3) - solid curves - fit the MC data - rectangles - slightly better than the DHX model-crosses - especially very close to contact.

Thus, equations (1) and (3) are not only good approximations between t = 4 and 120, but also very close to contact. An enormous increase in the ≫ local concentration ≪ of counterions takes place very close to contact. This corresponds to ≫ contact adsorption ≪ of some counterions in Bjerrum ion pairs. Ramanathan and Jensen [23] also predict such a boundary layer with ion association and a matching ≫ outer solution ≪ for the potential of mean force which is Debye-Hückelian with a certain charge neutralisation from ion association.

In Figure 4, the tails of the RDF's are shown, and it is seen that the MC-data, the values calculated from equations (1) and (3) and the DHX values are practically coinciding, although the DHX values may deviate very slightly close to contact.

In analogy with the treatment of the *one particle distribution functions* performed in grand canonical MC-simulations of ions in small charged pores [13–14], one might introduce the following *mean radial distribution function* around an ion:

$$G_0(t) \equiv \sqrt{(g_{+-}(t) \cdot g_A(t))} \tag{6}$$

If such models as DHX or EXP were completely correct at high dilution, the mean radial distribution function should simply be constant = 1. In the inverse

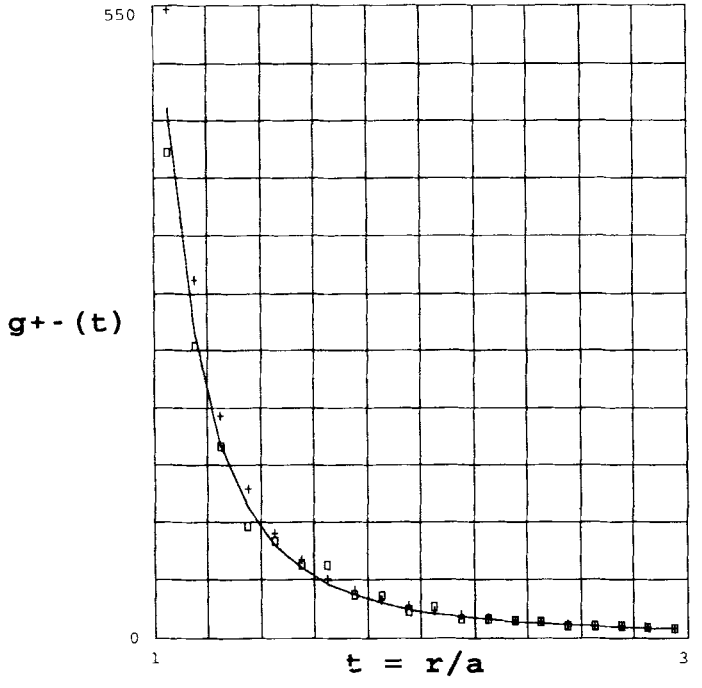

Figure 2 The RDF $g_{+-}(t)$ close to contact for the 2:2 electrolyte with B = 6.8116, $\rho^* = 8.924.10^{-6}$ and N = 1000 (8 million configurations). The rectangles are the directly sampled MC-data. DHX is denoted by + + + + , and the solid curve is calculated using the regression equation (1) for the potential of mean force.

Debye-Hückel problem treated in References [13–14] - ion distribution inside a charged sphere - variations in the corresponding mean of the one particle distribution functions reflected hard sphere oscillations at higher concentrations and repulsion from the wall (with the same dielectric constant!) because of the impossibility of forming a symmetric, optimally shielding ionic cloud around ions near the wall. Figure 5 exhibits the analogous situation in the present case. For t between 20 and 120, the MC-values are indeed equal to unity within 2 per mille or less! Notice, however, the very slight but systematic repression below unity at large separations. For $t < 10$, $G_0(t)$ *rises* very steeply, indicating that $g_{+-}(t)$ is increased by a factor greater than the factor by which the $g_A(t)$ is lowered. The most likely explanation of this is that the discretisation error due to the finite thickness of the sampling shells are much more important for $g_{+-}(t)$ due to the ≫ Bjerrum-Ramanathan boundary layer ≪ of ion pairs, but the usual ≫ attractive forces ≪ found in the potential of mean force in hard sphere systems might also be of importance, since the ≫ local concentration ≪ of counterions is very large close to contact.

Returning to the ≫ contact adsorption layer ≪ in Figure 2, it is well to notice that in spite of the drastic increase of $g_{+-}(t)$ *within a distance which is only* 0.2 from contact, the actual counterion adsorption is very small because of the low bulk concentration. If we denote by $n(\tau)$ the number of counterions around a given ion,

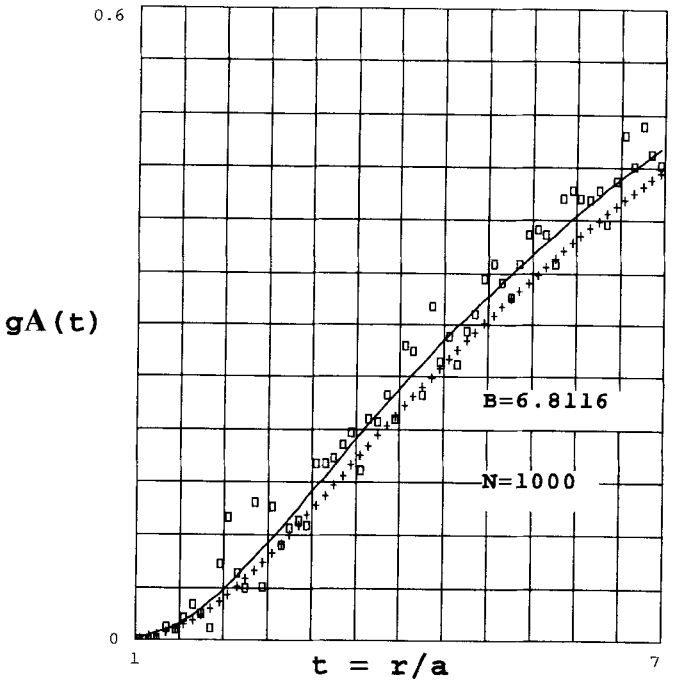

Figure 3 The RDF $g_A(t)$ close to contact for the 2:2 electrolyte with B = 6.8116, $\rho^* = 8.924.10^{-6}$ and N = 1000 (8 million configurations). The rectangles are the directly sampled MC-data. DHX is denoted by + + + + , and the solid curve is calculated using the regression equation (3) for the potential of mean force. The solid curve fits the MC-data very well, whereas the DHX values are systematically too low.

which is contained in the spherical shell between t = 1 and t = τ, we have (the bulk concentration of counterions is $\rho^*/2$):

$$n(\tau) = 2\pi\rho^* \int_1^\tau t^2 g_{+-}(t)\, dt \tag{7}$$

By $n_0(\tau)$ we denote the corresponding number with the counterions evenly distributed:

$$n_0(\tau) \equiv (2\pi\rho^*/3)\tau^3 \tag{8}$$

The *excess number of counterions* is:

$$n_{ex}(\tau) \equiv n(\tau) - n_0(\tau) \tag{9}$$

Now it is quite clear, that models with $a\, g_{+-}(t)$ approaching unity always from the same side when $t \to \infty$ (such as the DHX model) cannot be entirely correct. For large t, we have for the DHX, that $g_{+-}(t) \approx 1 + (B/t)\exp(\kappa a)\exp(-\kappa at)/[1 + \kappa a]$ (like in the original linearised Debye-Hückel theory), and $dn_{ex}(\tau)/d\tau$ is proportional to $(t \cdot B \cdot \exp(\kappa a)\exp(-\kappa at)/[1 + \kappa a])$ which is always positive. Thus, $n_{ex}(\tau)$ is never decreasing. However, close to contact there is an excess of counterions, and for

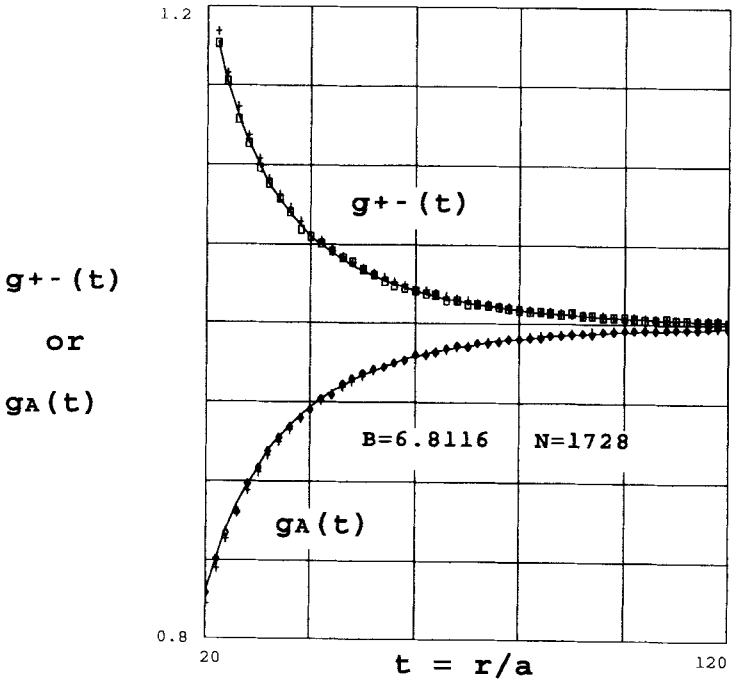

Figure 4 The tails of the RDF's for the 2:2 electrolyte with B = 6.8116, $\rho^* = 8.924.10^{-6}$ and N = 1728 (15 million configurations). MC values - rectangles for $g_{+-}(t)$ and diamonds for $g_A(t)$ - coincide with values calculated from equations (1) and (3) - solid curves - and with DHX(+ + +). Below t = 40, the DHX values for $g_{+-}(t)$ are very slightly higher and the DHX values for $g_A(t)$ very slightly lower, however.

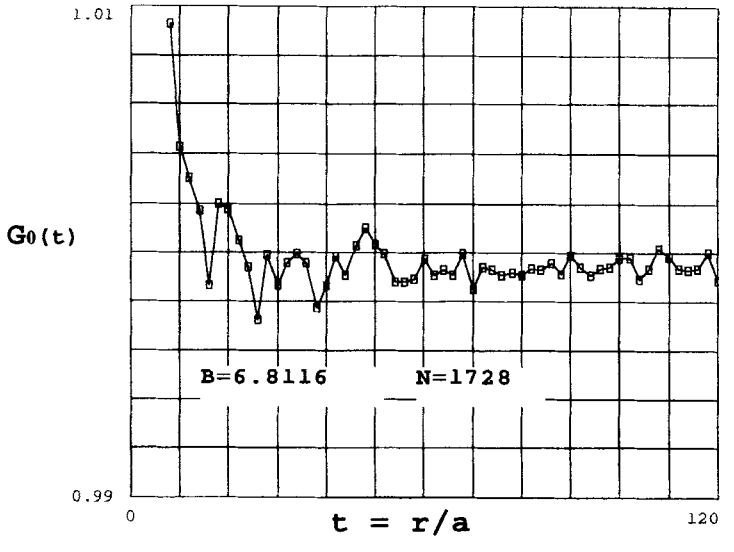

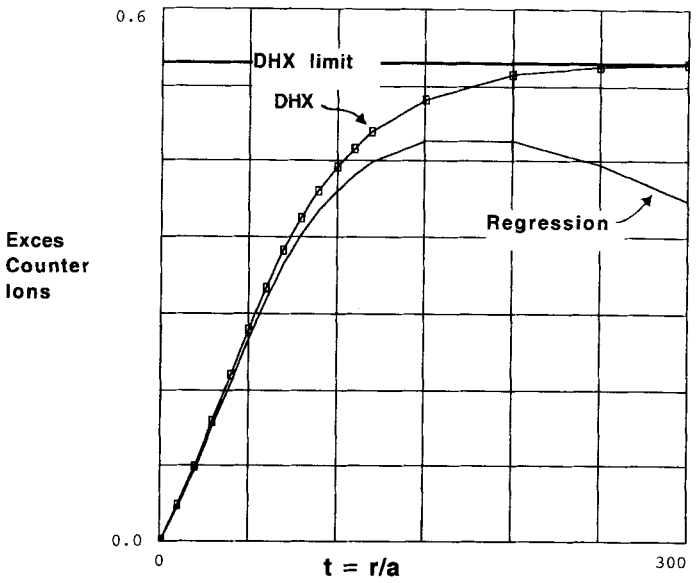

Figure 6 The excess number of counterions as a function of t = r/a. DHX-values are indicated by rectangles. The solid curve is values calculated from the regression (1). The fit to MC-data only extends to t = 120, but the extrapolation to t = 300 is more realistic for the regression than for DHX.

$\tau \to \infty$ we must have that $n_{ex}(\tau) \to 0$ because of *bulk electroneutrality*. Therefore, $dn_{ex}(\tau)/d\tau$ has to be negative for high values of τ.

Figure 6 shows the excess number of counterions inside a spherical shell of radius t as a function of t. Close to contact, the number of adsorbed ions is too small to be observed on the scale used. This is a combination of the low bulk concentration and the little space available close to contact. Indeed we calculate $n_{ex}(1.1) \approx 0.003$, $n_{ex}(1.2) \approx 0.005$, $n_{ex}(1.5) = 0.009$ and $n_{ex}(2.0) = 0.012$. Thus, only 1.2% of the ions have counterions between r = a and r = 2a.

The excess number calculated by DHX increases steadily to a constant positive value value, which is wrong. The solid curve based on equation (1) is probably better in the region from $t \approx 80$ to $t \approx 120$, which is the limit of the MC simulation to which equation (1) was fitted. A decrease in $n_{ex}(t)$ is correctly predicted, and $g_{+-}(t)$ crosses the unity line at the maximum exhibited in Figure 6 (at $t \approx 170$ and an excess of ≈ 0.55 counterions if the curve extrapolates correctly). At much higher t-values than shown it is clear, that also equation (1) is wrong, since n_{ex} calculated this way does not approach zero. This is easily understood: At κat $\gg 1$, the radial distribution function using equation (1) becomes $g_{+-}(t) \approx 1 - 0.056/t$ and $n_{ex}(t)$

Figure 5 The mean RDF, $G_0(t)$ for the 2:2 electrolyte with B = 6.8116, $\rho^* = 8.924.10^{-6}$ and N = 1728 (15 million configurations). The MC-data (rectangles) are connected with a broken curve. Above t = 10 the deviation from unity is less than 2 per mille. A very slight depression below unity ($\approx$0.5 per mille) is seen at large separations.

diverges towards $-\infty$ without limit. A way to rescue this would be to propose instead of equation (1):

$$t \cdot W_{+-}(t) = 0.056 \exp(-\lambda a t) - 6.686 \exp(-\kappa a t) \quad (\lambda a \ll \kappa a) \qquad (10)$$

If $\lambda a \ll \kappa a$, the first exponential would be close to unity up to at least ≈ 120, but at higher t-values the divergence of $n_{ex}(t)$ is prevented, and $n_{ex}(t) \to 0$.

A way to fix the value of λa would be to use the *Kirkwood-Buff* equations for calculation of $\ln y_{\pm}$ directly from the RDF. Such calculations are very sensitive to small changes in the long-tail properties of the RDF. The Kirkwood-Buff values should be identical to the excess chemical potentials calculated through other routes, see Reference [10]. In this paper, the chemical potentials calculated by Kirkwood-Buff + DHX were found to be much less precise than the chemical potential calculated from lower moments of g(t). However, we shall not pursue this matter further here.

MODERATELY DILUTE Z:Z ELECTROLYTES WITH INCREASING BJERRUM PARAMETER

Thermodynamic values

With $B \geq 6.8116$ and the concentration $\rho^* = 5.590 \cdot 10^{-3}$, small system MC simulations have been performed, see Table 4.

Table 4 MC simulations with small N and $\rho^* = 5.590 \cdot 10^{-3}$.

B	κa	N	$-E_{ex}NkT$	$-\Delta F_{ex}/NkT$	$C_{V,ex}/Nk$	$-\ln y_+$ (PW)	$-\ln y_-$ (PW)
6.8116	0.6917	32	1.903	1.318	1.353	1.119	1.118
8.8116	0.7868	44	2.976	2.231	2.201	1.750	1.742
10	0.8381	44	3.699	2.740	2.660	2.134	2.130
10	0.8381	100	3.700	(3.119)	2.615	2.277	2.328
12	0.9181	100	5.006	(4.396)	2.794	2.968	3.036
12	0.9181	150	4.996	(4.517)	2.836	3.150	3.079

First 3 simulations: 30 million configurations Last 3 simulations: 20 million configurations.

Some quantities of significance for the correction of the small system data to the thermodynamic limit are given in Table 5. The ≫ plain Widom ≪ (PW) values of $\ln y_{\pm}$ are corrected to electroneutrality subtracting the correction terms CORR (see Appendix), which are large compared to the plain Widom values. Else, the systems

Table 5 Some useful quantities for the correction of the data in Table 4.

B	N	L	$x = 2/(L\kappa a)$	$CORR$
6.8116	32	17.889	0.16163	0.4531
8.8116	44	19.892	0.12779	0.5272
10	44	19.892	0.11996	0.5982
10	100	26.153	0.09125	0.4550
12	100	26.153	0.08330	0.5460
12	150	29.938	0.07276	0.4770

are close to the thermodynamic limit in spite of their smallness, since $x \equiv 2/(L\kappa a)$ is small. We use the previously found polynomials in x to correct the thermodynamic quantities to the thermodynamic limit (∞), see Appendix. However, from the $\ln\gamma_\pm$ values corrected to electroneutrality one must first subtract the hard sphere contribution to obtain the electrostatic part of $\ln\gamma_\pm$. Then, this quantity is corrected by the same polynomial as E_{ex}/NkT, as found in Reference [11]. The latter is a very small correction compared to the correction with CORR. The *hard sphere* contribution is calculated by the following relation derived from the Carnahan-Starling expression [24]:

$$\ln\gamma^{HS} = (\eta)\,(3\eta^2 - 9\eta + 8)/(1-\eta)^3 \tag{11}$$

$$\eta \equiv \pi\rho^*/6 \tag{12}$$

All the systems in Table 4 are at the same concentration, so they all share the same value of $\ln\gamma^{HS} = 0.023544$. When this is added to $\ln\gamma_\pm^{el}(\infty)$, one obtains $\ln\gamma_\pm^{tot}(\infty)$. The corrected quantities are summarized in Table 6. One value has been calculated before by other authors, namely $-E_{ex}/NkT$ with B = 6.8116. Rogde and Hafskjold [21] obtained the value 1.898 ± 0.007 with N = 216, 4 million configurations and Ewald summation. The direct MC value (1.903) in Table 4 based upon one simulation with N = 32 without Ewald summation is within the uncertainty range of the figure of Rogde and Hafskjold, whereas the polynomial-extrapolated value in Table 6 (−1.890) is just below this uncertainty range. However, comparison of the two couple of values at B = 10 and B = 12 in Table 6 shows, that the uncertainty of the figures in Table 6 is of the same order of magnitude as the Rogde and Hafskjold uncertainty. Thus, the value in Table 6 is also statistically identical to the value of Rogde and Hafskjold.

Table 6 Corrected thermodynamic quantities for $N \to \infty$ and $\rho^* = 5.590 \cdot 10^{-3}$.

B	N	$-E_{ex}(\infty)/NkT$	$-\Delta F_{ex}(\infty)/NkT$	$C_{V,ex}(\infty)/Nk$	$-\ln\gamma_\pm^{el}(\infty)$	$-\ln\gamma_\pm^{tot}(\infty)$
6.8116	32	1.890	1.28	1.38	1.58	1.56
8.8116	44	2.964	2.19	2.23	2.29	2.26
10	44	3.686	2.70	2.69	2.74	2.72
10	100	3.693	(3.09)	2.63	2.78	2.75
12	100	4.999	(4.36)	2.81	3.57	3.54
12	150	4.991	(4.49)	2.85	3.61	3.59

Valleau, Cohen and Card [18] also simulated E_{ex}/NkT for this system with MI cut-off and 80,000 configurations. With N = 32 they obtained 1.920 ± 0.020, for N = 64 they found 1.907 ± 0.011 and for N = 200 a figure 1.905 ± 0.016 was found. Extrapolating linearly vs. 1/N to $N \to \infty$, they found finally 1.900 ± 0.017. According to the findings in References [10–11], it is in principle wrong to extrapolate in 1/N, although the error committed is only large at very low concentrations. The leading term in the variation is of order $[2/L\kappa a]^2$ which is proportional to $N^{-2/3}$. Regression with respect to $N^{-2/3}$ leads to an extrapolated value of 1.897 ± 0.017. It is seen, that the value in Table 6 is well within the uncertainty belt of both these extrapolated Valleau, Card and Cohen values.

In order to test for the activity coefficients, comparison is made with the expansion made by Poirier in terms of the exponential integral, see e.g. the discussion

Table 7 Values of $\ln y_\pm$ according to Poirier.

B	ρ^*	$-\ln y_\pm$ (*Poirier*)							
	Terms:	*2*	*4*	*6*	*8*	*10*	*12*	*14*	*16*
6.8116	$8.924\cdot10^{-6}$	.091566	.098158	.101989	.103815	1.04448	*.104610*	*.104642*	*.104647*
6.8116	$5.590\cdot10^{-3}$	1.56831	1.58103	1.57746	1.57598	*1.57574*	*1.57571*	*1.57571*	*1.57571*
8.8116	$5.590\cdot10^{-3}$	*2.27126*	*2.27777*	2.26170	2.25467	2.25318	*2.25297*	*2.25295*	*2.25295*
10	$5.590\cdot10^{-3}$	*2.72538*	*2.72289*	2.69263	2.67840	2.67497	*2.67443*	*2.67437*	*2.67437*
12	$5.590\cdot10^{-3}$	*3.54721*	3.51982	3.45092	3.41419	3.40361	3.40157	*3.40130*	*3.40127*

and tabulation made by Falkenhagen [25], section 15.2. For a z:z electrolyte (with z^2 included in B) one obtains in the present nomenclature:

$$\ln y_\pm = (-B/2)\kappa a + (4\pi/3)\rho^* - \sum_{k=1,2\ldots} B^{2k-1} b_{2k}(\kappa a) \qquad (13)$$

The first term is clearly the limiting law expression, whereas the second is an ≫excluded volume≪ term. The functions $b_2(\kappa a)$, $b_4(\kappa a)$ ..... $b_{16}(\kappa a)$ have been calculated by Poirier, see the Tabelle 81 in Falkenhagen [25], By ≫ Poirier 14 ≪ for example, I shall mean the series in (13) *including* the b_{14} term, but *omitting* the b_{16} term. Some results are shown in Table 7.

The values in Italics are either values, which are ≫ plateau values ≪ (quite independent of the number of terms) or values, which are close to the MC values extrapolated to $N = \infty$. The extremely dilute system is seen to converge slowly, but after inclusion of b_{12} the value is constant to 4 digits ($\ln y_\pm = -0.1046$), which value can not be distingued from the -0.1043 ± 0.0009 found by MC (Table 2). At the higher concentration $\rho^* = 5.590\cdot10^{-3}$ and $B = 6.81116$, Poirier 10 is satisfactory to 5-6 constant digits, and the value $\ln y_\pm = -1.57571$ is excellently in agreement with the MC-value -1.56 cited in Table 6. In the case $B = 8.8116$, Poirier 12 is satisfactory to 5 digits and the value -2.25295 is in excellent agreement with the MC-value-2.26. However, there is some indication of another plateau for Poirier 2-4, and indeed all the Poirier figures are within the uncertainty range of the MC calculations. For $B = 10$ there is also an initial plateau, and the plateau value ≈ -2.725 is better in accordance with the MC value (-2.73 ± 0.02) than the final plateau value -2.67437. For $B = 12$ there cannot be said to be any reasonable initial plateau value, but the Poirier 2 value -3.5472 is in very good agreement with the MC value -3.56 ± 0.02, whereas the final plateau value -3.4013 is not. Thus, for high B it seems to be a better approximation to truncate the series after the b_2-function than to take the whole series. Indeed, only for very low values of κa is it necessary to take more than this term, if the precision does not have to be more than three digits.

On the other hand, the additional functions of Poirier have important consequences in the dilute regime. For 2:2 and higher valency symmetric electrolytes, the values of $-\ln y_\pm$ will *overshoot* the limiting law value $B\kappa a/2$ below a certain critical concentration. Figs 7a-b shows $\ln y_\pm$(Poirier) *vs.* κa for the system with $B = 6.8116$, and the two MC-simulated values are inserted. It is seen, that $\ln y_\pm$ for the low concentration is indeed on the ≫ wrong side ≪ of the limiting law. This slight tendency becomes very dominating for larger values of B according to the Poirier expression, see Figure 8 for $B = 12$.

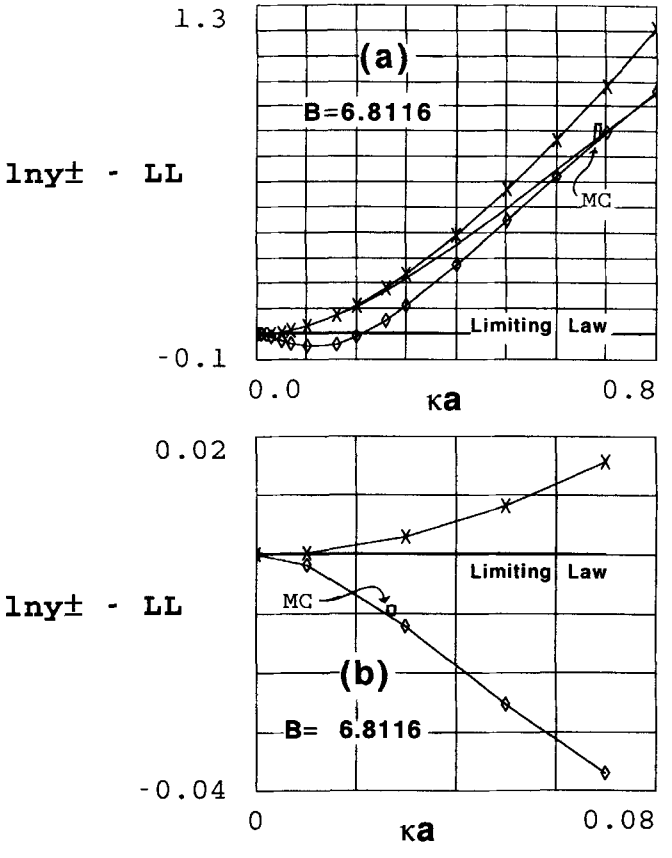

Figure 7 The difference between $\ln\gamma_{\pm}$ and $\ln\gamma_{\pm}$(limiting law) vs. κa for B = 6.8116 in the interval from (a) $\kappa a = 0$ to 0.8 and (b) in the interval from $\kappa a = 0$ to 0.08. Corrected and extrapolated MC-simulations: Rectangles with heights indicating estimated uncertainties. Limiting law, $\ln\gamma_{\pm}(LL) = -(B/2)\kappa a$: Horizontal base line at value zero. Debye-Hückel law, $\ln\gamma_{\pm}(DH) = -(B/2)\kappa a/(1 + \kappa a)$: Upper curves with X X X X X. Poirier 16: Curve with diamonds. Poirier 2: Curve without symbols in Figure 7a (asymptotic to DH at low concentrations and to Poirier 16 at moderate concentrations).

From Figures 7-8 it is also obvious that Poirier 2 cannot for account for the negative deviation from the limiting law. Poirier 2 just follows the usual Debye-Hückel expression $\ln\gamma \pm (DH) = -(B/2)\kappa a/(1 + \kappa a)$ for small κa. At higher values of κa it corrects slightly the DH expression and coincides with Poirier 16 and the MC-results at moderate concentrations. The usual DH-expression (curves with X X X X) are never correct and even deviates to the wrong side at low concentrations! Addition of a ≫ hard sphere ≪ contribution by the argument, that $\ln\gamma_{\pm}(DH)$ is only the electric part of the excess chemical potential - such as done in an attempt to interpret experimental data in an early paper of Sørensen *et al.* [40] - would only make things worse.

To finish this section, it is shown in Table 8, that Poirier 16 is *also* in good agreement (≈ 3 digits) with our previously simulated and corrected MC Widom test

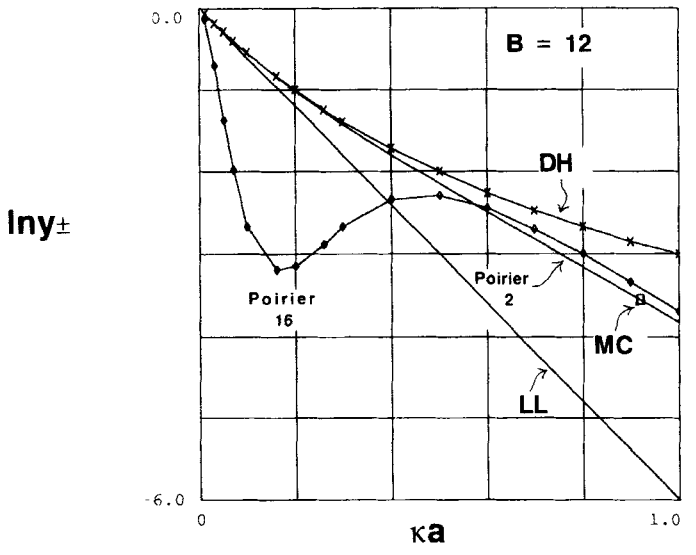

Figure 8 $\ln\gamma_{\pm}$ vs κa for B = 12 in the interval from κa = 0 to 1.0. Corrected and extrapolated MC-simulation: Rectangle with height indicating estimated uncertainty.
Limiting law: Solid straight line marked LL.
Debye-Hückel law: Upper curve with X X X X (marked DH).
Poirier 16: Curve with diamonds. Poirier 2; Curve without symbols.

particle results for $\ln\gamma_{\pm}$ for the considerably more ≫tame≪ 1:1 electrolytes with equal ionic radii (B = 1 correspond to very large ions in water at 25°C). In summary, the Poirier formula is very powerful and rather precise for low as well as high Bjerrum parameters at least for κa up to ≈ 1, except possibly for extreme values of B(> 10, say).

Table 8 Comparison between $\ln\gamma_{\pm}$(Poirier, 16) and corrected $\ln\gamma_{\pm}$ (MC, Widom) [11].

B	κa	$\ln\gamma_{\pm}^{el}(CORR, N=\infty)$	$\ln\gamma^{HS}$¶	$\ln\gamma_{\pm}^{tot}(MC)$	$\ln\gamma_{\pm}(Poirier)$
1	0.11210	−0.0511	0.00419	−0.0470	−0.04654
1.546	0.13938	−0.0963	0.00419	−0.0921	−0.09158
1.546	0.44077	−0.246	0.0423	−0.204	−0.20907
1.681	0.45021	−0.272	0.0406	−0.231	−0.23747
2	0.02242	−0.0221	0.00008	−0.0221	−0.02197
2	0.04011	−0.0391	0.00027	−0.0388	−0.03863
2	0.05605	−0.0540	0.00052	−0.0535	−0.05313
2	0.07927	−0.0749	0.00105	−0.0739	−0.07337
2	0.11210	−0.1033	0.00210	−0.1012	−0.10031

¶ Hard sphere contribution, equations (11-12).

RDF and triplet formation with increasing B

As shown in Figure 9, the RDF's between ions of like charge $g_A(r)$ become more and more different from the usual DHX-RDF's when B increases at fixed concentration $\rho^* = 0.00559$. For B = 6.8116 a shoulder is already observed, which for B increasing through 8.8116 and 10 to 12 evolves to a characteristic, sharp peak centered around r = 2a. Clearly, this peak must reflect *linear triplets* + − + and − + − favoured by the high Bjerrum parameter (~ electrostatic energy /kT at contact). It is well known that ionic clusters for *e.g.* in air and in organic solvents (low dielectric constants), indeed the process may easily continue to make the salt insoluble in the medium. For B = 12, the + + (or − −) distances 1.5a and 2.5a are also quite probable, so the angle of the triplet is not always 180° and there exist also clusters, where the ions are not quite in contact. Some admixture of quadruplets may also be reflected in the RDF's. The RDF's $g_{+-}(r)$ are not shown, since they look very DHX-like. It is always in the $g_A(r)$ the greatest deviations from DHX have been found at moderate concentrations even in 1:1 electrolytes, so it may be a reflection of a very small formation of triplets not accounted for in the Debye-Hückel approach. The slight systematic deviation in $g_A(r)$ in an extremely dilute 2:2 electrolyte (Figure 3) may also be explained in that way. In that case, it was seen in Ref. [11] that the DHX gave nevertheless quite reliable thermodynamic values (even for the excess heat capacity). This is so because of the dominance of the much greater $g_{+-}(r)$ near to contact in the integration formulae for the thermodynamic quantities.

Rogde and Hafskjold [21] have also found a (much less pronounced) triplet peak in their MC simulations of 2:2 electrolytes (B = 6.8116) at higher concentrations ($\rho^* = 0.1787 \approx 2$M). At lower concentrations ($\rho^* \leq 0.08961 \approx 1$M) they found no maximum, whereas the HNC theory erroneously predicted a significant peak even at $\rho^* = 0.0004461 \approx 0.005$ M). Abramo *et al.* [26] have found, that the triplet peak of Rogde and Hakfskjold becomes higher and sharper, when the cations and anions are of different sizes.

Very recently Laria *et al.* [27] have reconsidered the cluster theory of electrolyte solutions. They find the population of single ions and clusters which minimizes the Helmholtz free energy for different concentrations and Bjerrum parameters. Cluster formation are more dominating at intermediate concentrations than for low or for high concentrations. For B =6.8 there is only single ions and some ion pairs (see [27] Figure 1). For B = 10.3, ion pairs dominate, but there are also some triplets. Increasing B to 12, ion pairs dominate even more, but the amount of triplets is also increased, and it seems that there are almost just as many quadruplets. These might be the reason for the broadening of the peak in Figure 9 into separations between r = a and 2a (tetrahedral quadruplets). So even if such cluster calculations are crude from a strict statistical mechanical point of view, they seem to hit some right features.

AN EXTREMELY DILUTE 2:1 ELECTROLYTE

In order to perform a severe test of the simulation of for example *single ion activities* it was decided to simulate an extremely dilute 2:1 electrolyte with equal ionic radii, where $\ln y_{2+}$ according to the limiting law and the extended Debye-Hückel law should be about four times the value of $\ln y_{-}$. Also, it would be interesting to see if the DHX description of the RDF's may be generalized in a natural way.

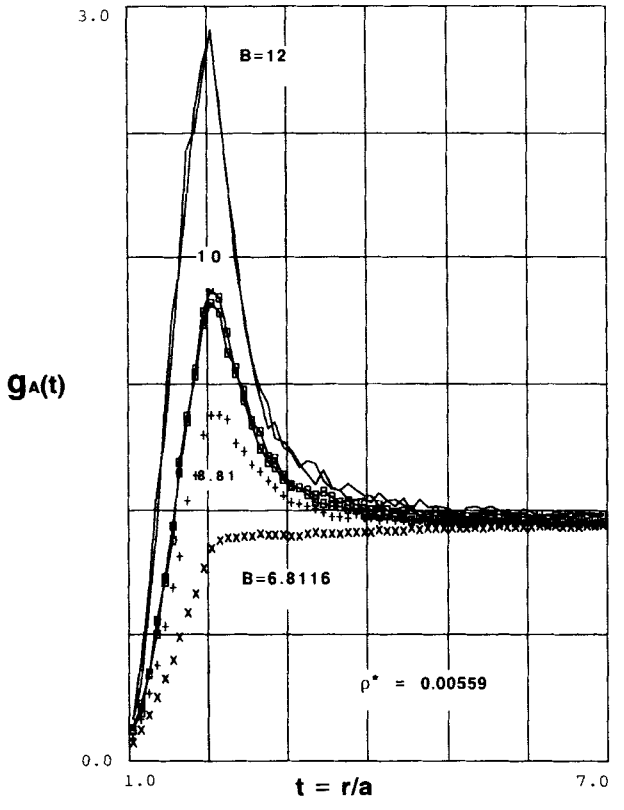

Figure 9 RDF between ions of like charges in symmetric electrolytes. The amount of linear triplets increases, when B increases in the succession 6.8116 (x x x x, N = 32, 30 million configurations), 8.8116 (+ + + +, N = 44, 30 million), 10 (two, curves with rectangles, N = 44, 30 million, N = 100, 20 million), 12 (upper two broken curves, N = 100 and N = 150, 20 million).

Thermodynamic properties: Extrapolation to the thermodynamic limit

In Tables 9–10, the MC data and some useful quantities have been summarized. The total number of particles (N) varied between 30 and 999. Mostly *ca.* 8 million configurations were used. In most cases, it was sufficient to reject the first 10,000 to 20,000 configurations, but in some few cases a quite large variation in especially the sampled excess chemical potentials was observed, and it was necessary to throw away the first 500,000 configurations. The (reduced) Bjerrum parameter $B \equiv e_o^2/(4\pi\epsilon kTa)$ is set to 1.546. Later, we shall also investigate a dilute 2:1 electrolyte with B = 3.

Figure 10 shows the uncorrected (plain Widom) as well as the electroneutrality corrected values of $\ln\gamma_{2+}$ plotted against $N^{-1/3}$ (see References [4–5] for a discussion of the choice of this particular power). The variation of the corrected values is much less. Furthermore, the leading term in the finite system effect of the corrected values seems rather to be proportional to $N^{-2/3}$, like the other thermodynamic

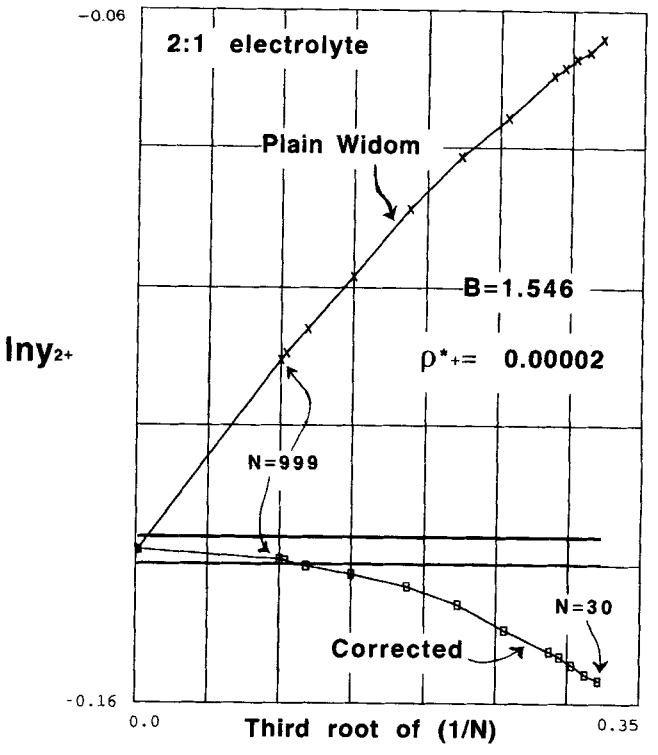

Figure 10 The MC single ion exces chemical potential for the doubly charged cation in a 2:1 electrolyte plotted against $(1/N)^{1/3}$. Plain Widom: Upper curve with x x x x. Corrected for deviation from electroneutrality: Lower curve with rectangles. Extrapolated value: $\ln y_{2+}(\infty) = -0.1380 \pm 0.0020$ between the two horizontal thick lines.

Table 9 Plain Widom samplings and corrected values of $\ln y_{2+}$ and $\ln y_{-}$. (2:1 Electrolyte. B = 1.546. $\rho_+^* = N_+/L^3 = 2 \cdot 10^{-5}$. $\kappa a = 0.0482837$).

Millions of configurations	N	N_+	L	$2/(L\kappa a)$	$-\ln y_{2+}(PW)$	$-\ln y_{-}(PW)$	$-\ln y_{2+}(corr)$	$-\ln y_{-}(corr)$
8.00(*a*)	30	10	79.37	0.5219	0.06398	0.01914	0.15670	0.04232
8.22(*b*)	33	11	81.93	0.5056	0.06590	0.01961	0.15572	0.04207
8.27(*a*)	36	12	84.34	0.4911	0.06705	0.01988	0.15430	0.04169
8.00(*a*)	39	13	86.62	0.4782	0.06836	0.02004	0.15332	0.04128
8.00(*a*)	42	14	88.79	0.4665	0.06949	0.02040	0.15237	0.04112
8.00(*a*)	60	20	100	0.4142	0.07569	0.02184	0.14928	0.04024
8.00(*a*)	90	30	114.47	0.3619	0.08133	0.02396	0.14562	0.04003
8.00(*c*)	150	50	135.72	0.3052	0.08891	0.02560	0.14313	0.03915
8.00(*c*)	300	100	171.00	0.2422	0.09847	0.02747	0.14151	0.03823
8.00(*a*)	600	200	215.44	0.1923	0.10610	0.03015	0.14026	0.03869
8.27(*c*)	900	300	246.62	0.1680	0.10960	0.02963	0.13944	0.03709
20.00(*a*)	999	333	255.35	0.1622	0.11050	0.03082	0.13932	0.03802

(a) 10,000 to 20,000 initial configurations rejected. No systematic effect of rejecting up to 500,000.
(b) Great effect of rejecting several 100,000 initial configurations 500,000 configurations rejected.
(c) 500,000 initial configurations rejected with a small effect.
B is the reduced Bjerrum parameter (not including the valency product).

Table 10 MC samplings of E_{ex}/NkT, $\Delta F_{ex}/NkT$ and $C_{v,ex}/Nk$ (2:1 Electrolyte. B = 1.546. $\rho_+^* = N_+/L^3 = 2\cdot10^{-5}$. $\kappa a = 0.0482837$).

N	$-E_{ex}/NkT$	$-\Delta F_{ex}/NkT$	$C_{v,ex}/Nk$
30	0.08116	0.06400	0.03632
33	0.08036	0.06289	0.03683
36	0.08012	0.06227	0.03752
39	0.07955	0.06159	0.03767
42	0.07901	0.06088	0.03744
60	0.07759	0.05829	0.03889
90	0.07639	0.05625	0.04053
150	0.07516	0.05235	0.04051
300	0.07434	0.05168	0.04208
600	0.07352	0.05423	0.04254
900	0.07359	0.05637	0.04388
999	0.07340	0.05534	0.04367

parameters. Thus for N = 999, corrected values are already inside the estimated uncertainty belt of the extrapolated value, whereas the plain Widom value is far away.

Figure 11 shows the sampled value of E_{ex}/NkT and the calculated values of $\ln\gamma_\pm = (1/3)\ln\gamma_+ + (2/3)\ln\gamma_-$ (calculated for each value of N after initial correction to electroneutrality) *vs.* the ⩾distance⩽ from the thermodynamic limit $x^2 = 4/(L\kappa a)^2$. The plots are linear and the regression lines are shown. The plot is very interesting, since in the Debye-Hückel theory there is no difference between E_{ex}/NkT and $\ln\gamma_\pm$, but here it is clearly seen, that the two quantities extrapolate significantly differently to the thermodynamic limit, and the slopes as well as the intercepts are different. Thus, the corresponding *calibration polynomials* for MC simulations in dilute 2:1 electrolytes ($\ln\gamma_\pm^{el} \approx \ln\gamma_\pm^{tot}$ in this extremely dilute system)

$$\ln\gamma_\pm^{el}(\mathrm{MC, corr})/\ln\gamma_\pm^{el}(\infty) = 1 + 0.5017\cdot x^2 \tag{14}$$

$$E_{ex}(\mathrm{MC})/E_{ex}(\infty) = 1 + 0.4277\cdot x^2 \tag{15}$$

are *not identical* as was found for z:z electrolytes [10–11]. On the other hand, they are simpler, since 4th degree polynomials in x seem not to be needed for dilute 2:1 systems. There is some weak indication of curvature in each plot, however, and indeed the following polynomials fit slightly better:

$$\ln\gamma_\pm^{el}(\mathrm{MC, corr})/\ln\gamma_\pm^{el}(\infty) = 1 + 0.423090\cdot x^2 + 0.267126\cdot x^4 \tag{16}$$

$$E_{ex}(\mathrm{MC})/E_{ex}(\infty) = 1 + 0.326752\cdot x^2 + 0.344037\cdot x^4 \tag{17}$$

The uncertainty of the extrapolated quantities may be judged by using either the set (14–15) or the set (16–17).

When the sampled and corrected *single ion* exces chemical potentials are plotted against x^2 (Figure 12), $\ln\gamma_-$ is almost a straight line, whereas $\ln\gamma_{2+}$ is considerably more curved. However, for the sake of uniformity, both have been fitted by second order polynomials in x^2. Thus, the following calibration polynomials are adopted:

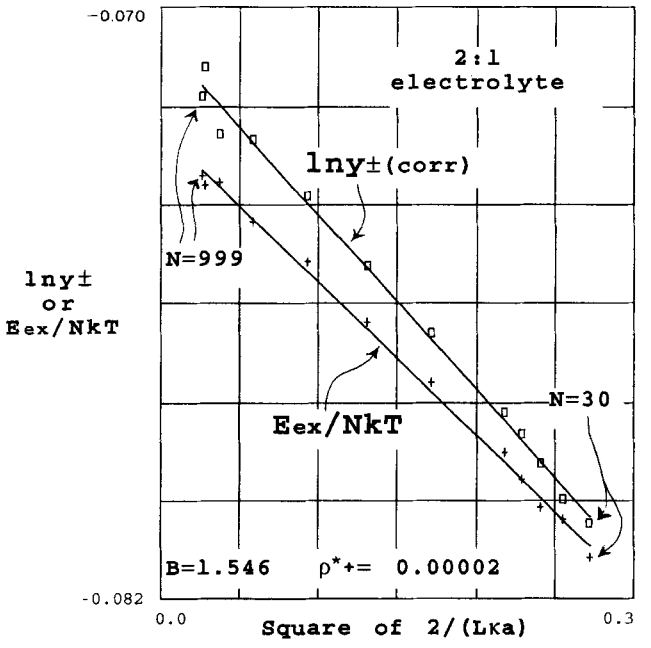

Figure 11 The corrected values of $\ln\gamma_{\pm}$(MC) (rectangles, upper curve) and the sampled values of E_{ex}/NkT (lower curve + + + +) as a function of $x^2 = (2/L\kappa a)^2$. The two regression lines are given by: $\ln\gamma_{\pm}(MC) = -0.070654 - 0.035447\ x^2$ (correlation coefficient r = 0.997) and $E_{ex}(MC)/NkT = -0.072467 - 0.030994\ x^2$ (correlation coefficient r = 0.998). There is a slight indication of curvature in the plots. Slightly better fit with the polynomials: $\ln\gamma_{\pm}(MC) = -0.070888 - 0.029992\ x^2 - 0.018936\ x^4$ and $E_{ex}(MC)/NkT = -0.072777 - 0.023780\ x^2 - 0.025038\ x^4$.

$$\ln\gamma_{2+}(\mathrm{MC,\ corr})/\ln\gamma_{2+}(\infty) = 1 + 0.384012\ x^2 + 0.442702 \cdot x^4 \qquad (18)$$

$$\ln\gamma_{-}(\mathrm{MC,\ corr})/\ln\gamma_{-}(\infty) = 1 + 0.495234x^2 - 0.057265 \cdot x^4 \qquad (19)$$

Figure 12 is also an interesting plot, showing that even at this extremely low concentration, the cation excess chemical potential is *not precisely* four times the exces chemical potential of the anions as predicted by the Debye-Hückel theory, but it is almost so! The two curves in Figure 12 clearly extrapolate to two significantly different values.

Finally, Figure 13 shows the sampled electrostatic excess Helmholtz free energies and the heat capacities as a function of $4/(L\kappa a)^2$. Straight lines are satisfactory, although deviations occur for $N \geq 90$ in the case of $-\Delta F_{ex}/NkT$. It has been reported repeatedly in the previous papers [1-3, 10-11], that although the direct Metropolis sampling of exp(+ U/kT) does *in principle* lead to the electrostatic part of the configuration integral [1], the method is only functioning for feasible lengths of the Markov chain in case of very small concentrations and/or number of particles. With this restriction we have:

$$\Delta F_{ex}(MC)/\Delta F_{ex}(\infty) = 1 + 1.1186x^2 \qquad (20)$$

$$C_{v,ex}(MC)/C_{v,ex}(\infty) = 1 - 0.6435x^2 \qquad (21)$$

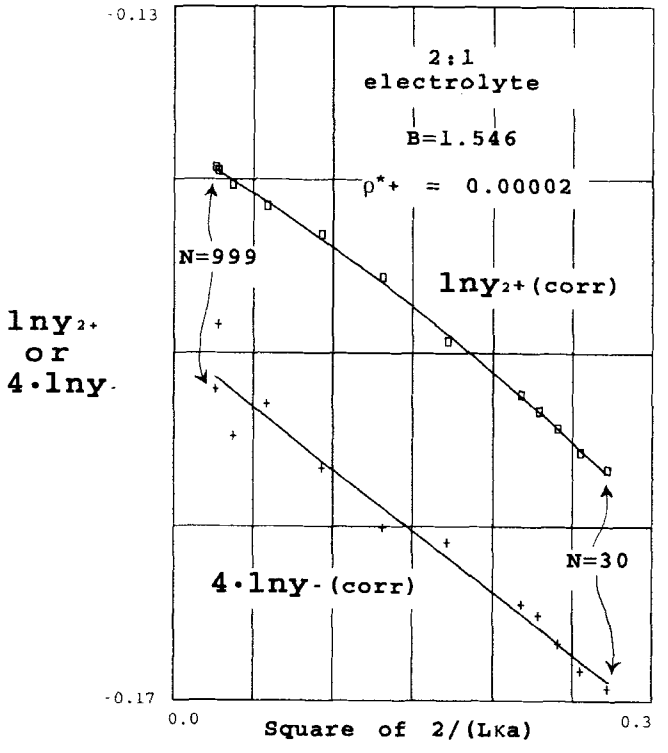

Figure 12 The corrected, sampled values of $\ln y_{2+}$ (rectangles, upper curve) and the sampled values of $4 \cdot \ln y_{-}$ (lower curve + + + +) as a function of $x^2 = (2/L\kappa a)^2$ The least square polynomials (solid curves) are: $\ln y_{2+}(MC) = -0.13798 - 0.052986\ x^2 - 0.061084\ x^4$ and $4 \cdot \ln y_{-}(MC) = 4 \cdot [-0.037344 - 0.018494\ x^2 + 0.0021385\ x^4]$.

In Table 11 we summarize the results for the extrapolated values of the different thermodynamic quantities. The uncertainties are best estimated by comparing different extrapolation formulae. Notice, that the value of $-\Delta F_{ex}/NkT$ is very close to 2/3 of the value of $-E_{ex}/NkT$, as it is in the Debye-Hückel limiting law case.

An extremely dilute 2:1 electrolyte with B = 3

Tables 12–13 shows the simulation results for an extremely dilute 2:1 electrolyte with Bjerrum parameter B = 3. The plain Widom results for the exces chemical potentials in Table 12 have been corrected to electroneutrality.

In Table 14, the values of the sampled thermodynamic quantities have been extrapolated to the thermodynamic limit using the equations (15–21), and in Table 15 the values of $\ln y_{\pm}(\infty)$ are compared with the 16 terms expansion of Poirier. For a 2:1 electrolyte, the expression of Poirier see (25], section 15.2) is given by the following expressions:

$$\ln y_{\pm} = -B\kappa a + 4\pi \cdot \rho_{+}^{*} + \Delta \ln y_{\pm} = -B\kappa a + (\kappa a)^2/(6B) + \Delta \ln y_{\pm} \qquad (22)$$

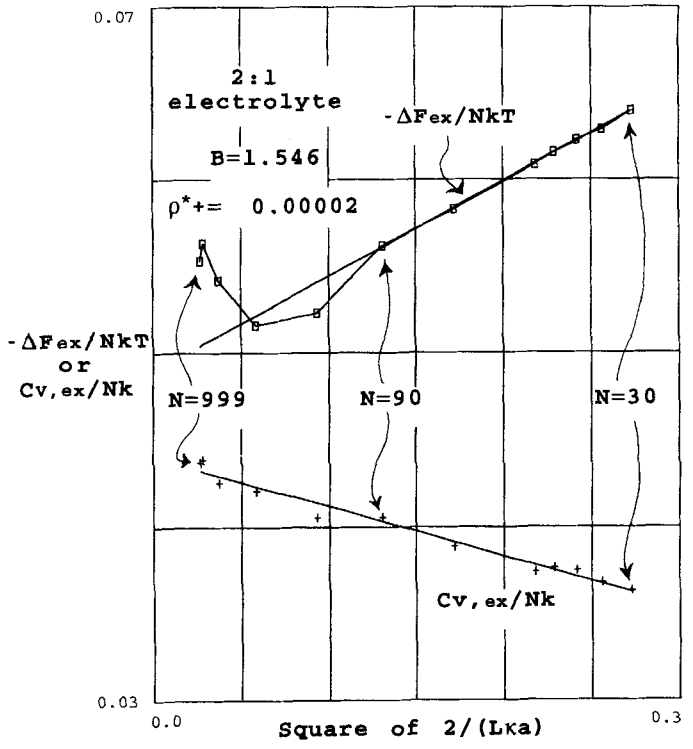

Figure 13 The sampled values of $\Delta F_{ex}/NkT$ (rectangles, upper curve) and of $C_{v,ex}/Nk$ (lower curve + + + +) as a function of $x^2 = (2/L\kappa a)^2$. The regressions (solid lines) are: $-\Delta F_{ex}/NkT = 0.04900 + 0.05481\ x^2$ and $C_{v,ex}/Nk = 0.04398 - 0.02830\ x^2$.

Table 11 Extrapolated MC-values for dilute 2:1 electrolyte (B = 1.546. $\rho_+^* = N_+/L^3 = 2\cdot10^{-5}$. $\kappa a = 0.0482837$. HS contribution ≈ 0).

$-E_{ex}/NkT$	$-E_{ex}/NkT$	$-\Delta F_{ex}/NkT$	$C_{v,ex}/Nk$	$-\ln\gamma_\pm$	$-\ln\gamma_\pm$	$-\ln\gamma_{2+}$	$-\ln\gamma_-$	$-\ln\gamma_\pm$
Eq: [15]	*[17]*	*[20]*	*[21]*	*[14]*	*[16]*	*[18]*	*[19]*	*[18–19]*
0.0725	0.0728	0.0490	0.0440	0.0707	0.0709	0.1380	0.0373	0.0709

Uncertainties ≈ 1–2 on the last digit.

$$\begin{aligned}\Delta\ln\gamma_\pm = &-(B/2)\cdot2^2\cdot b_2(\kappa a) + (B^2/2)\cdot2^2\cdot b_3(\kappa a) - (B^3/2)\cdot6^2\, b_4(\kappa a)\\ &+ (B^4/2)\cdot10^2\cdot b_5(\kappa a) - (B^5/2)\cdot22^2\cdot b_6(\kappa a) + (B^6/2)\cdot42^2\cdot b_7(\kappa a)\\ &- (B^7/2)\cdot86^2\cdot b_8(\kappa a) + (B^8/2)\cdot170^2\cdot b_9(\kappa a) - (B^9/2)\cdot342^2\cdot b_{10}(\kappa a)\\ &+ (B^{10}/2)\cdot682^2\cdot b_{11}(\kappa a) - (B^{11}/2)\cdot1366^2\cdot b_{12}(\kappa a) + (B^{12}/2)\cdot2730^2\cdot b_{13}(\kappa a)\\ &- (B^{13}/2)\cdot5462^2\cdot b_{14}(\kappa a) + (B^{14}/2)\cdot10922^2\cdot b_{15}(\kappa a) - (B^{15}/2)\cdot21846^2\cdot b_{16}(\kappa a)\end{aligned} \tag{23}$$

$$(\kappa a)^2 = 24\pi B\rho_+^* \tag{24}$$

Table 12 Plain Widom samplings and corrected values of $\ln y_{2+}$ and $\ln y_{-}$.
(2:1 Electrolyte. B = 3. $\rho_+^* = N_+/L^3 = 2\cdot10^{-5}$. $\kappa a = 0.0672599$).

Millions of configs.	N	N_+	L	$2/(L\kappa a)$	$-\ln y_{2+}(PW)$	$-\ln y_{-}(PW)$	$-\ln y_{2+}(corr)$	$-\ln y_{-}(corr)$
27.0(c)	60	20	100	0.2974	0.2601	0.08768	0.4029	0.1234
20.0(a)	90	30	114.47	0.2598	0.2730	0.09112	0.3978	0.1223
16.0(a)	999	333	255.35	0.1164	0.3414	0.1101	0.3973	0.1241

(a) 20,000 to 30,000 initial cfgs. rejected. No systematic effect of rejecting up to 500,000.
(c) ca. 500,000 initial cfgs. rejected with a small effect.
B is the reduced Bjerrum parameter (not including the valency product).

Table 13 MC samplings of E_{ex}/Nkt, $\Delta F_{ex}/NkT$ and $C_{v,ex}/Nk$
(2:1 Electrolyte. B = 3. $\rho_+^* = N_+/L^3 = 2\cdot10^{-5}$. $\kappa a = 0.0672599$).

N	$-E_{ex}/NkT$	$-\Delta F_{ex}/NkT$	$C_{v,ex}/Nk$
60	0.2606	0.1528	0.3701
90	0.2590	0.1539	0.3750
999	0.2549	(0.1976)	0.3603

The functions $b_k(\kappa a)$ (k = 2 . . . . 16) in Equation (23) have been tabulated in Reference [25], Table 81. Comparing the Poirier expression for a 2:1 electrolyte with the expression for a symmetric electrolyte (13), we observe that the coefficients to $b_3(\kappa a)$, $b_5(\kappa a)$ . . . . (and even powers of B) do *not* vanish for a 2:1 electrolyte.

From Table 14 (B = 3) it is apparent, that the extrapolation formula (17) for E_{ex}/NkT is better than Equation [15]. The values of $-\Delta F_{ex}(\infty)/NkT$ are increasing with N and probably the value for N = 90 and certainly the value for N = 999 are too high for the reasons indicated previously. Clearly, the value of $-4\cdot\ln y_{-} > -\ln y_{+}$ as the case were also for B = 1.546 (see Figure 12). However, the relative difference is 20% for B = 3 as compared to 8% for B = 1.546. It is also seen, that $-E_{ex}(\infty)/NkT$ is 17% larger than $-\ln y_{\pm}(\infty)$ for B = 3. For B = 1.546 it is only 2.5% larger. Thus, there is a drastical increase in the non-Debye-Hückelian features with increasing Bjerrum parameter!

From Table 15, it is seen that the 16 term expansion of Poirier describes the values of $\ln y_{\pm}$ very well also in the case of dilute 2:1 electrolytes. For B = 3, the value of $-\ln y_{\pm}$ overshoots the limiting law value as the case where for dilute z:z electrolytes at high dilution. The curves of $\ln y_{\pm}$ vs. κa as predicted by the Poirier formula for B = 1.546 and B = 3 are shown in Figure 14-15. It is seen that in case of 2:1 electrolytes in water at 25°C with quite large contact distance (B ≈ 1.5), the

Table 15 Comparison between $\ln y_{\pm}$(Poirier, 16) and corrected $\ln y_{\pm}$(MC, Widom)
(2:1 electrolyte, hard sphere contribution negligible).

B	ρ_+^*	κa	$\ln y_{\pm}(MC, N = \infty)$	$\ln y_{\pm}(Poirier)$	$\ln y_{\pm}(LL)$	$\ln y_{\pm}(DH)$
1.546	$2\cdot10^{-5}$	0.048284	−0.0709 ± 0.0002	−0.07124	−0.07465	−0.07121
3	$2\cdot10^{-5}$	0.067260	−0.210 ± 0.004	−0.2145	−0.2018	−0.1891

The limiting law values (LL) are given by $-B\kappa a$ and the Debye-Hückel values (DH) by $-B\kappa a/(1 + \kappa a)$

Table 14 Calculation extrapolated MC-values for dilute 2:1 electrolyte (B = 3. $\rho_+^* = N_+/L^3 = 2\cdot10^{-5}$. $\kappa a = 0.0672599$. HS contribution ≈ 0).

N	$x = 2/(L\kappa a)$	$-E_{ex}(\infty)/NkT$	$-E_{ex}(\infty)/NkT$	$-\Delta F_{ex}(\infty)/NkT$	$C_{v,ex}(\infty)/Nk$	$-lny_{2+}(\infty)$	$-4\cdot lny_{-}(\infty)$
		Eq: [15]	*[17]*	*[20]*	*[21]*	*[18]*	*[19]*
60	0.2974	0.2511	0.2526	0.1390	0.3924	0.3884	0.4732
90	0.2598	0.2517	0.2530	(0.1431)	0.3920	0.3870	0.4736
999	0.1164	0.2534	0.2538	(0.1946)	0.3635	0.3952	0.4932
∞	0	-	0.2531	0.139	0.383	0.390	0.480
			±0.0005	±0.005	±0.010	±0.005	±0.012

Debye-Hückel law (without addition of hard sphere contribution) is *fortuitously* very good up to at least $\kappa a \approx 0.5$ and the limiting law is quite good up to $\kappa a \approx 0.1$. (Indeed, the solubility curve of $Ba(IO_3)_2$ as a function of added ionic strength has for many years been used as a student exercise in our laboratory demonstrating an $\gg$ unreasonable $\ll$ good fit of the limiting law up to 0.01 molar. For 1:1 electrolytes it is very difficult to demonstrate the limiting law convincingly by experiment!). Figure 14 (b) exhibits the very small deviation of $\ln\gamma_\pm$ from the limiting law up to $\kappa a \approx 0.05$ as predicted by the DH (curve) as well as by the Poirier 16 (rectangles) expression. It is impressive to see how the corrected and extrapolated Widom value (MC) are supporting these values within the uncertainty level. The same is the case for B = 3 (Figure 15 b), where there is considerable deviation between DH and Poirier 16 at small κa, and where the MC-value supports the negative deviation from the limiting law.

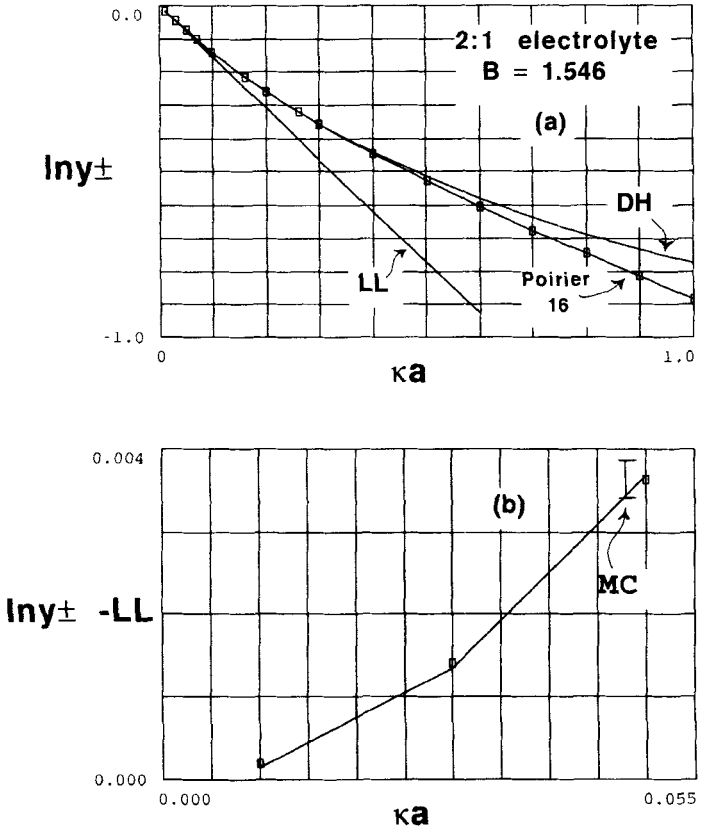

Figure 14 The logarithm of the mean ionic activity coefficient as a function of κa for a 2:1 electrolyte with reduced Bjerrum parameter B = 1.546. (a) The Poirier 16 term expansion and the Debye-Hückel expression without addition of hard sphere term ($-B\kappa a/[1 + \kappa a]$) coincide fortuitously up to $\kappa a \approx 0.5$ (b) Magnification of the deviation from the limiting law (LL) at small κa. The vertical bar is the Widom MC value (with uncertainty) corrected to electroneutrality and to the thermodynamic limit. Rectangles are Poirier 16 values and the curve represents the DH values.

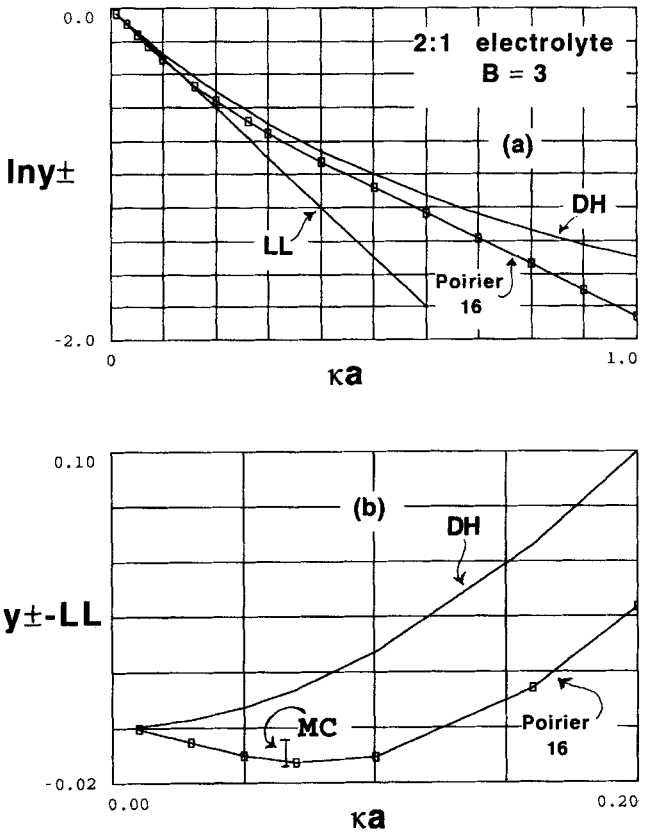

Figure 15 The logarithm of the mean ionic activity coefficient as a function of κa with reduced Bjerrum parameter B = 3. (a) In this case, the Poirier 16 term expansion and the Debye-Hückel expression ($-B\kappa a/[1 + \kappa a]$) are clearly different for all concentrations. (b) Magnification of the deviation from the limiting law (LL) at small κa. The vertical bar is the Widom MC value (with uncertainty) corrected to electroneutrality and to the thermodynamic limit. The curve with rectangles are Poirier 16 values and the curve without symbols represents the DH values. The Poirier 16 values slightly ≫ overshoot ≪ the limiting law values below $\kappa a \approx 0.13$. This is confirmed by the MC value, see also Table 15.

RDF for extremely dilute 2:1 electrolytes

In Figure 16, the values of the potentials of mean force W_{++}, W_{--} and W_{+-} multiplied by $t = r/a$ have been plotted vs. $\exp(-\kappa at)$. The regression lines (solid) given by

$$tW_{+-}(t) = 0.05 - 3.153\exp(-\kappa at) \tag{25}$$

$$tW_{++}(t) = 0.105 - 6.118\exp(-\kappa at) \tag{26}$$

and

$$tW_{--}(t) = 0.052 - 1.405\exp(-\kappa at) \tag{27}$$

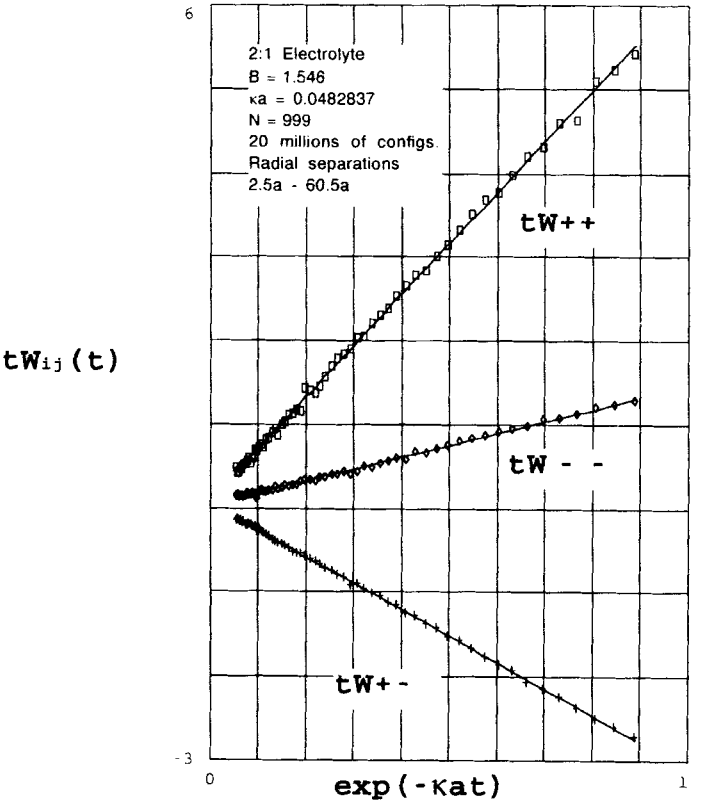

Figure 16 The potentials of mean force (multiplied by t = r/a) in a 2:1 electrolyte with reduced Bjerrum parameter B = 1.546 and $\kappa a = 0.0482837$. The abscissa is $\exp(-\kappa at)$. The points are calculated from the sampled values of the RDF's between t = 2.5 and t = 60.5 after 20 millions of configurations. The number of ions are N = 999. Rectangles calculated from $g_{++}(t)$, diamonds from $g_{--}(t)$ and crosses from $g_{+-}(t)$. The solid straight lines are the regressions (25-27).

fit the points calculated from the sampled values of $g_{+-}(t)$, $g_{++}(t)$ and $g_{--}(t)$ from 2.5a to 60.5a (N = 999, 20 millions of configurations, B = 1.546, $\kappa a = 0.0482837$) very well with correlation coefficients 0.998 − 1.000. Like in the case of z:z electrolytes the ≫ true expression ≪ is probably rather of the biexponential form as in equation (10), but the very long decay length (λ) is practically indeterminable by MC studies.

It is noticed, that $2B = 3.092 \approx 3.153$ and $4B = 6.184 \approx 6.118$. Furthermore, $\exp(\kappa a)/(1 + \kappa a) = 1.00113$ so the DHX and the EXP model are practically indistinguishable. The (generalized) DHX expressions for the RDF's (with B = reduced Bjerrum parameter and common contact distance) are given by:

$$g_{ij}(t) \approx \exp\{z_i z_j [B/t] \cdot [\exp(\kappa a)/(1 + \kappa a)] \cdot \exp(-\kappa at)\} \qquad (28)$$

Figures 17-19 shows that the DHX approximation is quite exact near to contact, where one would intuitively expect the potential of mean force calculated by the Debye-Hückel linearization to be of little value! In the ≫ tail ≪ of the distribution,

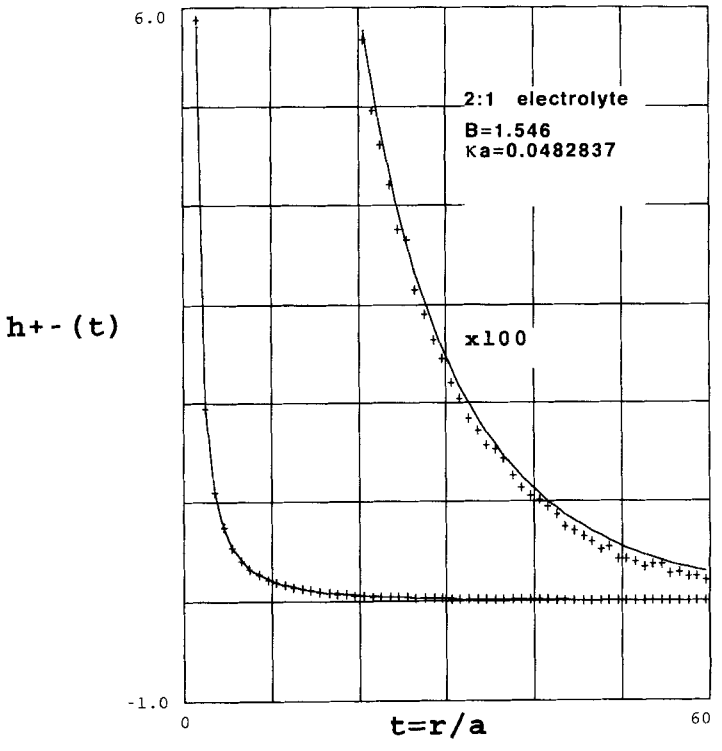

Figure 17 The sampled values (+) of the correlation function $h_{+-}(t)$ as compared with the DHX-values (solid curves) for a 2:1 electrolyte with B = 1.546 and κa = 0.0482837. Near contact the DHX values are practically exact, in the ≫ tail ≪ the percentage deviation becomes appreciable (see the curve with the correlation function magnified by 100). N = 999 and 20 millions of configurations.

the percentage deviations of the correlation functions $h_{+-}(t)$ and $h_{++}(t)$ from the DHX profiles are quite large, however, whereas $h_{--}(t)$ seems almost exact in the whole range from contact to r = 60a.

As with equation (6) for z:z electrolytes, we may define *mean radial distribution functions*, but now there is not only one electroneutral combination but two - one around the doubly charged cation and one around the singly charged anion:

$$G_{+0}(t) \equiv [g_{++}(t) \cdot g_{+-}(t)^2]^{1/3} \tag{29}$$

$$G_{-0}(t) \equiv [g_{+-}(t) \cdot g_{--}(t)^2]^{1/3} \tag{30}$$

As shown in Figure 20 these correlation functions are very close to unity in the whole range of separations. They both have a very slight systematic depression below unity, however, which has not completely vanished at r = 60a. (This depression *might* be due to the periodic boundary conditions and the MI energy cut-off. However, this is not very likely since the half of the edge length of the simulation box L/2 is ≈ 128 units of the contact distance, whereas the radial distribution functions are sampled to at most 60 contact distances). Near to contact this depression

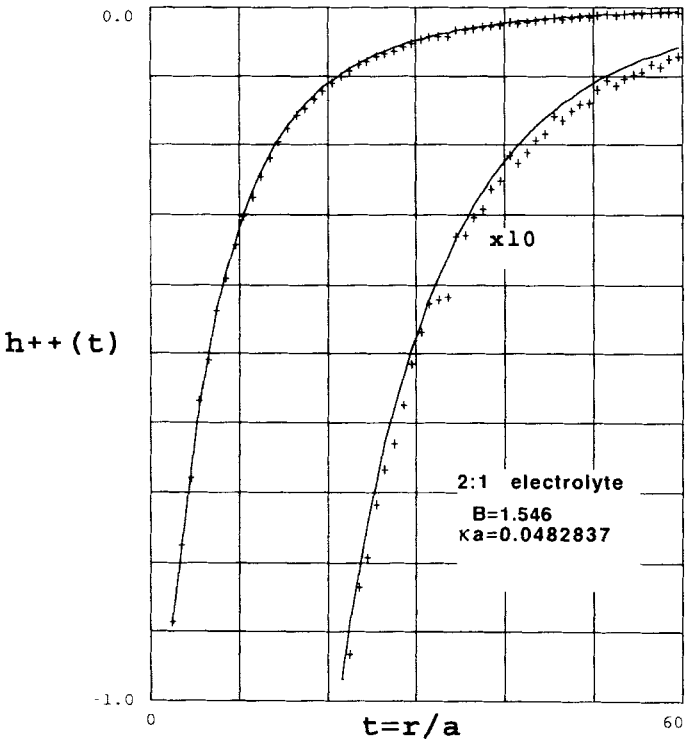

Figure 18 The sampled values (+) of the correlation function $h_{++}(t)$ as compared with the DHX-values (solid curves) for a 2:1 electrolyte with B = 1.546 and κa = 0.0482837. Near contact, the DHX values are practically exact, in the ≫ tail ≪ the percentage deviation becomes appreciable (see the curve with the correlation function magnified by 10). N = 999 and 20 millions of configurations.

is reinforced in the case of $G_{+0}(t)$, indicating a slightly larger repulsion between the cations and/or a slightly smaller attraction between cation and anion than predicted by the DHX model. The opposite is the case for $G_{-0}(t)$. These initial perturbations of the mean RDF's correlate well with the Debye length ≈ 21 a.

In the case of the extremely dilute 2:1 electrolyte with B = 3, we investigate the sampled RDF's with N = 999 ions after 16 millions of configurations. The values are compared to the DHX values in Figures 21-23. The correlation function $h_{+-}(t)$ (Figure 21) is very well described by DHX close to contact, but deviates in the tail in a similar way as for B = 1.546 (Figure 17). The same can be said in the case of $h_{++}(t)$, compare Figures 22 and 18. With the high Bjerrum parameter, $h_{++}(t)$ becomes sigmoid so that there is a small zone around each cation, where there are absolutely no other cations. This is well predicted also by DHX. Figure 23 shows, that $h_{--}(t)$ is quite badly represented by DHX for B = 3, also close to contact, which is in contrast to the situation for B = 1.546 (Figure 19).

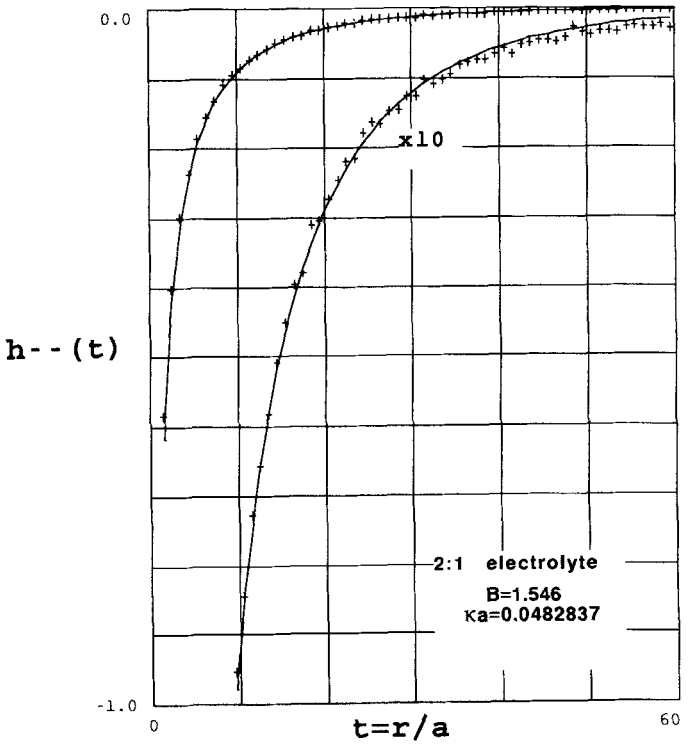

Figure 19 The sampled values (+) of the correlation function h__(t) as compared with the DHX-values (solid curves) for a 2:1 electrolyte with B = 1.546 and κa = 0.0482837. The DHX values seem exact near to contact as well as in the ≫ tail ≪ (see the curve with the correlation function magnified by 10). N = 999 20 millions of configurations.

MODERATELY CONCENTRATED MIXTURES OF MODEL KF AND KCl

As the final case, mixtures of three different (primitive) ions shall be considered. A system will be considered which corresponds approximately to mixtures of KF and KCl with a total ionic strength equal to 1 mol/L. Experimentally, this - and closely related - systems have been studied by Bagg and Rechnitz [28] and by our group [6–7, 29]. Some acceptable fitted values of the ≫ primitive ionic diameters ≪ (including hydration shell) are 0.29 nm for K^+ as well as for Cl^- and 0.34 nm for F^-. A more clear distinction between the individual ionic activities are obtained in a system, where the diameter of the ≫ flouride ion ≪ is increased to 0.37 nm. The latter system will be called the ≫ exaggerated KF-KCl system ≪ to distinguish it from the ≫ normal KF-KCl system ≪. Very recently, the ≫ normal KF-KCl system ≪ was reconsidered by Molero, Outhwaite and Bhuiyan [30] in the light of a ≫ Symmetric Poisson-Boltzmann theory ≪ (SPB).

In Reference [7] a number of simulation results were reported for both of the above mentioned systems, but only the ≫ plain Widom ≪ values of the single ion activity

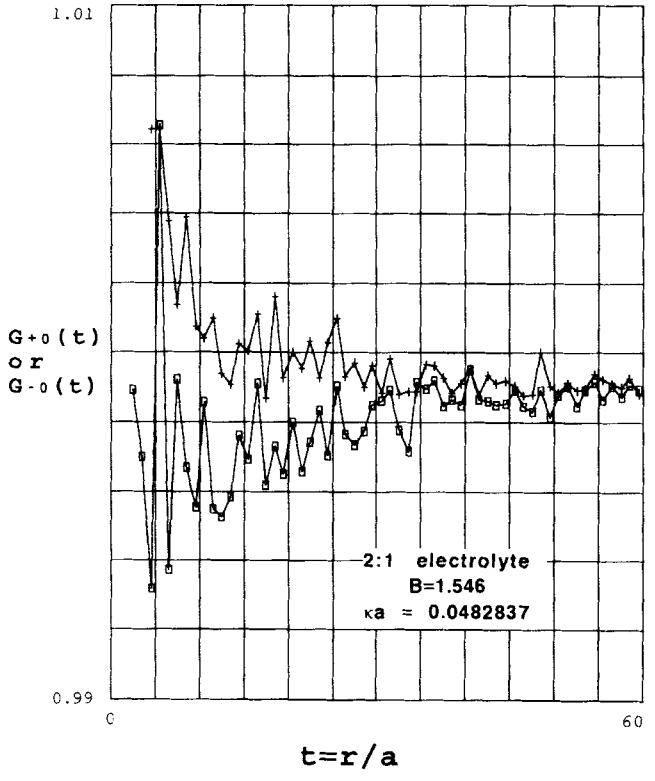

Figure 20 The sampled mean RDF's around the cation ($G_{+0}(t)$, rectangles connected with broken curve) and around the anion ($G_{-0}(t)$, + + + connected with broken curve) for a 2:1 electrolyte with B = 1.546 and κa = 0.0482837. The curves are within 0.5% from unity with a systematic slight depression at large separations. Close to contact, there is an additional depression for $G_{+0}(t)$, whereas $G_{-0}(t)$ exhibits a systematic elevation. N = 999 and 20 millions of configurations.

coefficients were given. The excess energy, the excess heat capacity and the RDF's were not discussed. Furthermore, we did not correct the excess chemical potentials for the three ions to electroneutrality. Instead we made a quite risky extrapolation against $(1/N)^{1/3}$ to estimate the thermodynamic limit. This will be ameliorated here, and furthermore some supplementary long-run MC-simulations with a higher number of ions (N) will be discussed. Some few RDF's will also be presented.

Thermodynamic values

In Table 16, the simulation values of the excess chemical potentials for the ≫ normal ≪ KF-KCl system are given together with the values corrected to electroneutrality. The corresponding values of E_{ex}/NkT and $C_{v,ex}/Nk$ are given in Table 17.

The values of E_{ex}/NkT and $C_{v,ex}/Nk$ - as well as the corrected values of the excess chemical potentials for the ions ($\ln y_i$) - extrapolate to the thermodynamic

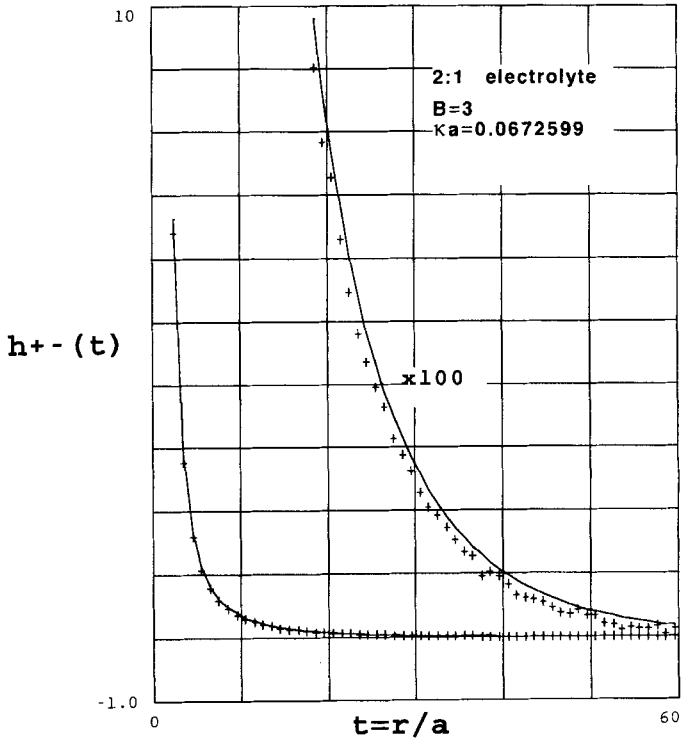

Figure 21 The sampled value (+) of the correlation function $h_{+-}(t)$ as compared with the DHX-values (solid curves) for a 2:1 electrolyte with B = 3 and $\kappa a = 0.0672599$ (N = 999 ions and 16 millions of configurations) Near contact the DHX values are practically exact, in the ≫ tail ≪ the percentage deviation becomes appreciable (see the curve with the correlation function magnified by 100). A plot of $t \cdot W_{+-}(t)$ vs. $\exp(-\kappa at)$ yields the regression curve $0.069 - 5.891 \exp(-\kappa at)$ with a correlation coefficient 1.000 (with t from 2.5 to 60.5).

limit with a leading term proportional to $x^2 = (2/L\kappa a)^2 \sim (1/N)^{2/3}$. All systems mentioned here are sufficiently close to the thermodynamic limit to ensure that the leading term is the only one. Figures 24–28 show examples of these extrapolations. The correlation coefficients of the regressions are in many situations not impressively high. This is a consequence of the fact that mostly only a half million of configurations have been performed. It is clear from the figures, that the correction formulae for finite size are not the same as in the dilute regime (even for the restricted primitive model case of two equally sized ions). This is not unexpected, since we have here that $\kappa a \approx 1$ and the simple physical interpretation of the Debye length and of $2/(L/\kappa a)$ is not possible. This is weighed up by the fact, that a simple linear plot against $(1/N)^{2/3}$ is sufficient for extrapolating even quite small systems to the thermodynamic limit. It is also apparent that the electric parts of lny's do not scale like the excess energies, as was found earlier for simulations for 1:1 and 2:2 electrolytes in the dilute regime, see Reference [11] Figures 6–7. In the present study, the common scaling was shown remove to break down also in the case of dilute 2:1 electrolytes.

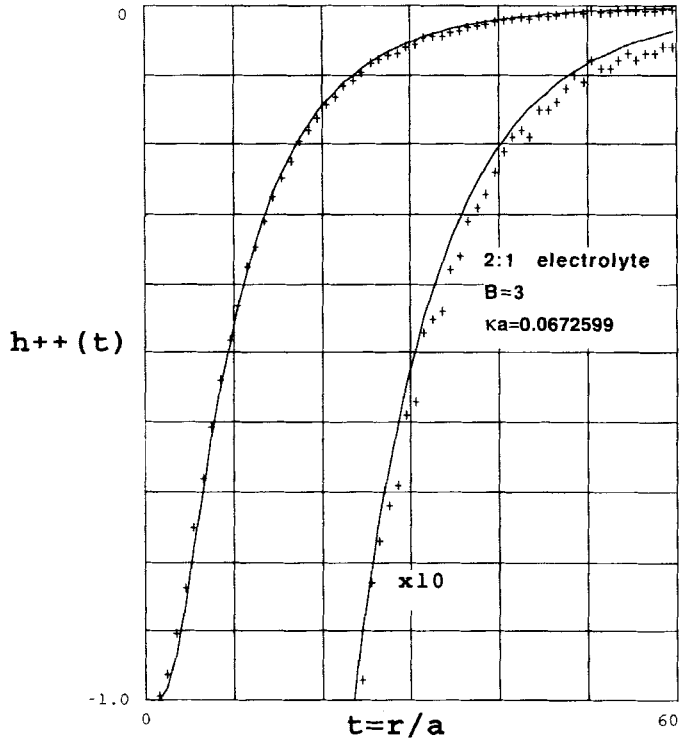

Figure 22 The sampled values (+) of the correlation function $h_{++}(t)$ as compared with the DHX-values (solid curves) for a 2:1 electrolyte with B = 3 and κa = 0.0672599. Near contact the DHX values are practically exact, in the ≫ tail ≪ the percentage deviation becomes appreciable (see the curve with the correlation function magnified by 10). There is a ≫ forbidden zone ≪ from r = a to r ≈ 2a where there are no other cations. (N = 999 ions and 16 millions of configurations).

Tables 18-19 summarize the values of the extrapolated thermodynamic quantities. It is noticed, that no systematic variation of $C_{v,ex}/Nk$ with the mixture ratio can be observed within the quite large uncertainty of this parameter. For the other two parameters, where three values are determined, we have *perfect Harned linearity* (X_{KCl} and X_{KF} are in the following formulae the salt fractions of KCl and of KF in the mixture, and $X_{KCl} = 1 - X_{KF}$):

$$E_{ex}/NkT = -0.6293 - 0.0260X_{KCl} \qquad (r = 1.000) \tag{31}$$

$$\ln y_{K^+} = -0.461 - 0.057X_{KCl} \qquad (r = 1.000) \tag{32}$$

Assuming likewise Harned linearity for the remaining excess chemical potentials (we shall see this to be verified for the ≫ exaggerated ≪ KF/KCl system) we have:

$$\ln y_{Cl^-} = -0.518 - 0.002X_{KF} \tag{33}$$

$$\ln y_{F^-} = -0.448 - 0.004X_{KCl} \tag{34}$$

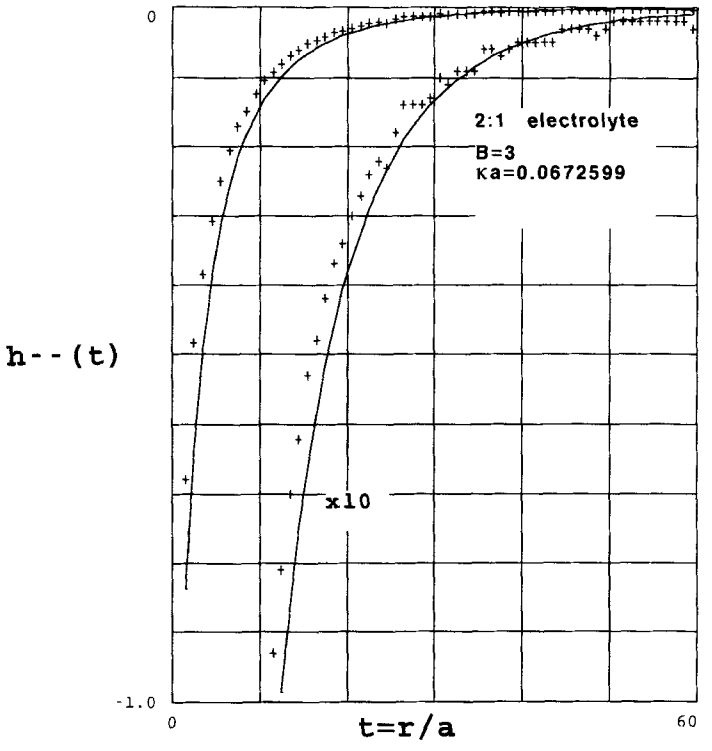

Figure 23 The sampled values (+) of the correlation function $h_{--}(t)$ as compared with the DHX-values (solid curves) for a 2:1 electrolyte with B = 3 and κa = 0.0672599. The DHX values are quite bad in the whole range of radial separations. (N = 999 ions and 16 millions of configurations).

Notice, that there is very little variation in the single-ion activity coefficients of Cl^- and F^-. Indeed, Bagg and Rechnitz [28] found experimentally, that the estimated single-ion activity coefficient of the fluoride ion for mixtures of trace concentrations of NaF in NaCl up to 1 mol/kg or of trace concentrations of KF in KX solutions up to 4 mol/kg (with X = Cl, Br and I) were *the same as in pure NaF, respectively KF solutions at the same ionic strength.* Although such electrochemical $\gg$ measurements $\ll$ of single-ion activities based on the use of salt bridges are always somewhat risky because of the complicated behaviour of the diffusion potential of zones with more than two diffusing ions - see for example References [32–35] - we obtain here the same result for the model KF-KCl system. Furthermore, we see that *also the single-ion activity of the chloride ion remains practically constant.* To obtain directly measurable quantities, we define (dimensionless) *Harned coefficients* in the usual way [36]:

$$\ln\gamma_{\pm}(KCl) = -0.518 - \alpha_{KCl}X_{KF} \tag{35}$$

$$\ln\gamma_{\pm}(KF) = -0.454 - \alpha_{KF}X_{KCl} \tag{36}$$

Thus, we calculate the following Harned coefficients from the extrapolated MC-data:

$$\alpha_{KCl}(MC) \approx -0.028; \qquad \alpha_{KF}(MC) \approx +0.032 \tag{37}$$

The calculated values of the single-ion activity coefficients and the excess energy may be compared to Mean Spherical Approximation (MSA) calculations following the procedure of Ebeling and Scherwinski [31]. This procedure also involves introduction of a neutralising background charge in the derivation of the single-ion activities. Furthermore, the hard sphere contribution is calculated by the generalised Carnahan-Starling formulae of Mansoori *et al.* [37]. Table 20 exhibits the results.

From Table 20 we calculate (perfect Harned linearity is exhibited):

$$E_{ex}(MSA)/NkT = -0.6198 - 0.0213X_{KCl} \qquad (r = 1.000) \tag{38}$$

$$\ln y_{K^+}(MSA) = -0.4642 - 0.0503X_{KCl} \qquad (r = 1.000) \tag{39}$$

$$\ln y_{Cl^-}(MSA) = -0.5144 + 0.0036X_{KF} \qquad (r = 1.000) \tag{40}$$

$$\ln y_{F^-}(MSA) = -0.4452 - 0.0056X_{KCl} \qquad (r = 1.000) \tag{41}$$

Comparison with (31-34) shows that the MSA agrees quite well for E_{ex}/NkT, $\ln y_{K^+}$ and $\ln y_{F^+}$. However, the MSA theory predicts a slight *increase* in $\ln y_{Cl^-}$ with increasing X_{KF} whereas the MC results indicates a slight *decrease* (cf.equation 33).
(The text is continued on p. 437

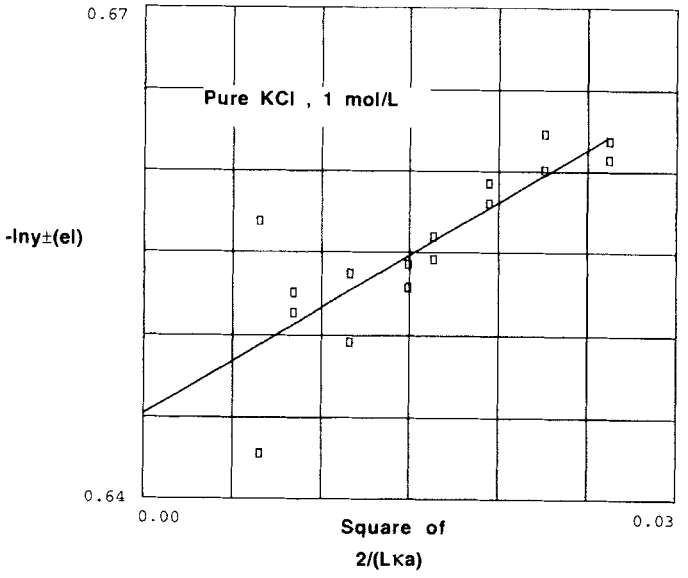

Figure 24 Extrapolation to the thermodynamic limit of the corrected values of the sampled Widom-values of the excess, chemical potentials in pure (model) KCl at 25°C, 1 mol/L and with pressure = osmotic pressure. The hard sphere contribution lny(HS) = 0.1267 has been subtracted to show the electric part $\ln y_{\pm}$(el). For each value of $(2/L\kappa a)^2$ there are two values (one for K^+ and one for Cl^-) which are identical apart from statistical scatter, since the ionic radii are assumed equal. The correlation coefficient of the linear regression with all points included is r = 0.82, and the extrapolated value is $\ln y \pm$(el) = −0.6455. If the two highly scattering values for N = 512 are omitted, the correlation coefficient is r = 0.93 and $\ln y \pm$(el) = − 0.6452 ± 0.0030. The correction formula is then given by: $\ln y_{\pm}(el, N)/\ln y_{\pm}(el,\infty) \approx 1 + 1.001x^2$ (shown).

Table 16 Monte Carlo results for $\ln\gamma_i$ for the ≫ normal ≪ KF-KCl system.

N_{K^+}	N_{Cl^-}	N_{F^-}	*KF/KCl*	$-\ln\gamma_{K^+}$	$-\ln\gamma_{Cl^-}$	$-\ln\gamma_{F^-}$	*B*	ρ^*	*Configurations (millions)*
				(bracketed values corrected to electroneutrality)					
16	0	16	∞	0.2096	-	0.1950	2.26522	0.03765	1.0
				[0.4942]		[0.4796]			
32	0	32	∞	0.2530	-	0.2435	2.26522	0.03765	0.5
				[0.4789]		[0.4694]			
40	0	40	∞	0.2709	-	0.2566	2.26522	0.03765	0.5
				[0.4806]		[0.4663]			
50	0	50	∞	0.2763	-	0.2686	2.26522	0.03765	0.5
				[0.4710]		[0.4633]			
75	0	75	∞	0.2986	-	0.2911	2.26522	0.03765	0.5
				[0.4686]		[0.4611]			
108	0	108	∞	0.3141	-	0.3127	2.26522	0.03765	0.5
				[0.4647]		[0.4633]			
175	0	175	∞	0.3421	-	0.3161	2.26522	0.03765	0.5
				[0.4703		[0.4443]			
256	0	256	∞	0.3682	-	0.3513	2.26522	0.03765	0.67
				[0.4811]		[0.4642]			
500	0	500	∞	0.3679	-	0.3544	2.26522	0.03765	0.5
				[0.4582]		[0.4447]			
50	25	25	1	0.3081	0.3404	0.2742	2.32678	0.03474	0.5
				[0.5028]	[0.5351]	[0.4689]			
70	35	35	1	0.3311	0.3597	0.2951	2.32678	0.03474	0.5
				[0.5051]	[0.5337]	[0.4691]			
80	40	40	1	0.3340	0.3657	0.2978	2.32678	0.03474	0.5
				[0.5004]	[0.5321]	[0.4642]			
108	54	54	1	0.3471	0.3743	0.3109	2.32678	0.03474	0.5
				[0.4977]	[0.5249]	[0.4615]			
180	90	90	1	0.3565	0.4031	0.3333	2.32678	0.03474	0.5
				[0.4835]	[0.5301]	[0.4603]			
256	128	128	1	0.3827	0.4047	0.3345	2.32678	0.03474	0.5
				[0.4956]	[0.5176]	[0.4474]			
32	32	0	0	0.3082	0.3093	-	2.4605	0.02938	0.5
				[0.5341]	[0.5352]				
40	40	0	0	0.3237	0.3259	-	2.4605	0.02938	0.5
				[0.5334]	[0.5356]				
50	50	0	0	0.3379	0.3367	-	2.4605	0.02938	0.5
				[0.5326]	[0.5314]				
65	65	0	0	0.3495	0.3509	-	2.4605	0.02938	0.5
				[0.5279]	[0.5293]				
75	75	0	0	0.3562	0.3576	-	2.4605	0.02938	0.5
				[0.5262]	[0.5276]				
108	108	0	0	0.3723	0.3764	-	2.4605	0.02938	0.5
				[0.5229]	[0.5270]				
175	175	0	0	0.3977	0.3965	-	2.4605	0.02938	0.5
				[0.5259]	[0.5247]				
256	256	0	0	0.4173	0.4032	-	2.4605	0.02938	0.5
				[0.5302]	[0.5161]				

Diameters K^+ ~ 0.29 nm, Cl^- ~ 0.29 nm, F^- ~ 0.34 nm; λ_B = 0.7136 nm; I = 1 mol/L. The mean contact distance (a) is the mean diameter (of 2 or 3 ions), the Bjerrum parameter $B \equiv \lambda_B/a$ and the dimensionless total concentration $\rho^* \equiv a^3\rho_{total}$.

Table 17 MC results for E_{ex}/NkT and $C_{v,ex}/NK$ for the » normal « KF-KCl system.

N	N_{K^+}	N_{Cl^-}	N_{F^-}	L	κa	$x = 2/(L\kappa a)$	$-E_{ex}/NkT$	$C_{v,ex}/Nk$
32	16	0	16	9.472	1.03525	0.2039	0.6458	0.1828
64	32	0	32	11.935	1.03525	0.1619	0.6396	0.1856
80	40	0	40	12.856	1.03525	0.1503	0.6385	0.1895
100	50	0	50	13.849	1.03525	0.1395	0.6355	0.1896
150	75	0	75	15.853	1.03525	0.1219	0.6351	0.1926
216	108	0	108	17.902	1.03525	0.1079	0.6334	0.1993
350	175	0	175	21.027	1.03525	0.0919	0.6328	0.2042
512	256	0	256	23.869	1.03525	0.0809	0.6315	0.1940
1000	500	0	500	29.836	1.03525	0.0648	0.6318	0.2003
100	50	25	25	14.225	1.00786	0.1395	0.6489	0.2097
140	70	35	35	15.913	1.00786	0.1247	0.6478	0.2041
160	80	40	40	16.638	1.00786	0.1193	0.6465	0.1937
216	108	54	54	18.388	1.00786	0.1079	0.6466	0.2082
360	180	90	90	21.802	1.00786	0.0910	0.6450	0.1980
512	256	128	128	24.518	1.00786	0.0809	0.6446	0.2051
64	32	32	0	12.963	0.95309	0.1619	0.6641	0.2109
80	40	40	0	13.964	0.95309	0.1503	0.6622	0.2080
100	50	50	0	15.042	0.95309	0.1395	0.6597	0.2087
130	65	65	0	16.417	0.95309	0.1278	0.6602	0.2045
150	75	75	0	17.219	0.95309	0.1219	0.6597	0.2061
216	108	108	0	19.445	0.95309	0.1079	0.6592	0.2113
350	175	175	0	22.839	0.95309	0.0919	0.6590	0.2135
512	256	256	0	25.926	0.95309	0.0809	0.6566	0.2147

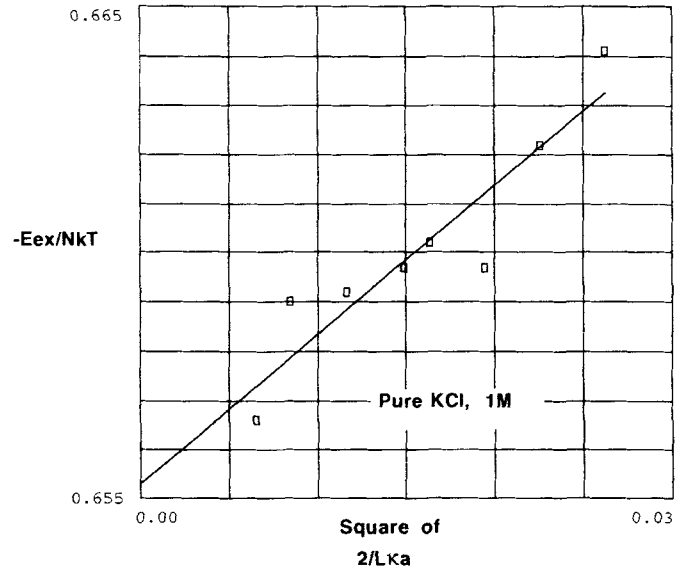

Figure 25 Extrapolation to the thermodynamic limit of $-E_{ex}/NkT$ in pure KCl at 1 mol/L. The regression line has a correlation coefficient r = 0.93 and extrapolates to $E_{ex}(\infty)/NkT = -0.6553 \pm 0.0008$. The correction formula amounts to $E_{ex}(N)/E_{ex}(\infty) \approx 1 + 0.464\ x^2$, which is clearly different from $\ln\gamma_{\pm}(\text{el}, N)/\ln\gamma_{\pm}(\text{el}, \infty) \approx 1 + 1.001x^2$ (see Figure 24).

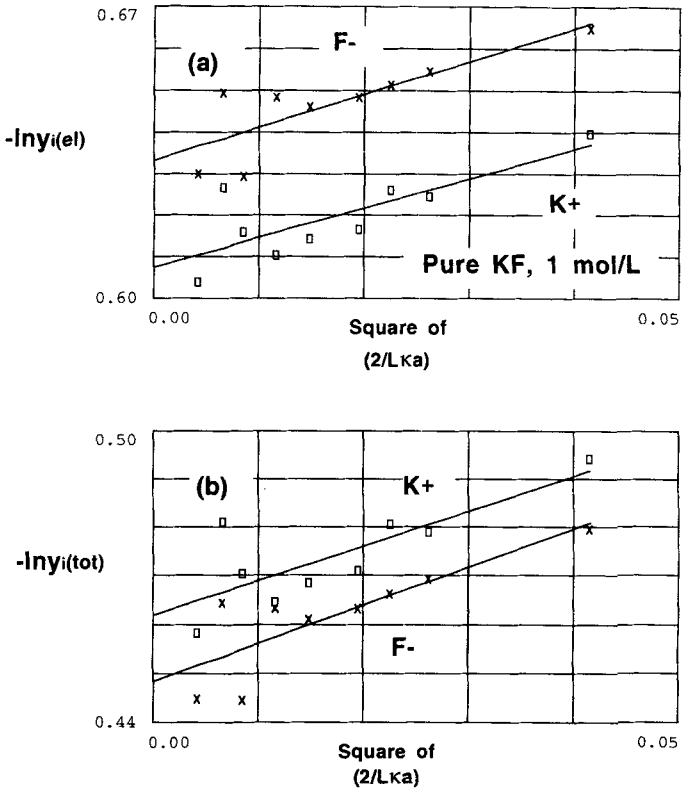

Figure 26 Extrapolation to the thermodynamic limit of the corrected values of the sampled Widom-values of the excess, chemical potentials in pure (model) KF at 25°C, 1 mol/L and osmotic pressure. In (a) the hard sphere contributions $\ln\gamma_{K^+}(HS) = 0.1456$ and $\ln\gamma_{F^-}(HS) = 0.1851$ have been subtracted to show the electric parts of the individual ionic, excess chemical potentials of K^+(rectangles) and F^-(crosses). These clearly separate and extrapolate to $\ln\gamma_{K^+}(el) = -0.607 \pm 0.005$ and to $\ln\gamma_{F^-}(el) = -0.633 \pm 0.007$. The correction formulae (solid lines) are $\ln\gamma_{K^+}(el, N)/\ln\gamma_{K^+}(el, \infty) \approx 1 + 1.179x^2$ and $\ln\gamma_{F^-}(el, N)/\ln\gamma_{F^-}(el, \infty) \approx 1 + 1.248x^2$, respectively. Correlation coefficients 0.79 and 0.83.

In (b) the total excess chemical potentials are plotted. These are quite difficult to separate for the two ions with the given statistical noise. The differences in the electric parts and the hard sphere parts due to the difference in radii seem almost to cancel.

Table 18 Summary of extrapolated Widom results for the ≫ normal ≪ KF-KCl system.

KF / *KCl*	$\ln\gamma_{K^+}(el)$	$\ln\gamma_{Cl^-}(el)$	$\ln\gamma_{F^-}(el)$	$\ln\gamma_{K^+}(HS)$	$\ln\gamma_{Cl^-}(HS)$	$\ln\gamma_{F^-}(HS)$	$\ln\gamma_{K^+}$	$\ln\gamma_{Cl^-}$	$\ln\gamma_{F^-}$
∞	−0.607	-	−0.633	0.1456	-	0.1851	−0.461	-	−0.448
	±0.005		±0.007				±0.005		±0.007
1:1	−0.626	−0.655	−0.624	0.1361	0.1361	0.1739	−0.490	−0.519	−0.450
	±0.008	±0.003	±0.003				±0.008	±0.003	±0.003
0	−0.645	−0.645	-	0.1267	0.1267	-	−0.518	−0.518	-
	±0.003	±0.003					±0.003	±0.003	

Hard sphere contributions calculated from generalised Carnahan-Starling [31] or from Equations (11-12) for pure KCl.

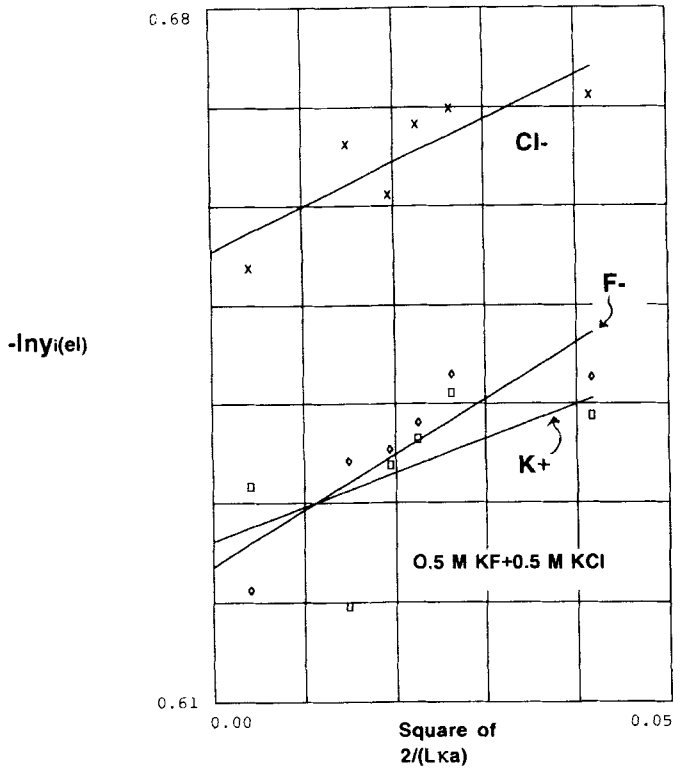

Figure 27 Extrapolation to the termodynamic limit of the corrected values of the sampled Widom-values of the excess, chemical potentials in the ≫ normal ≪ KF-KCl system at 25°C, total ionic strength 1 mol/L with 50% KF and 50% KCl at osmotic pressure. The hard sphere contributions $\ln\gamma_{K^+}(HS) = 0.1361$, $\ln\gamma_{Cl^-}(HS) = 0.1361$ and $\ln\gamma_{F^-}(HS) = 0.1739$ have been subtracted to show the electric parts of the individual ionic, exces chemical potentials of K^+ (rectangles), of Cl^- (crosses) and of F^- (diamonds). These extrapolate to $\ln\gamma_{K^+}(el) = -0.626 \pm 0.008$, $\ln\gamma_{Cl^-}(el) = -0.655 \pm 0.003$ and $\ln\gamma_{F^-}(el) = -0.624 \pm 0.003$. The correction formulae (solid lines) are $\ln\gamma_{K^+}(el, N)/\ln\gamma_{K^+}(el, \infty) \approx 1 + 0.559x^2$, $\ln\gamma_{Cl^-}(el, N)/\ln\gamma_{Cl^-}(el, \infty) \approx 1 + 0.683\,x^2$ and $\ln\gamma_{F^-}(el, N)/\ln\gamma_{F^-}(el, \infty) \approx 1 + 0.910\,x^2$ respectively. Correlation coefficients 0.57, 0.85 and 0.88.

Table 19 Extrapolated E_{ex}/NkT and $C_{v,ex}/Nk$ results for the ≫ normal ≪ KF-KCl system. (r = correlation coefficient).

KF/KCl	E_{ex}/NkT	$C_{v,ex}/NkT$
∞	−0.6293 ± 0.0007	0.202 ± 0.005
	(r = 0.990)	(r = 0.870)
1:1	−0.6424 ± 0.0005	0.203 ± 0.007
	(r = 0.978)	(mean value §)
0	−0.6553 ± 0.0008	0.210 ● 0.005
	(r = 0.927)	(mean value ¶)

§ The linear regression has r = 0.26. ¶ The linear regression has r = 0.49.

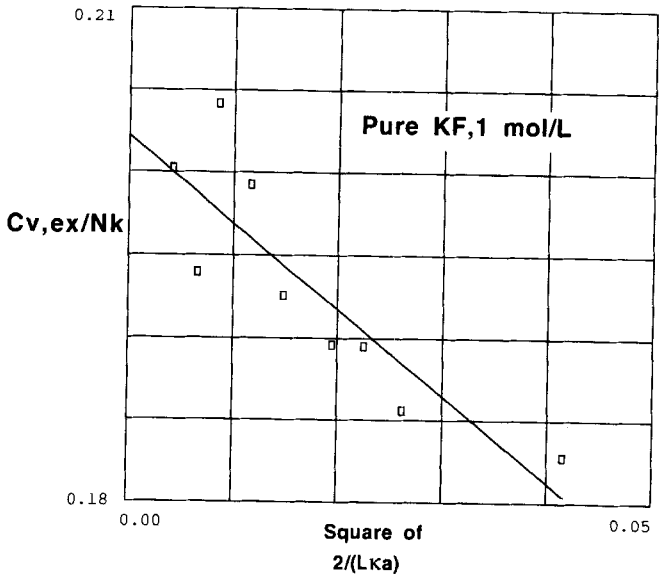

Figure 28 Extrapolation to the thermodynamic limit of the values of the sampled exces heat capacity of constant volume in the case of pure 1 mol/L KF. The extrapolated value is 0.202 ± 0.005. The correction formula for finite size is $C_{v,ex}(N)/C_{v,ex}(\infty) \approx 1 - 2.59x^2$ (solid line). Correlation coefficient r = 0.87.

Table 20 MSA values of thermodynamic quantities for the ≫ normal ≪ KF-KCl system.

X_{KCl}	E_{ex}/NkT	$lny_{K^+}(el)$	$lny_{K^+}(HS)$	$lny_{Cl^-}(el)$	$lny_{Cl^-}(HS)$	$lny_{F^-}(el)$	$lny_{F^-}(HS)$
0.001	−0.61983	−0.60974	+0.14555	−0.65632	+0.14555	−0.63035	+0.18512
0.5	−0.63035	−0.62546	+0.13609	−0.64873	+0.13609	−0.62196	+0.17390
0.999	−0.64107	−0.64106	+0.12670	−0.64110	+0.12670	−0.61355	+0.16276

Nevertheless, both set of values support the thesis, that the variations of the single-ion activity coefficients of F^- and Cl^- are an order of magnitude less than the variation of the activity coefficient of K^+. The Harned expressions for the MSA model are in very good agreement with the MC expressions (35–37):

$$\ln y_{\pm}(KCl, MSA) = -0.5144 - \alpha_{KCl,MSA} X_{KF} \tag{42}$$

$$\ln y_{\pm}(KF, MSA) = -0.4547 - \alpha_{KF,MSA} X_{KCl} \tag{43}$$

$$\alpha_{KCl}(MSA) = -0.0270; \qquad \alpha_{KF}(MSA) = +0.0279 \tag{44}$$

The two mean ionic *trace activity coefficients* are given as:

$$\ln y_{\pm}(KCl, trace, MC) \approx -0.490; \qquad \ln y_{\pm}(KF, trace, MC) \approx -0.486 \tag{45}$$

$$\ln y_{\pm}(KCl, trace, MSA) = -0.4874; \qquad \ln y_{\pm}(KF, trace, MSA) = -0.4826 \tag{46}$$

These values are almost equal, and both set of values satisfy the rule of thumb stated in the monograph of Robinson and Stokes [36] that the trace activity coefficients tend to be (almost) equal for the two salts at constant ionic strength.

Molero, Outhwaite and Bhuiyan [30] have made calculations for the present system using the so-called symmetric Poisson-Boltzmann (SPB) approximation for the electric parts of the excess chemical potentials. The hard sphere parts were estimated as here. For 1 mol/L total ionic strength, they obtained (see [30] Figure 8 and Table 5):

$$\ln\gamma_{\pm}(KCl, SPB) = -0.482 - \alpha_{KCl,SPB}X_{KF} \quad (47)$$

$$\ln\gamma_{\pm}(KF, SPB) = -0.419 - \alpha_{KF,SPB}X_{KCl} \quad (48)$$

$$\alpha_{KCl}(SPB) = -0.0281; \qquad \alpha_{KF}(SPB) = +0.0297 \quad (49)$$

It is seen, that $\alpha_{KCl}(SPB) \approx \alpha_{KCl}(MSA) \approx \alpha_{KCl}(MCA) \approx -0.028$, whereas $\alpha_{KF}(SPB) \approx +0.030$ is midway between $\alpha_{KF}(MSA) \approx +0.028$ and $\alpha_{KF}(MC) \approx +0.032$. In that way the SPB is better than the MSA. However, the SPB is shifted towards too low absolute values. For example, $-\ln\gamma_{\pm}$(KCl, SPB, pure) = 0.482 as compared to $-\ln\gamma_{\pm}$(KCl, MC, pure) ≈ 0.518 and $-\ln\gamma_{\pm}$(KCl, MSA, pure) = 0.5144, and also $-\ln\gamma_{\pm}$(KCl, SPB, trace) = 0.454 as compared to $-\ln\gamma_{\pm}$(KCl, MC, trace) = 0.490 and $-\ln\gamma_{\pm}$(KCl, MSA, trace) = 0.4874.

Similarly, we have $-\ln\gamma_{\pm}$(KF, SPB, pure) = 0.419 as compared to $-\ln\gamma_{\pm}$(KF, MC, pure) ≈ 0.454 and $-\ln\gamma_{\pm}$(KF, MSA, pure) = 0.4547, and also $-\ln\gamma_{\pm}$(KF, SPB, trace) = 0.4487 as compared to $-\ln\gamma_{\pm}$(KF, MC, trace) = 0.486 and $-\ln\gamma_{\pm}$(KF, MSA, trace) = 0.4826. In all cases, the SPB model yields too small results in absolute values. This shift is also obvious in regarding Figure 8 in Reference [30]. In Reference [30] some comfort was seeked in the finding that the trace activity coefficients of SPB were closer to our previous MC-extrapolations from Reference [7] than the MSA values. However, with the more accurate extrapolations performed in the present paper, this is not the case anymore, and the MSA seems to be a very well functioning model for 1:1:1 mixtures at such moderately concentrated systems.

In Table 21, the variation of the Harned coefficients with varying total ionic strength (I) - as predicted by the MSA and the SPB theories - is shown. Table 21 should replace Table 1 in Reference [7] - where the MSA values were erroneously stated in all other cases than the I = 1 M case as remarked by Molero, Outhwaite and Bhuiyan [30] - and it should also replace Table 5 in Reference [30], where the stated MC Harned coefficients α_{KCl}(MC) = −0.050 ± 0.011 and α_{KF}(MC) = +0.008 ± 0.017 should now be replaced with the better ones obtained here. (All the MSA calculations have been checked independently by reprogramming the voluminous Mansoori-Ebeling formulae in Pascal as well as MathCad). The sums of the two Harned coefficients are tabulated as a check of the thermodynamic consistency, since this sum should be proportional to the ionic strength, because of the Maxwell identity of the cross derivatives of the chemical potentials [36].

Table 21 Harned coefficients by MC, MSA and SPB for ≫ normal ≪ KF-KCl mixtures.

I (*mol/L*)	α_{KCl} (*MC*)	α_{KF} (*MC*)	*Sum* (*MC*)	α_{KCl} (*MSA*)	α_{KF} (*MSA*)	*Sum* (*MSA*)	α_{KCl} (*SPB*)	α_{KF} (*SPB*)	*Sum* (*SPB*)
0.5	-	-	-	−0.0149	+0.0152	+0.0003	−0.0161	+0.0168	+0.0007
1.0	−0.028	+0.032	+0.004	−0.0270	+0.0279	+0.0009	−0.0281	+0.0297	+0.0016
1.5	-	-	-	−0.0390	+0.0409	+0.0019	−0.0399	+0.0428	+0.0029
2.0	-	-	-	−0.0516	+0.0547	+0.0031	−0.0522	+0.0564	+0.0042

This is not so. Plotting the sums against the total ionic strength, one obtains a curve through I = 0 with upward curvatures. The MSA is deviating more from a straight line than the SPB. Thus, these models are not consistent which is not surprising, since they are approximations! We have:

$$\alpha_{KCl}(MSA) + \alpha_{KF}(MSA) \approx 0.0003\,\mathrm{I} + 0.0006\,\mathrm{I}^2 \tag{50}$$

$$\alpha_{KCl}(SPB) + \alpha_{KF}(SPB) \approx 0.0012\,\mathrm{I} + 0.0004\,\mathrm{I}^2 \tag{51}$$

If the MC results are really exact, we should predict

$$\alpha_{KCl}(MC) + \alpha_{KF}(MC) \approx 4.10^{-3}\,\mathrm{I} \tag{52}$$

for similar MC calculations at other ionic strengths. To demonstrate this is left as a challenge for the future.

We now pass to exactly similar calculations for the ≫ exaggerated ≪ KF-KCl system, where the total ionic strength is also 1 mol/L, but the diameter of the ≫ fluoride ion ≪ is increased from 0.34 nm to 0.37 nm (the diameters of the potassium and the chloride ion still being 0.29 nm). Tables 22-23 exhibit the MC results for $\ln\gamma_i$, E_{ex}/NkT and $C_{v,ex}/Nk$. Tables 24-25 show the extrapolated values. The corresponding MSA values are found in Table 26. Figures with examples of extrapolations will not be shown, since they look similar to the extrapolations shown in Figures 29-33 for the ≫ normal ≪ KF-KCl system.

Harned linearity is found in all the thermodynamic quantities (now also in the exces heat capacity):

$$E_{ex}/NkT = -0.6163 - 0.0388\,X_{KCl} \qquad (r = 0.999) \tag{53}$$

$$C_{V,ex}/Nk = 0.183 + 0.026\,X_{KCl} \qquad (r = 0.996) \tag{54}$$

$$\ln\gamma_{K^+} = -0.426 - 0.094\,X_{KCl} \qquad (r = 0.994) \tag{55}$$

$$\ln\gamma_{Cl^-} = -0.516 - 0.017\,X_{KF} \qquad (r = 0.953) \tag{56}$$

$$\ln\gamma_{F^+} = -0.418 + 0.002\,X_{KCl} \qquad (r = 0.884) \tag{57}$$

It is seen once again that the fluoride activity coefficient is practically independent of the salt fraction, whereas the chloride activity coefficient varies somewhat, though much less than the potassium activity coefficient. For the mean ionic activity coefficients one obtains the following Harned relations:

$$\ln\gamma_{\pm}(\mathrm{KCl}) = -0.518 - \alpha_{KCl}X_{KF}; \qquad \alpha_{KCl} = -0.035 \qquad (r = 0.993) \tag{58}$$

$$\ln\gamma_{\pm}(\mathrm{KF}) = -0.422 - \alpha_{KF}X_{KCl}; \qquad \alpha_{KF} = +0.047 \qquad (r = 0.992) \tag{59}$$

In Table 26 the MSA values of E_{ex}/NkT and the single-ion exces chemical potentials are shown for the ≫ exaggerated system ≪. Perfect Harned linearity is obtained for all thermodynamic quantities:

$$E_{ex}(MSA)/NkT = -0.6083 - 0.0327\,X_{KCl} \tag{60}$$

$$\ln\gamma_{K^+}(MSA) = -0.4320 - 0.0825\,X_{KCl} \tag{61}$$

$$\ln\gamma_{Cl^-}(MSA) = -0.5145 + 0.0065\,X_{KF} \tag{62}$$

$$\ln\gamma_{F^-}(MSA) = -0.3985 - 0.0123\,X_{KCl} \tag{63}$$

Table 22 Monte Carlo results for $\ln\gamma_i$ for the ≫ exaggerated ≪ KF-KCl system.

N_{K^+}	N_{Cl^-}	N_{F^-}	*KF/KCl*	$-\ln\gamma_{K^+}$	$-\ln\gamma_{Cl^-}$	$-\ln\gamma_{F^-}$	*B*	ρ^*	*Configurations (millions)*
				(bracketed values corrected to electroneutrality)					
40	0	40	∞	0.2310	-	0.2113	2.16225	0.04329	0.5
				[0.4407]		[0.4210]			
50	0	50	∞	0.2544	-	0.2240	2.16225	0.04329	0.5
				[0.4491]		[0.4187]			
75	0	75	∞	0.2637	-	0.2477	2.16225	0.04329	0.5
				[0.4337]		[0.4177			
108	0	108	∞	0.2865	-	0.2647	2.16225	0.04329	0.5
				[0.4371]		[0.4153]			
175	0	175	∞	0.2988	-	0.2896	2.16225	0.04329	0.5
				[0.4270]		[0.4178]			
256	0	256	∞	0.3095	-	0.3064	2.16225	0.04329	0.5
				[0.4224]		[0.4193]			
500	0	500	∞	0.3456	-	0.3289	2.16225	0.04329	0.5
				[0.4360]		[0.4193]			
65	5	60	12	0.2678	0.3521	0.2381	2.2533	0.03825	0.78
				[0.4461]	[0.5304]	[0.4164]			
130	10	120	12	0.3007	0.3846	0.2670	2.2533	0.03825	0.5
				[0.4423]	[0.5262]	[0.4086]			
195	15	180	12	0.3148	0.4020	0.2930	2.2533	0.03825	0.5
				[0.4385]	[0.5257]	[0.4167]			
260	20	240	12	0.3206	0.4223	0.2952	2.2533	0.03825	0.5
				[0.4329]	[0.5346]	[0.4075]			
325	25	300	12	0.3438	0.4327	0.3208	2.2533	0.03825	0.5
				[0.4481]	[0.5370]	[0.4251]			
494	38	456	12	0.351944	0.435126	0.325165	2.2533	0.03825	4.0
				[0.442657]	[0.525839]	[0.415878]			
494	38	456	12	0.1549728	0.1549728	0.2246418	0 (NB!)	0.03825	4.0
32	16	16	1	0.2690	0.3081	0.2018	2.2533	0.03825	0.5
				[0.4949]	[0.5340]	[0.4277]			
40	20	20	1	0.2786	0.3248	0.2171	2.2533	0.03825	0.64
				[0.4883]	[0.5345]	[0.4268]			
50	25	25	1	0.2940	0.3406	0.2299	2.2533	0.03825	0.6
				[0.4887]	[0.5353]	[0.4246]			
70	35	35	1	0.3156	0.3511	0.2434	2.2533	0.03825	0.5
				[0.4896]	[0.5251]	[0.4174]			
80	40	40	1	0.3192	0.3671	0.2546	2.2533	0.03825	0.5
				[0.4856]	[0.5335]	[0.4210]			
108	54	54	1	0.3274	0.3748	0.2749	2.2533	0.03825	0.5
				[0.4780]	[0.5254]	[0.4255]			
180	90	90	1	0.3616	0.4034	0.2970	2.2533	0.03825	0.5
				[0.4886]	[0.5304]	[0.4240]			
256	128	128	1	0.3661	0.4247	0.3031	2.2533	0.03825	0.5
				[0.4790]	[0.5376]	[0.4160]			
500	250	250	1	0.39231	0.43237	0.32801	2.2533	0.03825	4.06
				[0.48266]	[0.52272]	[0.41836]			
52	48	4	1/12	0.32924	0.33979	0.23446	2.2533	0.03825	1.54
				[0.52136]	[0.53191]	[0.42658]			
65	60	5	1/12	0.3455	0.3491	0.2415	2.2533	0.03825	0.58
				[0.5238]	[0.5274]	[0.4198]			
130	120	10	1/12	0.3759	0.3936	0.2879	2.2533	0.03825	0.5
				[0.5175]	[0.5352]	[0.4295]			
195	180	15	1/12	0.3874	0.4024	0.2972	2.2533	0.03825	0.5
				[0.5111]	[0.5261]	[0.4209]			
260	240	20	1/12	0.4042	0.4194	0.3072	2.2533	0.03825	0.5
				[0.5165]	[0.5317	[0.4195]			
325	300	25	1/12	0.4175	0.4112	0.3160	2.2533	0.03825	0.5
				[0.5218]	[0.5155]	[0.4203]			
494	456	38	1/12	0.41914	0.41766	0.32044	2.2533	0.03825	3.8
				[0.50985]	[0.50837]	[0.41115]			

Table 23 MC results for E_{ex}/NkT and $C_{v,ex}/Nk$ for the ≫ exaggerated ≪ KF-KCl system.

N	N_{K^+}	N_{Cl^-}	N_{F^-}	L	κa	$x = 2/(L\kappa a)$	$-E_{ex}/NkT$	$C_{v,ex}/Nk$
80	40	0	40	12.272	1.08455	0.1503	0.6245	0.1754
100	50	0	50	13.219	1.08455	0.1395	0.6218	0.1790
150	75	0	75	15.132	1.08455	0.1219	0.6215	0.1743
216	108	0	108	17.088	1.08455	0.1079	0.6191	0.1873
350	175	0	175	20.070	1.08455	0.0919	0.6188	0.1934
512	256	0	256	22.784	1.08455	0.0809	0.6178	0.1795
1000	500	0	500	28.480	1.08455	0.0647	0.6178	0.1752
130	65	5	60	15.035	1.04071	0.1278	0.6255	0.1841
260	130	10	120	18.943	1.04071	0.1014	0.6208	0.1870
390	195	15	180	21.684	1.04071	0.0886	0.6232	0.1754
520	260	20	240	23.867	1.04071	0.0805	0.6221	0.1906
650	325	25	300	25.710	1.04071	0.0747	0.6212	0.1842
988	494	38	456	29.560	1.04071	0.06501	0.62100	0.1832
64	32	16	16	11.872	1.04071	0.1619	0.6447	0.1948
80	40	20	20	12.789	1.04071	0.1503	0.6442	0.1886
100	50	25	25	13.776	1.04071	0.1395	0.6417	0.1951
140	70	35	35	15.411	1.04071	0.1247	0.6404	0.1942
160	80	40	40	16.113	1.04071	0.1193	0.6405	0.1982
216	108	54	54	17.808	1.04071	0.1079	0.6419	0.1924
360	180	90	90	21.120	1.04071	0.0910	0.6388	0.1880
512	256	128	128	23.744	1.04071	0.0809	0.6385	0.2062
1000	500	250	250	29.679	1.04071	0.06475	0.63721	0.1957
104	52	48	4	13.957	1.04071	0.1377	0.6580	0.2076
130	65	60	5	15.035	1.04071	0.1278	0.6579	0.2023
260	130	120	10	18.943	1.04071	0.1014	0.6531	0.2083
390	195	180	15	21.684	1.04071	0.0886	0.6534	0.1965
520	260	240	20	23.867	1.04071	0.0805	0.6546	0.1957
650	325	300	25	25.710	1.04071	0.0747	0.6529	0.2205
988	494	456	38	29.560	1.04071	0.06501	0.65378	0.2089

Diameters K^+ ~ 0.29 nm, Cl^- ~ 0.29 nm, F^- ~ 0.37 nm; λ_B = 0.7136 nm; I = 1 mol/L. The mean contact distance (a) is the mean diameter (of 2 or 3 ions), Bjerrum parameter $B \equiv \lambda_B/a$ and the dimensionless total concentration $\rho^* \equiv a^3 \rho_{total}$.

Table 25 Extrapolated E_{ex}/NkT and $C_{v,ex}/Nk$ results for the ≫ exaggerated ≪ KF-KCl system.

KF/KCl	E_{ex}/NkT	$C_{v\,ex}/Nk$
∞	−0.6157 ± 0.0007	0.184 ± 0.005
12:1	−0.6196 ± 0.0009	0.184 ± 0.005
1:1	−0.6363 ± 0.0005	0.198 ± 0.005
1:12	−0.6514 ± 0.0007	0.207 ± 0.007
0	−0.6553 ● 0.0008	0.210 ± 0.005

Table 26 MSA values for the ≫ exaggerated ≪ KF-KCl system.

X_{KCl}	E_{ex}/NkT	$lny_{K^+}(el)$	$lny_{K^+}(HS)$	$lny_{Cl^-}(el)$	$lny_{Cl^-}(HS)$	$lny_{F^-}(el)$	$lny_{F^-}(HS)$
0.001	−0.60842	−0.59055	+0.15860	−0.66647	+0.15860	−0.62734	+0.22889
1/13	−0.61083	−0.59444	+0.15615	−0.66456	+0.15615	−0.62513	+0.22569
0.5	−0.62449	−0.61595	+0.14257	−0.65385	+0.14257	−0.61277	+0.20799
12/13	−0.63850	−0.63724	+0.12912	−0.64306	+0.12912	−0.60036	+0.19050
0.999	−0.64106	−0.64104	+0.12672	−0.64112	+0.12672	−0.59813	+0.18739

Table 24 Summary of extrapolated Widom results for the ≫ exaggerated ≪ KF-KCl system.

$\frac{KF}{KCl}$	lny_{K^+} (el)	lny_{Cl^-} (el)	lny_{F^-} (el)	lny_{K^+} (HS)	lny_{Cl^-} (HS)	lny_{F^-} (HS)	lny_{K^+}	lny_{Cl^-}	lny_{F^-}
∞	−0.579 ±0.007	-	−0.647 ±0.002	0.1586	-	0.2289	−0.420 ±0.007	-	−0.418 ±0.002
12	−0.594 ±0.005	−0.687 ±0.005	−0.643 ±0.005	0.1562	0.1562	0.2257	−0.438 ±0.005	−0.531 ±0.005	−0.417 ±0.005
	(−0.593	−0.686	−0.642)	(MC:0.1550	0.1550	0.2246)	(B = 0 simulation)		
1	−0.621 ±0.005	−0.670 ±0.007	−0.625 ±0.003	0.1426	0.1426	0.2080	−0.478 ±0.005	−0.527 ±0.007	−0.417 ±0.003
1/12	−0.641 ±0.005	−0.644 ±0.007	−0.607 ±0.007	0.1291	0.1291	0.1905	−0.512 ±0.005	−0.515 ±0.007	−0.416 ±0.007
0	−0.645 ±0.003	−0.645 ±0.003	-	0.1267	0.1267	-	−0.518 ±0.003	−0.518 ±0.003	-

Hard sphere (HS) contributions calculated by the formulae in References [31] and [37]. One MC simulation given for comparison (Values for B = 0 in Table 22).

$$\ln\gamma_{\pm}(KCl, MSA) = -0.5145 - \alpha_{KCl,MSA}X_{KF} \quad (64)$$

$$\alpha_{KCl,MSA} = -0.0445 \quad (65)$$

$$\ln\gamma_{\pm}(KF, MSA) = -0.4152 - \alpha_{KF,MSA}X_{KCl} \quad (66)$$

$$\alpha_{KF,MSA} = +0.0474 \quad (67)$$

The Harned coefficient is α_{KF} is very well predicted by the MSA theory, but the coefficient $\alpha_{KCl,MSA}$ is too high compared to the MC result. In the ≫ normal ≪ KF-KCl system, the situation was just the reverse. The MSA-values of the $\ln\gamma\pm$ of the pure salts are acceptable. We have the following mean ionic trace activity coefficients:

$$\ln\gamma_{\pm}(KCl, trace, MC) = -0.483 \pm 0.005; \quad \ln\gamma_{\pm}(KF, trace, MC) = -0.469 \pm 0.005 \quad (68)$$

$$\ln\gamma_{\pm}(KCl, trace, MSA) = -0.4700; \quad \ln\gamma_{\pm}(KF, trace, MSA) = -0.4626 \quad (69)$$

These are also acceptably predicted by MSA. However, the details are not well predicted. For example it appears from (56) that $\ln\gamma_{Cl^-}$ *decreases* with *increasing* X_{KF}, but MSA predicts a (small) *increase* with X_{KF}- see equation (62). The same feature was found for the ≫ normal ≪ KF-KCl system.

For the exaggerated system, the MC value of the fluouride activity coefficient varies very little, and the chloride activity coefficient somewhat more, equations. (56–57). The MSA predicts just the reverse, see equations (62–63). In short, the MSA theory is only a fair approximation and cannot predict properly details in the variation of single ion activities or even Harned coefficients. There seems to be no short circuit to bypass detailled MC studies here.

Some sampled RDF's for the ≫ exaggerated ≪ KF-KCl system

In the KF-KCl primitive model electrolyte system, there are the following 6 RDF's: $g_{KCl}(r)$, $g_{KF}(r)$, $g_{KK}(r)$, $g_{FF}(r)$, $g_{ClCl}(r)$, $g_{FCl}(r)$. Thus, a presentation of all the sampled RDF's in all the cases simulated here is out of scope. One example is selected, namely the ≫ exaggerated ≪ KF-KCl system with 494 K^+ ions, 38 Cl^- ions, and 456 F^- ions. The simulation of this system was carried out to 4 millions of configurations, and the RDF's were also simulated for the same system with all charges removed (B = 0, see Table 22). This makes possible an estimation of the hard sphere contribution to the RDF.

Figures 29–34 show the simulated values of the 6 RDF's (in the form of dimensionless potentials of mean force). The curves with crosses connected with broken lines correspond to the potential of mean force between chargeless particles of the same sizes and in the same proportions. A zone near contact with the usual ≫ attractive ≪ potential for hard spheres is clearly identified in all figures. The hard sphere contribution is small compared to the electric contribution, but it is not negligible near to contact. The electric potential of mean force is defined as the difference between the total and the hard sphere potential of mean force, i.e.

$$W_{tot,ij}(r) = W_{el,ij}(r) + W_{HS,ij}(r) \quad i\,\&\,j = K, Cl, F \quad (70)$$

$$g_{tot,ij}(r) = exp(-W_{tot,ij}) = g_{el,ij}(r)\cdot g_{HS,ij}(r) \quad (71)$$

In Figures 29-34 the calculated electric contributions to the potential of mean force in 60 equally spaced spherical shells between contact and r ≈ 7a are indicated by rectangles. The solid smooth curves are calculated by the (generalized) DHX formula:

$$W_{el,DHX,ij}(t) = \pm B\,[\exp(\kappa a_{ij})/(1 + \kappa a_{ij})] \cdot [\exp(-\kappa a t)/t] \qquad (72)$$

The radial separation t is measured in units of a, which is the mean contact distance of the ions in the mixture, and a_{ij} is the contact distance between ions of species i and j. The Bjerrum parameter B is the Bjerrum length divided by the mean contact distance. The + sign should be applied for ions of the same sign, whereas the minus is for ions of opposite sign. In other words we have (generalizing to mixtures of ions of any valency):

$$W_{el,DHX,ij}(r) = z_i z_j\,[e_0^2/(4\pi\varepsilon kT)] \cdot [\exp(\kappa a_{ij})/(1 + \kappa a_{ij})] \cdot [\exp(-\kappa r)/r] \qquad (73)$$

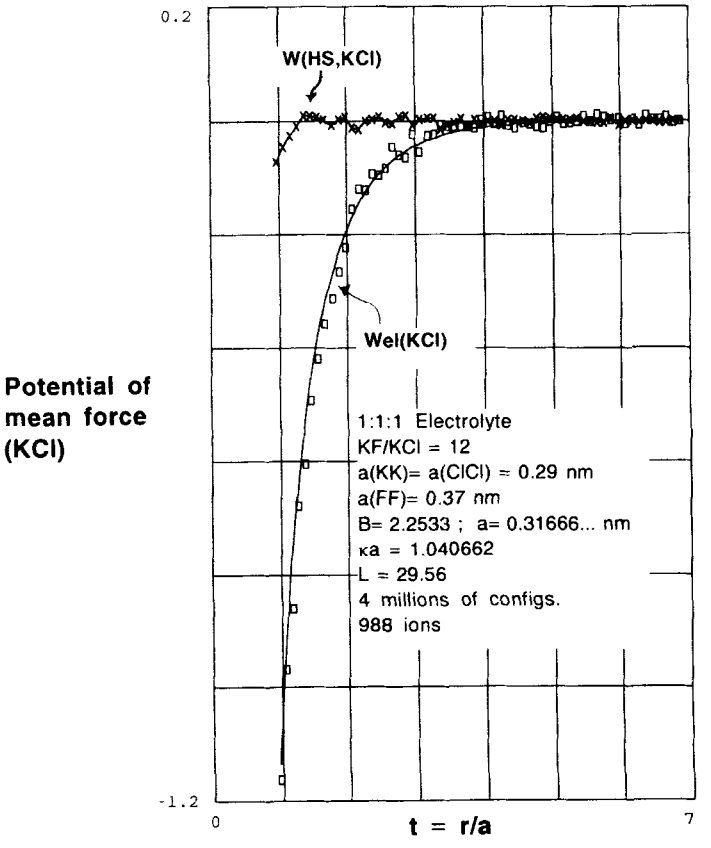

Figure 29 The hard sphere (HS, x-x-x-x) and the electric (el, rectangles) contributions to the dimensionless potential of mean force between the ions K^+ and Cl^- calculated from simulated data for the RDF. The values for W(HS, KCl) is calculated from the simulated RDF in a system with B = 0. The values for W_{el}(KCl) are calculated from the simulated RDF for B = 2.2533 by means of equation (70). The smooth solid curve are the DHX values calculated by equation (72): $W_{el,DHX}(KCl) = -2.9923 \cdot \exp(-\kappa a t)/t$. The contact is at t (contact) = $a_{KCl}/a \approx 0.9158$.

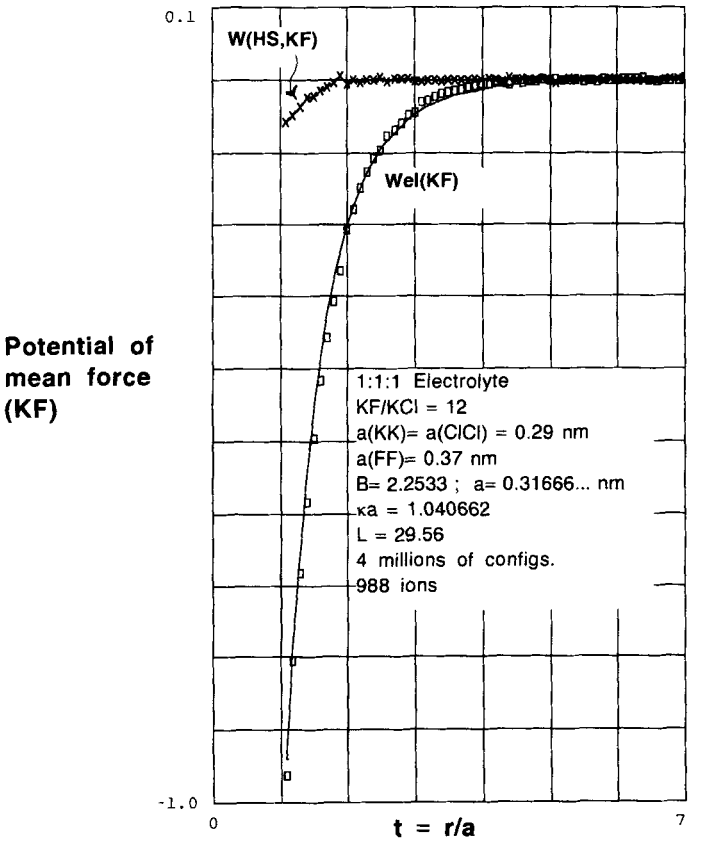

Figure 30 The hard sphere (HS, x-x-x-x) and the electric (el, rectangles) contributions to the dimensionless potential of mean force between the ions K^+ and F^- calculated from simulated data for the RDF for the same KF-KCl system as in Figure 29. The smooth solid curve are the DHX values calculated by equation (72): $W_{el,DHX}(KF) = -3.1974 \cdot \exp(-\kappa at)/t$. The contact is at t (contact) $= a_{KF}/a \approx 1.0407$.

This is simply the Debye-Hückel potentials-normalized as in the usual linearized theory. It is surprising how well this potential satisfies the simulated values of $W_{el,ij}(r)$ even in this complicated system with ionic strengths corresponding to $\kappa a \approx 1$, and it is astonishing how much physical meaning the Debye length κ^{-1} still has! The most significant deviations from the prediction of the formula (73) seems to be for $W_{el}(KK)$, see Figure 31, but even there the deviation is quite small. (In the tail of the distributions, however, there may well be significant deviations as indicated previously in this paper).

CONCLUSIONS

We have considered canonical ensemble MC simulations of primitive model electrolytes with up to N = 1728 ions in the simulation cell and with up to 30 million

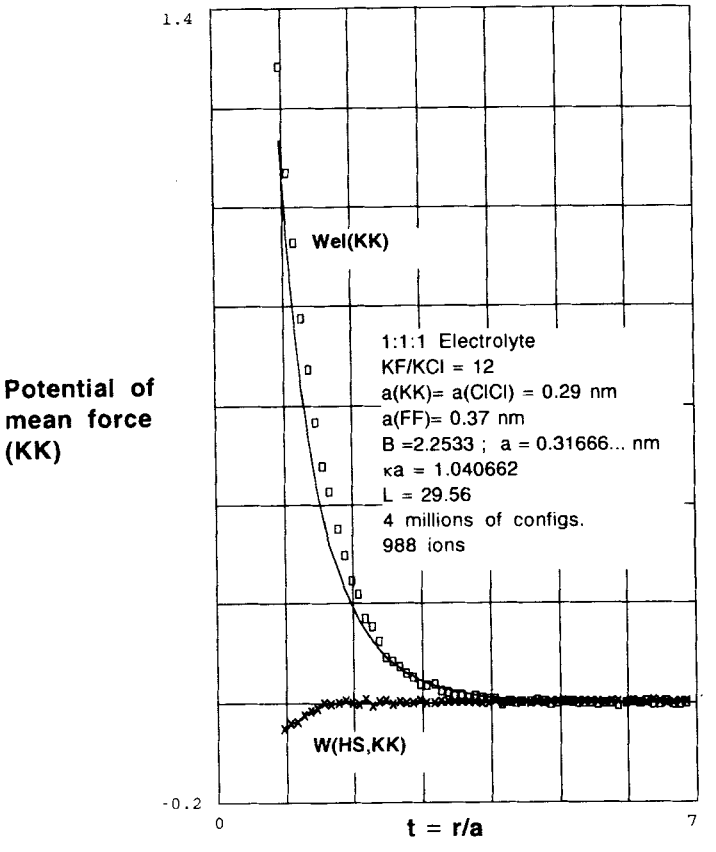

Figure 31 The hard sphere (HS, x-x-x-x) and the electric (el, rectangles) contributions to the dimensionless potential of mean force between the ions K^+ and K^+ calculated from simulated data for the RDF for the same KF-KCl system as in Figure 29. The smooth solid curve are the DHX values calculated by equation (72): $W_{el,DHX}(KK) = +2.9923 \cdot \exp(-\kappa at)/t$. The contact is at t (contact) = $a_{KK}/a \approx 0.9158$. The DHX potential slightly underestimates the electric potential of mean force in the region from contact to $t \approx 2.5$.

of configurations for very dilute ($\kappa a \ll 1$) z:z and 2:1 electrolytes and for moderately concentrated mixtures of 1:1 electrolytes with a common ion. From the above analysis, the following conclusions may be drawn:

Fast MC is possible under suitable circumstances

In the first part of the paper, the simulated values of E_{ex}/NkT, $-\Delta F_{ex}/NkT$, $C_{v,ex}/Nk$ and $\ln\gamma_{\pm}$ in a long run N = 1728 simulation of an extremely dilute 2:2 electrolyte are compared to extrapolated values from shorter simulations with smaller values of N and with the values of E_{ex}/NkT obtained by other authors. The previously established extrapolation methods for dilute z:z electrolyte systems are validated. With the same number of configurations, the statistical spread of the

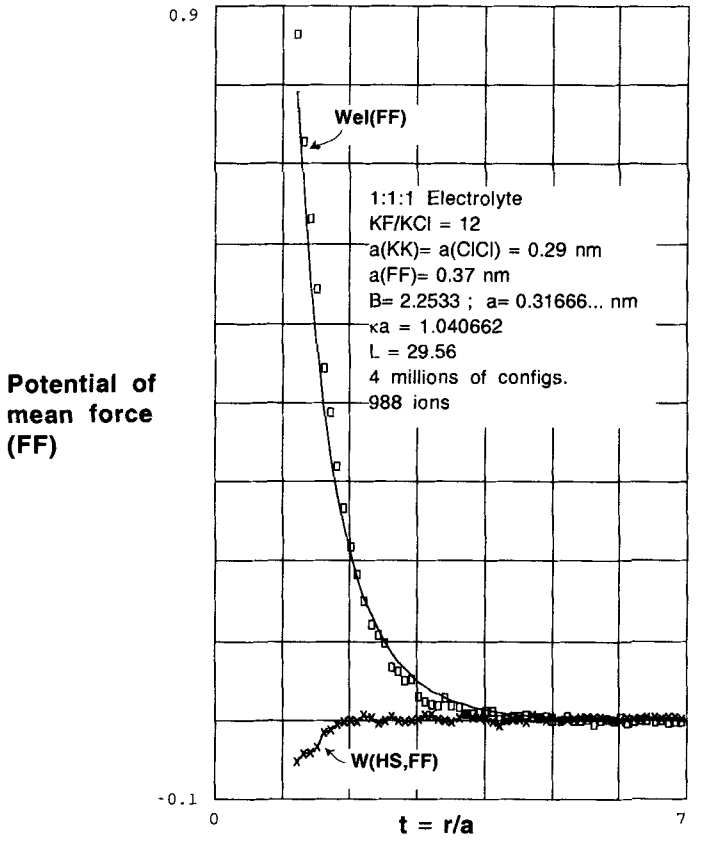

Figure 32 The hard sphere (HS, x-x-x-x) and the electric (el, rectangles) contributions to the dimensionless potential of mean force between the ions F^- and F^- calculated from simulated data for the RDF for the same KF-KCl system as in Figure 29. The smooth solid curve are the DHX values calculated by equation (72): $W_{el,DHX}(FF) = +3.4303 \cdot \exp(-\kappa at)/t$. The contact is at t (contact) = $a_{FF}/a \approx 1.168$.

parameters increases with N and the time consumption increases linearly with N. Thus, it is possible to perform fast MC simulations using a range of small N values carried to a high number of configurations and then extrapolating the results. It is better not to include large N-values with a high statistical spread.

For dilute 2:1 electrolytes new extrapolation formulae are found, which are quantitatively different from the z:z electrolyte extrapolations. Qualitatively the procedure is the same: E_{ex}/NkT, $-\Delta F_{ex}/NkT$, $C_{V,ex}/Nk$ have a leading correction term proportional to x^2, with $x = (L/2\kappa a)$. For a series with different N but constant ion density and Bjerrum parameter, the leading term is proportional to $(1/N)^{2/3}$. For $\ln\gamma_i$ simulated by the Widom method, there is an analytic correction to electroneutrality of order $(1/N)^{1/3}$ which is very dominant and has to be removed first. Then, the further corrections are made on the corrected $\ln\gamma_i^{el}$ with empirical (but universal for dilute systems) polynomials in x with a leading term in x^2. For

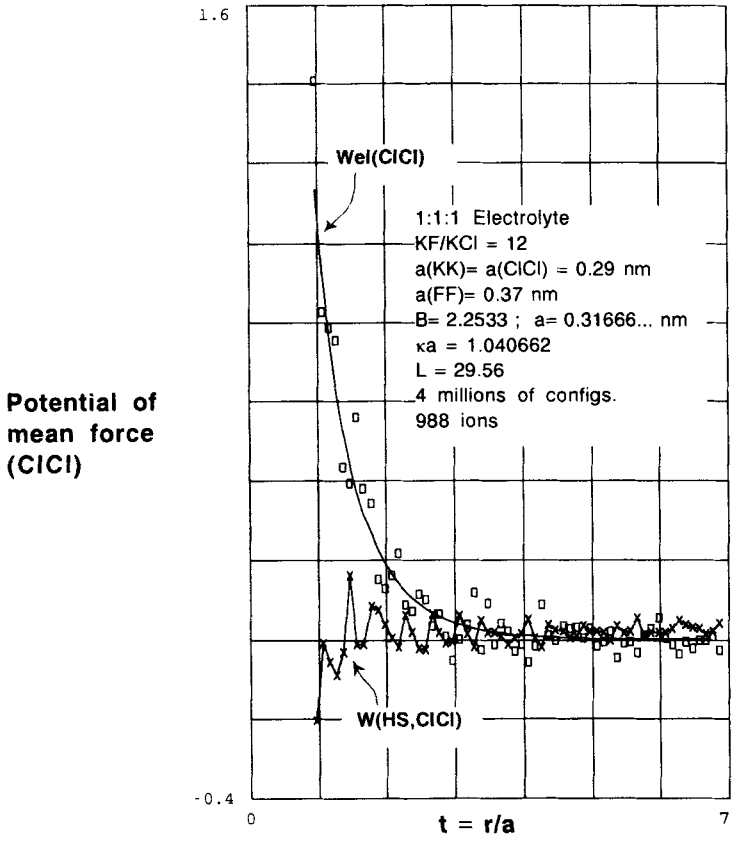

Figure 33 The hard sphere (HS, x-x-x-x) and the electric (el, rectangles) contributions to the dimensionless potential of mean force between the ions Cl^- and Cl^- calculated from simulated data for the RDF for the same KF-KCl system as in Figure 29. The smooth solid curve are the DHX values calculated by equation (72): $W_{el,DHX}(ClCl) = +2.9923 \cdot \exp(-\kappa at)/t$. The contact is at t (contact) = $a_{ClCl}/a \approx 0.9158$. There is more statistical noise than in the other figures, since only 38 of the 988 ions are Cl^- ions.

z:z electrolytes the extrapolation polynomials seem identical for E_{ex}/NkT and for the corrected $\ln\gamma_{\pm}^{el}$. The precise reason for this is at present not clear to the author. The ≫ rule ≪ is also not true for 2:1 electrolytes, where the two (universal) polynomials for E_{ex}/NkT and for $\ln\gamma_{\pm}^{el}$ are different.

For moderately concentrated mixtures of 1:1 electrolytes (and for moderately concentrated pure 1:1 electrolytes), the ≫ universal ≪ extrapolation polynomials in x are not valid any more. However, the leading term is still in $(1/N)^{2/3}$ - for $\ln\gamma_i$ after removal of the analytic term in $(1/N)^{1/3}$ - and one term seems to be enough. Thus, linear regression vs. $(1/N)^{2/3}$ easily leads to the thermodynamic value with values of N being less than 100, say. In short, with some care, fast MC simulations may be made for all systems with not too high density. (For a high density simulation with a 2:1 electrolyte, where N-extrapolation is without any value, see Sloth and Sørensen, Reference [9] Figure 3).

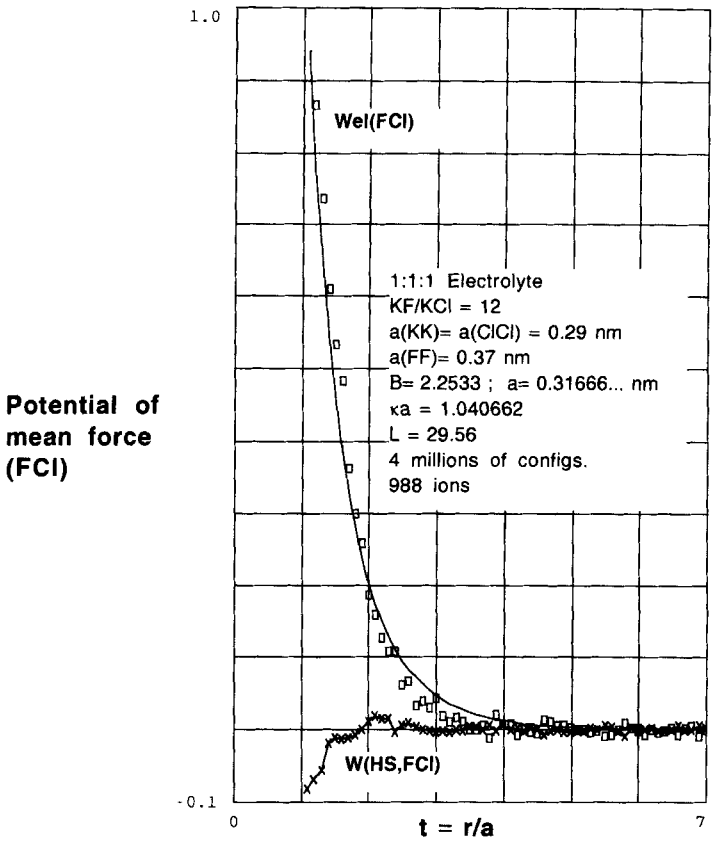

Figure 34 The hard sphere (HS, x-x-x-x) and the electric (el, rectangles) contributions to the dimensionless potential of mean force between the ions F^- and Cl^- calculated from simulated data for the RDF for the same KF-KCl system as in Figure 29. The smooth solid curve are the DHX values calculated by equation (72): $W_{el,DHX}(FCl) = +3.1975 \cdot \exp(-\kappa at)/t$. The contact is at t (contact) = $a_{FCl}/a \approx 1.042$.

Linear, non-neutral triplets are found in increasing amounts with increasing B for dilute z:z electrolytes

A hump with maximum around r = 2a is growing up with increasing Bjerrum parameter in dilute z:z electrolyte in the RDF between ions of similar charge. This corresponds to linear triplets + − + or − + − with all three ions in contact. The two similar charges are as far away as possible from each other in a linear configuration.

The (exponential integral) formula of Poirier for lny± seems to be valid for dilute as well as for moderately concentrated z:z and 2:1 systems

The formulae (13) and (22-24) of Poirier for $\ln\gamma_\pm$ of z:z and 2:1 electrolytes (with equal ionic radii) have been tested by comparison with MC simulations. For high

enough values of B, a region in the ultradilute regime is found with ≫ negative deviation ≪ from the limiting law. For increasing B, the deviation becomes more and more drastic and extends to higher concentrations. It is in this region, where inclusion of many terms (up to the 15th power in B, say) in the Poirier formulae are necessary in order to describe the nonlinearities in the model, which the classical Debye-Hückel model as well as the MSA model are totally unable to describe. At higher concentrations only a few terms seem to be necessary. We have verified the Poirier formulae both in cases with negative deviation from the limiting law and in moderately concentrated systems, but more work (for example using fast MC as described) should be done for the final validation. For 2:1 electrolytes with relatively large ions (in water at 25°C) the limiting law and the extended Debye-Hückel law may *fortuituously* be quite good in an extended concentration range according to the Poirier formula.

The ratio between lny2+ and ln y− is deviating from 4 in very dilute 2:1 electrolytes

It has been effectively demonstrated, that it is possible to calculate physically significant single ion activity coefficients using corrected and extrapolated Widom simulations. For example, in an extremely dilute 2:1 electrolyte the ratio $\ln y_{2+}/\ln y_{-}$ is close to 4, but there is a significant deviation from this value (8%) for B = 1.546. For B = 3 the deviation from 4 is 20%. This is well in accordance with the assumption that the Debye-Hückel results are valid strictly only in the B → 0 limit. Another non-Debye Hückel feature is the significant differences found between $\ln y_{\pm}^{el}$ and E_{ex}/NkT. For an extremely dilute 2:1 electrolyte the deviation is 2.5% at B = 1.546 compared to 17% for B = 3.

The real significance of the Debye-Hückel theory

Careful analysis of a number of sampled radial distribution functions of 2:2 and 2:1 electrolytes has shown, that the ≫ potential ≪ (73) from the usual linearized Debye-Hückel theory is a very good approximation to the *electric* contribution to the potential of mean force in the simulated systems - except possibly far out in the ≫ tails ≪ of the RDF's. This is so even for very dilute 2:2 and 2:1 electrolytes, where the linearisation Ansatz for the potential is very bad close to contact and also for (mixtures of) moderately concentrated 1:1 electrolytes, where $\kappa a \approx 1$ and one would not assume that the Debye length has much physical significance. When (small) systematic deviations from these so-called DHX RDF's are found, it is mostly in the case of RDF's between ions with charges of similar sign. In the DHX approximation, the electric potential of mean force just changes sign in a z:z electrolyte when interactions between similar charges or opposite charges are considered. That it is almost so - but not completely - is demonstrated by calculating mean radial distribution functions for example by equation (6), see Figure 5. Also, calculations of the excess number of counterions, see equation (7) and Figure 6, demonstrates that monotonous RDF's as predicted by the DHX model cannot be completely correct in the tail. A comprehensive study of the thermodynamic consistency of the DHX model for 1:1 electrolytes [10] has revealed that thermodynamic quantities calculated from integrals of the type $\int g(r) r dr$ such as E_{ex}/NkT, the osmotic coefficient and derived values for $C_{V,ex}/Nk$, $\Delta F_{ex}/NkT$ and $\ln y_{\pm}$ are quite consistent (independent of route of calculation) up to at least $\kappa a \approx 0.5$, whereas

Kirkwood-Buff calculations from integrals of the type $\int g(r)r^2dr$ - like the excess number of ions - are less consistent. This also indicates deviations from DHX in the far tail of the distributions.

The feature of the Debye-Hückel theory, which seems to survive, is that it almost correctly predicts the electric potentials of mean force in the neighbourhood of the ions. Normally, one solves the linearized Poisson-Boltzmann equation

$$\nabla^2\Phi^{(i)} = -\rho_q^{(i)}/\varepsilon \approx \kappa^2\Phi^{(i)} \tag{74}$$

in the geometry given and normalizes the (conditioned) charge density $\rho_q^{(i)}$ around the chosen ≫ central ion ≪ of species no. i, so that the charge in the ≫ ionic cloud ≪ cancels with the charge of the central ion. This gives rise to the factor $\exp(\kappa a_{ij})/(1 + \kappa a_{ij})$ in equation (72), and in the moderately concentrated KF-KCl systems studied, this factor varies very significantly for the various RDF's, see Figures 34–39. Thus there seems to be an identification between the (conditioned) electric potential in the Debye-Hückel theory and the electric potential of mean force. However, in the derivation of the last part of (74) it was assumed, that $|z_j e_0^2 \Phi^{(i)}|/kT \ll 1$ which is obviously not the case close to contact, so this is kind of a paradox.

Now assume, that a more ≫ true ≪ expression of the Debye-Hückel relation is the equation (75):

$$\nabla^2\rho_q^{(i)} \approx \kappa^2\rho_q^{(i)} \tag{75}$$

In that case, the solution around an ion would be of the form $\rho_q^{(i)}(r) = A^{(i)}\exp(-\kappa r)/r$ and the factor A could be found by charge cancellation. Using the Poisson equation we then have $\nabla^2\Phi^{(i)} = -\rho_q^{(i)}/\varepsilon = -(A^{(i)}/\varepsilon)\exp(-\kappa r)/r$. Since $\exp(-\kappa r)/r$ is an eigen-function to the spherical Laplacian, the potential $\Phi^{(i)}$ will have the same form + possibly any physically feasible spherical harmonics. There are only two such spherical harmonics without angular dependence, namely the constant $B^{(i)}$ and $C^{(i)}/r$. In the present case, where the potential is assumed to vanish when $r \to \infty$, we must have $B^{(i)} = 0$, but $C^{(i)}$ might be different from zero. Indeed, we saw in eqs. (1), (3) and (25–27) that expressions of the form $[A\exp(-\kappa r) + C]/r$ were excellent approximations for the sampled RDF's of dilute 2:2 and 2:1 electrolytes. Nevertheless, there are problems with a $C \neq 0$, since the excess of counterions will not go to zero when $r \to \infty$ (Figure 8). Thus, we end up with the classical Debye-Hückel solution for $\Phi^{(i)}$ but without having used the condition $|z_j e_0^2 \Phi^{(i)}|/kT \ll 1$.

The solution of the modified Debye-Hückel equation (75) *inside* a charged spherical pore the eigenfunction has the form $A\sinh(\kappa r)/r$, and the potential has the same form + a constant B. The term C/r must vanish, since r = 0 is now included. It is clear, that $B + [A\sinh(\kappa r)/r]$ does not satisfy the ordinary Debye-Hückel equation (74). This points to a general weakness of the usual derivation of Debye and Hückel. The electric potential is a gauge function and it is only determined up to an arbitrary additive constant. Thus, the condition $|z_j e_0^2 \Phi^{(i)}|/kT \ll 1$ is basically meaningless. In contrast, to state that the charge density is in some sense small is quite reasonable. In extensive grand canonical ensemble simulations of ions in small, charged spherical pores [14], it has indeed been shown that it is the charge density and not the potential, which satisfies a Debye-Hückel equation in dilute systems. It is a problem for the future to find out why precisely it is so. Here, I shall only point to the fact, that the formula (75) may be derived from Nernst-

Planck-Smoluchowski electro-diffusion equations with $\partial\rho_i/\partial t = 0$ by weighing with the ionic charges and summing - using the Poisson equation:

$$\nabla^2\rho_q - \kappa^2_{local}\rho_q - \varepsilon E\cdot\nabla(\kappa^2_{local}) = 0 \qquad (76)$$

In (76), κ_{local} is the inverse Debye length defined with local concentrations and E is the electric field strength. Equation (75) now follows from equation (76) by a linearisation, where the scalar product of the field strength and the local gradient in ionic strength is regarded as a second order quantity and where the values of κ_{local} may be replaced by a common mean value. In this derivation the traditional condition $|z_j e_0^2 \Phi^{(i)}|/kT \ll 1$ is not used.

The influence of different ionic sizes on the activity coefficients

One remarkable fact, which is an outcome of some of the present and some previous simulations, is that with a fixed mean contact distance (a), the single ion activities of the cation and the anion are almost the same without regard to the ratio of the radii between the two ions for pure 1:1 electrolytes. Table 27 shows that for a quite dilute 1:1 electrolyte with $\kappa a \approx 0.14$ and B = 1.546, there is no significant variation in the single ion activity coefficient of the anion, when the ratio between cation and anion radius is increased by a factor 3. For the cation, there is a very slight decrease in the absolute value. There are considerable variations in the electric and the hard sphere contributions taken separately, but these variations tend to cancel in the total activity coefficients. In pure ≫ normal ≪ KF at 1 mol/L, the table shows that there is probably not any significant difference between the single ion activity coefficient of K^+ (radius 0.145 nm) and of F^- (radius 0.17 nm). In ≫exaggerated≪ KF at the same concentration, the single ion activity coefficients of K^+ (radius 0.145 nm) and of F^- (radius 0.185 nm) are completely identical - in spite of quite large differences in the electric and in the hard sphere contributions taken separately! Thus, the assumption

$$\ln y_\pm \approx \ln y_+ \approx \ln y_- \qquad (77)$$

seems to be a quite good one for primitive model 1:1 electrolytes. In experimental situations, the assumption (77) might be called the *modified MacInnes assumption*, since MacInnes made the assumption, that the single ion activity coefficients of

Table 27 The influence of different ionic radii on single ion activity coefficients in pure 1:1 electrolytes. (a = mean contact distance).

B	*κa*	a_{++}/a_{--}	$\ln y_+$ (*tot*)	$\ln y_-$ (*tot*)	$\ln y_+$ (*el*)	$\ln y_-$ (*el*)	$\ln y_+$ (*HS*)	$\ln y_-$ (*HS*)	*Reference*
1.546	0.13938	1	−0.0921 ±0.0005	−0.0921 ±0.0005	−0.0963	−0.0963	0.00419	0.00419	[10–12]
1.546	0.13938	3	−0.0904 ±0.0006	−0.0923 ±0.0004	−0.0996	−0.0947	0.00918	0.00236	[10–12]
2.26522									Normal KF
	1.03524	1.1724	−0.461 ±0.005	−0.448 ±0.007	−0.607	−0.633	0.1456	0.1851	This paper
2.16225									Exagg. KF
	1.08455	1.2759	−0.420 ±0.007	−0.418 ±0.002	−0.579	−0.647	0.1586	0.2289	This paper

HS contributions from the formulae in References [31] and [37].

K^+ and Cl^- are equal, for example in mixtures of KCl and NaCl at the same ionic strength [38], [39]. Many ≫ purist ≪ electrochemists maintain, that single ion activities can never be measured by classical electrochemical methods, and they are of course right in principle. However, the purists point of view comes to an end, when one wishes to speak about ≫ ion selective electrodes ≪, ≫ the electrochemical definition of pH ≪, ≫ action potentials ≪ in nerves, ≫ diffusion potentials ≪ and ≫ Donnan potentials ≪ in membranes and as a matter of fact already in the precise definition of the ≫ series of standard electrode potentials ≪, so the purist point of view is certainly not a practical one. The present and previous MC studies may lend some support for just using (77) in all solutions of pure 1:1 electrolytes without having too bad a conscience afterwards!

Single ion activity coefficients and other thermodynamic quantities in mixtures

Tables 18 and 24 for the ≫ normal ≪ and for the ≫ exaggerated ≪ KF-KCl systems show the following features for the single ion activity coefficients for the ions in ternary mixtures of 1:1 electrolytes with a common ion at the same ionic strength:

(a) In the solutions of only one salt, the single ion activities of the cation and anion are practically the same, also when the ions have different radii (see the discussion above). However, the single ion activities ≈ the mean ion activities are different for pure KCl and pure KF at the same ionic strength.

(b) In mixtures the single ion activities of Cl^- and of F^- *vary very little* and this seems to be so even down to trace concentrations of the ion.

(c) The K^+ ion has to *strike a compromise*. In pure KCl, the activity coefficient is the same as for Cl^- (since the two ions have the same radii). In pure KF, the activity of K^+ has to be (almost) the same as the activity coefficient of F^- because of the ≫ principle ≪ (a) above. In mixtures, the dimensionless exces chemical potential of K^+ ($= \ln y_+$) varies linearly with the salt fraction between these extremes. Thus the traditional use of the Mac-Innes assumption (see the examples given if Reference [39]) seems *not* to be the correct one - at least not for the primitive electrolyte model.

It has been found, that there is perfect *Harned linearity* for the mean ionic excess chemical potentials (which is the classical Harned linearity) as well as for the single ion activity coefficients, the excess energy and the excess heat capacity at constant volume. (The two latter quantities are both for temperature independent permittivity, but they may easily be corrected to real experimental situations, when the temperature coefficient of ε is known). Let us consider what Harned linearity means for the exces energy in terms of the RDF's. In terms of the nomenclature of Reference [6], we have for a general mixture:

$$E_{ex}/NkT = (2\pi/\rho^*)\, B \sum_i \sum_j z_i z_j \rho_i^* \rho_j^* [2e_{ij} - d_{ij}^2] \tag{78}$$

$$e_{ij} \equiv \int_{d_{ij}}^{\infty} h_{ij}(t) \cdot t\, dt \tag{79}$$

$$d_{ij} \equiv a_{ij}/a \tag{80}$$

We have found here, that the electric potential of mean force is given very well by the Debye-Hückel potential (72) in 1:1:1 mixtures. Thus, as long as we have the same ionic strength (same κa), the functions $g_{el,ij}(t)$ seem to be quite *independent* of *the ratio of mixture* and the same is assumed for the hard sphere contribution $g_{HS,ij}(t)$. With this assumption we have for the KF-KCl mixture:

$$E_{ex}/NkT = (\pi B\rho^*/2)[c_o + c_1 X_{KCl} + c_2 (X_{KCl})^2] \tag{81}$$

$$c_o \equiv (e_{KK} + e_{FF} - 2e_{KF}) - (1/2)(d_{KK}^2 + d_{FF}^2 - 2d_{KF}^2) \tag{82}$$

$$c_1 \equiv 2(e_{KF} + e_{ClF} - e_{KCl} - e_{FF}) - (d_{KF}^2 + d_{ClF}^2 - d_{KCl}^2 - d_{FF}^2) \tag{83}$$

$$c_2 \equiv (e_{ClCl} + e_{FF} - 2e_{ClF}) - (1/2)(d_{ClCl}^2 + d_{FF}^2 - 2d_{ClF}^2) \tag{84}$$

Harned linearity requires $c_2 = 0$, which is not in general the case. In the case of Debye-Hückel linearity ($B \to 0$) and negligible hard sphere correlations we have for the correlation functions $h_{ij} \approx -W_{ij}(t)$ with the $W_{ij}(t)$ given by equation (72). One obtains in this limit for example:

$$e_{KK} \approx -(B/\kappa a)[1 + \kappa a\, d_{KK}]^{-1}; e_{ClF} \approx -(B/\kappa a)[1 + \kappa a\, d_{ClF}]^{-1}$$

$$e_{KF} \approx +(B/\kappa a)[1 + \kappa a\, d_{KF}]^{-1}$$

For not too large $\kappa a\, d_{ij}$ we have $[1 + \kappa a\, d_{ij}]^{-1} \approx 1 - \kappa a\, d_{ij}$ and

$$c_2 \approx (-B)[2d_{ClF} - d_{ClCl} - d_{FF}] - (1/2)[d_{ClCl}^2 + d_{FF}^2 - 2d_{ClF}^2].$$

Using the definitions of the d_{ij}'s we have that the first term is identically zero, and the second term may be simplified:

$$c_2 \approx -(1/4)[d_{FF} - d_{ClCl}]^2 \tag{85}$$

This term is of second order in the difference in ionic radii. However, for large differences there should be some curvature in the Harned plot even in the Debye-Hückel limit ($B \to 0$, $\kappa a \to 0$). By similar calculations (using also that $d_{KK} = d_{ClCl}$) we have:

$$c_1 \approx (2B)[d_{ClCl} - d_{FF}] + (1/2)d_{FF}^2[1 - (a_{KK}/a_{FF})]^2 \tag{86}$$

$$c_o \approx -(4B/\kappa a) + 4B\, d_{KF} \tag{87}$$

Since $\kappa a = \sqrt{(4\pi B\rho^*)}$ we obtain finally in the DH-limit (neglecting the square terms in the difference of the ionic radii, *i.e.* neglecting Harned nonlinearity:

$$E_{ex}/NkT \approx (-B\kappa a/2) + (1/4)B(\kappa a)^2[d_{KK}(1 + X_{KCl}) + d_{FF}(1 - X_{KCl})] \tag{88}$$

In the limit of pure KCl ($X_{KCl} = 1$) we obtain:

$$E_{ex}/NkT \approx (-B\kappa a/2)[1 - \kappa a\, d_{KK}] \approx (-\lambda_B \kappa/2)[1 + \kappa a_{KCl}]^{-1} \tag{89}$$

In the other limit ($X_{KCl} = 0$):

$$E_{ex}/NkT \approx (-B\kappa a/2)[1 - \kappa a\, d_{KF}] \approx (-\lambda_B \kappa/2)[1 + \kappa a_{KF}]^{-1} \tag{90}$$

These limits are exactly the expected limits for pure Debye-Hückel electrolytes. The above calculations show the consistency of the present approach. In the D.H. limit we have for mixtures:

$$(E_{ex}/NkT)_{DH,Mix} = (E_{ex}/NkT)_{DH,KF} - (B/4)(\kappa a)^2 (d_{FF} - d_{KK})X_{KCl} \quad (91)$$

For the ≫ normal ≪ KF-KCl system at 1 mol/L($B = 2.3268$, $\kappa a = 1.00786$, $d_{FF} - d_{KK} = 0.1630$) we obtain a ≫ Harned coefficient ≪ = 0.0963 which has the right sign, but is far too high compared to the MC value 0.0260 in equation (31) or the MSA value 0.0213 in equation (38). For the ≫ exaggerated ≪ KF-KCl system at 1 mol/L(B = 2.2533, $\kappa a = 1.04071$, $d_{FF} - d_{KK} = 0.2526$) the Harned coefficient from equation (91) is 0.1541 which is also much higher than the MC value 0.0388 in equation (53) or the MSA value 0.0327 in equation (60). The reason lies of course in the hard sphere contribution to h_{ij}, which contributes considerably to the e-integrals in (82–84). Also, the first part of the potential of mean force is too high to be linearized as in the D.H theory. It is not obvious to me, why the Harned linearity should be so perfect as it is in such systems. Nevertheless, the MC calculations as well as the MSA and the SPB calculations demonstrate Harned's rule to be true - also the usual one for the mean ionic activity coefficients. The Harned coefficients are well predicted by the MSA theory.

APPENDIX ON METHODOLOGY AND BASIC NOMENCLATURE

The dimensionless pair potential between two ions of species i and species j with valencies z_i and z_j in the primitive electrolyte model is the following:

$$U_{ij}(t_{ij})/kT = z_i z_j B/t_{ij} \quad (A1)$$

The Boltzmann constant is k and T is the absolute temperature. The dimensionless separation is defined by:

$$t_{ij} \equiv r_{ij}/a \quad (A2)$$

With n ionic species the mean contact distance is:

$$a \equiv (1/n) \sum_{i=1..n} a_{ii} \quad (A3)$$

The reduced Bjerrum parameter is defined by

$$B \equiv \lambda_B/a \quad (A4)$$

with the Bjerrum length:

$$\lambda_B \equiv e_o^2/(4\pi\varepsilon kT) \quad (A5)$$

In (A5), ε is the dielectric permittivity of the solvent (which is the only influence of solvent in the primitive model). The unit charge is e_o (SI units have been assumed). In the present paper, the Bjerrum parameter z^2 B for z:z electrolytes is simply referred to as B (with no consequence). The concentrations of ions of species i are ρ_i, and they are made dimensionless by scaling with the mean contact distance:

$$\rho_i^* \equiv \rho_i a^3 \quad (A6)$$

The total dimensionless concentration is given by:

$$\rho^* \equiv \sum_{i=1..n} \rho_i^* = N/(L)^3 \quad (A7)$$

N is the total number of ions in the MC simulation cell and L is the dimensionless edge length of the cell (scaled by the mean contact distance a). The central Debye-Hückel parameter κa may be calculated from (A8) for z:z and 1:1:1 electrolytes and by (A9) for 2:1 electrolytes:

$$\kappa a = \sqrt{(4\pi B \rho^*)} \quad \text{(z:z and 1:1:1 electrolytes)} \tag{A8}$$

$$\kappa a = \sqrt{(24\pi B \rho_+^*)} \quad \text{(2:1 electrolytes, cation doubly charged,)} \tag{A9}$$

The Debye length measured in mean contact distances is $\lambda_D/a = 1/(\kappa a)$.

The simulations are performed after the usual Metropolis scheme: Firstly, a lot is drawn between the ions to select a specific ion. Secondly, this ion is attempted to be moved. In the x-, y- and z- directions the movement is random up to a maximum displacement equal to $\pm \delta La$. In all simulations, $\delta = 1/2$ to ensure $\gg$ maximum stirring $\ll$. After the attempted displacement, the change in configurational energy ΔU of the central cube is calculated summing the pair potentials (A1) between the displaced ion and the N-1 other ions. If $\Delta U < 0$, the move is always accepted. If $\Delta U > 0$ the move is accepted with a probability proportional to $\exp(-\Delta U/kT)$ and rejected proportionally to $1 - \exp(-\Delta U/kT)$. If rejected, the original situation is counted once more in the samplings. The equilibrium distribution over states of the Markov chain will be the one of the canonical ensemble. The configurations are grouped in "samplings" of 10,000-20,000 configurations. After each sampling, the configurational energy between the N ions is calculated *ab initio* to avoid accumulation of errors from the summation of many ΔU's.

The Metropolis method is optimal for calculating the *exces (internal) energy*, where the sampled quantity is the configurational energy of the central cube. However, other quantities may be simulated simultaneously with very little additional time consumption. The *radial distribution functions* (RDF) have been sampled as normalized local concentrations of ions in 60 equally spaced spherical shells around each ion with averaging over all the relevant ions in the simulation cube. Closely related to the RDF's are the *dimensionless potentials of mean force* W_{ij} and the *correlation functions* h_{ij}:

$$W_{ij}(r_{ij}) \equiv -\ln g_{ij}(r_{ij}) \; ; \; h_{ij}(r_{ij}) \equiv g_{ij}(r_{ij}) - 1 \tag{A10}$$

The *exces heat capacity at constant volume* is calculated from the variance of the energy fluctuations and the *single ion exces chemical potentials* are found by the ingenious method of Widom. A number of non-disturbing $\gg$ test ions $\ll$ are introduced in the simulation cube. The test ions do not influence the Markov proces, but they are $\gg$ neutral observers $\ll$, since the interaction energy $U_{\text{test ion of type i} \Leftrightarrow N \text{ ions}}/kT$ is sampled. The exces chemical potential for the ions of species i may then be calculated from

$$-\mu_{i,ex}/kT = -\ln y_i = \ln \langle \exp(-U_{\text{test ion of type i} \Leftrightarrow N \text{ ions}}/kT) \rangle \tag{A11}$$

where y_i is the Plain Widom (PW) estimate of the (MacMillan-Mayer) single ion activity coefficient and $\langle\rangle$ denotes average over the Markov chain (canonical average). Notice, that when there is hard sphere overlap between the test ion and one of the $\gg$ real $\ll$ ions, the sampled quantity is counted as zero. The position of the test ion is of no importance, but in order to obtain good statistics, 64 test ions of each ion type were distributed in a regular lattice in the simulation box, and the averaging in (A11) was performed over all 64 replicas of the test ion. Finally, the *electrostatical* contribution to the exces Helmholtz free energy per ion may in

dilute systems and for not too large N be estimated by the following average:

$$\Delta F_{ex}/NkT = (1/N)ln\langle \exp(U_N/kT)\rangle \quad \text{(A12)}$$

This is a modification of the Salsburg-Chesnut method, where Δ stands for the electrostatical contribution (hard sphere contributions cannot be calculated by this method). The instantaneous configurational energy of the N-ion system is U_N, and when the exponential of this quantity is averaged over an infinite Metropolis chain, one obtains the ratio of the configuration integral of the hard sphere system to the total configuration integral [1].

The length of the Markov chains is a critical parameter. By a ≫ configuration ≪ in the present paper is meant one attempt to displace a particle, whether it is accepted or not. To obtain exact values, ≫ infinitely many ≪ configurations should be used. With finite chains there is some uncertainty and - for some parameters - even systematic deviations. Both of these are best estimated by repeating independently the simulations and by considering the spread of systematic deviations of series of simulations with various N-values (see later). The Metropolis method is optimal for the excess energy and values with a precision of 4-5 digits are obtained using only few millions of configurations. With the same number of configurations, the precision decreases somewhat with increasing N (but not to the extent that the same number of movements of each ions have to be performed to obtain the same precision). Much longer Markov chains have to be performed to obtain reliable radial distribution functions close to contact in very dilute systems - especially between electrostatically repelling ions. Also, the PW values of $\ln y_i$ and especially $C_{V,ex}/Nk$ fluctuate considerably at higher N-values and require longer MC runs. The values of $\Delta F_{ex}/NkT$ require an excessive number of configurations not to deviate systematically, except in very dilute systems and not too high values of N. This is so, since only very rare samplings with a large value of the configurational energy U_N/kT contribute significantly in the average given by (A12) and these rare values are more rare and more extreme the larger the number of N, B or ρ^*.

The simulations are started from regular lattices (sometimes with interstitial ions) and the initial parts of the Markov chains are not in statistical equilibrium and should be rejected or just majorized by the subsequent configurations. It is advantageous to reject the first configurations (10,000 or more). For some systems, especially $\ln y_i$ and $C_{V,ex}/Nk$ are found to be sensitive to the number of initial configurations rejected, and a higher number of configurations were rejected until no systematic effect could be seen.

In the simulations, the N ions in the central simulation cube are interacting with each other or with an ≫ image ion ≪ in neighbouring identical cubes, if the image ion is closer to the selected ion. This is the ≫ minimum image ≪ (MI) energy cut-off method. There are periodic boundary conditions, since if a given ion leaves the central cube, an image ion enters automatically. The combined artificial constraints of periodic boundary conditions (preventing fluctuations in N in the volume $(La)^3$) and MI energy cut-off (each ion interacts only with other ions inside a volume $(La)^3$ centered at the given ion) may be expressed through the ≫ distance from thermodynamic limit ≪ parameter

$$x \equiv (\lambda_D)/(La/2) = 2/(L\kappa a) \quad \text{(A13)}$$

expressing the ratio of the Debye length to the maximum interaction distance. The thermodynamic limit is reached for $x \to 0$. In a series of simulations with constant

concentration ρ^* and constant B, but different numbers of ions N, we have for example for z:z electrolytes using (A7-A8):

$$x = constant \cdot N^{-1/3}\,;\, constant(z{:}z) = (\pi B)^{-1/2}(\rho^*)^{-1/6} \qquad \text{(A14)}$$

Considering *several* such N-series each at *different* values of B and ρ^*, it has been documented in References [10–12], that in *extremely to moderately dilute* z:z electrolyte systems, the simulated MC quantities scaled relative to the values in the thermodynamic limit in the form of *universal* polynomials in x with the leading term proportional to x^2. By $\gg$ universal $\ll$ is meant, that the polynomials are the same for each N-series whatever the values of B and ρ^*. The following polynomials have been found *for z:z electrolytes which might have as different ionic diameters as a factor 3*:

$$E_{ex}(MC, N)/E_{ex}(\infty) = 1 + 0.152526\,x^2 + 0.783555\,x^3 - 0.45261\,x^4 \qquad \text{(A15)}$$

$$\Delta F_{ex}(MC, N)/\Delta F_{ex}(\infty) = 1 + 1.06734\,x^2 + 0.729190\,x^3 - 0.84083\,x^4 \qquad \text{(A16)}$$

$$C_{V,ex}(MC, N)/C_{V,ex}(\infty) = 1 - 0.695\,x^2 + 0.28\,x^5 \qquad \text{(A17)}$$

The leading N-dependence of these quantities are as $(1/N)^{2/3}$. In contrast, the leading N-dependence of the PW values of $\ln\gamma_i$ is rather found to be $(1/N)^{1/3}$. This is due to the violation of electroneutrality, when a Widom test ion is introduced in a finite system. Introducing a uniform *neutralizing background* (which vanishes in the limit $N \to \infty$) it has proven possible to remove the $(1/N)^{1/3}$ dependence completely by an *analytic correction* of the PW values to electroneutrality. One obtains for any electrolyte system [8,11]:

$$-\ln\gamma_i\,(\text{corrected to electroneutrality}) = -\ln\gamma_i\,(\text{plain Widom}) + \text{CORR} \qquad \text{(A18)}$$

$$\text{CORR} \equiv (K/32\pi kT\varepsilon\, La)\,[z_i^2 e_o^2 - 2\,z_i\,e_o\,Q_b(N)] \qquad \text{(A19)}$$

$$K \equiv 12 \cdot \ln(2 + \sqrt{3}) - 2\pi \approx 9.520309 \qquad \text{(A20)}$$

In (A19) the charge $Q_b(N)$ is the total value of the neutralizing background charge in the MC simulation cube with N ions present *without* regard to the test ions. It is given by

$$Q_b(N) = -\sum_{\substack{\text{all real ions}\\ \text{in MC cube}}} z_i\,e_o \qquad \text{(A21)}$$

and it is only different from zero, if one simulates systems with a non-electroneutral combination of cations and anions in the central simulation cube. It might sometimes be of value to simulate both N-series which are electroneutral and N-series with for example one cation in exces of the anions in order to check the extrapolations [5], but in all cases simulated in the present paper we have $Q_b(N) = 0$. In that case, the correction formula (A19) may be rewritten in terms of the reduced Bjerrum parameter and the dimensionless total concentration:

$$\text{CORR} = z_i^2 BK/(8L) = (\rho^*/N)^{1/3}(z_i^2 BK/8) \qquad \text{(A22)}$$

This term which is non-vanishing even for electroneutral systems is a consequence of the fact that the background charge has to be increased to $Q_b(N+1)$ when the test ion is introduced. For a careful discussion of this correction and for the

evaluation of the space integral leading to (A20), see Reference [11], pp. 481–483 and pp. 491–492.

When the plain Widom values of $\ln\gamma_i$ have been corrected to neutrality, the strong $N^{-1/3}$ dependence has been removed, but there is still some variation with a leading term of $x^2 \sim N^{-2/3}$. In *dilute z:z systems* it has been found that the *electric* part of the *corrected* Widom values for the *mean ionic activity coefficients* (i.e. with the estimated hard sphere contribution subtracted) *scale exactly like the exces energy*:

$$\ln\gamma_{\pm,el}(\text{corrected Widom}, N)/\ln\gamma_{\pm,el}(\infty) = E_{ex}(MC, N)/E_{ex}(\infty)$$
$$= 1 + 0.152526\,x^2 + 0.783555\,x^3 - 0.45261\,x^4 \qquad \text{(A23)}$$

In the present paper new extrapolation formulae of the same type as (A15–A17, A23) are proved for dilute 2:1 electrolytes, see equations (16–17) and equations (20–21). For such electrolytes E_{ex} and $\ln\gamma_{\pm,el}$ *scale differently*. In addition, we have scaling formulae for the corrected Widom values for the *single ion activity coefficients*, see equations (18–19). In the case of moderately concentrated ions, the scaling is found to be *linear* in $(1/N)^{2/3}$, so no scaling polynomials are needed here. It should be stressed, that the analytic correction formulae (A19) and (A22) are *always* valid for any type of electrolyte system and for any concentration, so the $(1/N)^{1/3}$ dependence of the single ion activity coefficients may *always* be removed.

References

[1] P. Sloth, T.S. Sørensen and J.B. Jensen, "Monte Carlo calculations of thermodynamic properties of the restricted, primitive model of electrolytes at extreme dilution using 32, 44, 100, 216 and 512 ions and *ca.* 10^6 configurations per simulation", *J. Chem. Soc., Faraday Trans. 2*, **83**, 881 (1987).

[2] T.S. Sørensen, P. Sloth, H.B. Nielsen and J.B. Jensen, "On the validity of the Debye-Hückel laws for dilute electrolyte solutions tested by high-precision Monte Carlo simulations", *Acta Chem. Scand.*, **A42**, 237 (1988).

[3] T.S. Sørensen and P. Sloth, "Computer modelling of thermodynamic properties of very dilute charged hard spheres in a dielectric continuum", in *Structure, coherence and chaos in dynamical systems*, P.L. Christiansen and R.D. Parmentier, eds., Manchester University Press, Manchester and New York, 1989, ch. 26.

[4] P. Sloth and T.S. Sørensen, "Monte Carlo simulations of single-ion chemical potentials. Preliminary results for the restricted primitive model", *Chem. Phys. Letters*, **143**, 140 (1988).

[5] P. Sloth and T.S. Sørensen, "Monte Carlo simulations of single-ion chemical potentials. Results for the unrestricted primitive model", *Chem. Phys. Letters*, **146**, 452 (1988).

[6] T.S. Sørensen and J.B. Jensen, "Mean activity coefficients in aqueous electrolyte mixtures. II. The generalized DHX model and its resolution of some seemingly paradoxical experimental results", *Acta Chem. Scand.*, **43**, 421 (1989).

[7] T.S. Sørensen, J.B. Jensen and P. Sloth, "Experimental activity coefficients in aqueous mixed solutions of KCl and KF at 25° compared to Monte Carlo Simulation and Mean Spherical Approximation Calculations", *J. Chem. Soc., Faraday Trans. 1*, **85**, 2649 (1989).

[8] P. Sloth and T.S. Sørensen, "Monte Carlo calculations of chemical potentials in ionic fluids by application of Widom's formula: Correction for finite-system effects", *Chem. Phys. Letters*, **173**, 51 (1990).

[9] P. Sloth and T.S. Sørensen, "Single-ion activity coefficients and structure of ionic fluids. Results for the primitive model of electrolyte solutions", *J. Phys. Chem.*, **94**, 2116 (1990).

[10] T.S. Sørensen, "How wrong is the Debye-Hckel approximation for dilute primitive model electrolytes with moderate Bjerrum parameter?" *J. Chem. Soc. Faraday Trans.*, **86**, 1815 (1990).

[11] T.S. Sørensen, "Error in the Debye-Hückel approximation for dilute primitive model electrolytes

with Bjerrum parameters of 2 and *ca.* 6.8 investigated by Monte Carlo Methods: Exces energy, Helmholtz free energy, heat capacity and Widom activity coefficients corrected for neutralising background" *J. Chem. Soc. Faraday Trans.*, **87**, 479 (1991).

[12] T.S. Sørensen, "Ions in solution and in weak ion exchange membranes" in *Capillarity Today. Lecture Notes in Physics, Vol. 386*, G. Pétré and A. Sanfeld, eds., Springer-Verlag, Berlin-Heidelberg-New York-London-Paris-Tokyo-Hong Kong-Barcelona-Budapest, 1991, pp. 164–221.

[13] P. Sloth and T.S. Sørensen, "Hard charged spheres in spherical pores. Grand canonical ensemble Monte Carlo calculations" *J. Chem. Phys.*, **96**, 548 (1992).

[14] T.S. Sørensen and P. Sloth, "Ion and potential distributions in charged and non-charged primitive spherical pores in equilibrium with primitive electrolyte solution calculated by grand canonical ensemble Monte Carlo simulation: Comparison with generalized Debye-Hückel and Donnan theory", *J. Chem. Soc. Faraday Trans.*, **88**, 571 (1992).

[15] D.N. Card and J.P. Valleau, "Monte Carlo study of the thermodynamics of electrolyte solutions" *J. Chem. Phys.*, **52**, 6232 (1970).

[16] B. Widom, "Some topics in the theory of fluids" *J. Chem. Phys.*, **39**, 2808 (1963).

[17] B. Widom, "Potential-distribution theory and the statistical mechanics of fluids" *J. Phys. Chem.*, **86**, 869 (1982).

[18] J.P. Valleau, L.K. Cohen and D.N. Card, "Primitive model electrolytes. II. The symmetrical electrolyte" *J. Chem. Phys.*, **72**, 5942 (1980).

[19] W. van Megen and I.K. Snook, "The grand canonical ensemble Monte Carlo method applied to electrolyte solutions" *Molecular Phys.*, **39**, 1043 (1980).

[20] J.P. Valleau and L.K. Cohen, "Primitive model electrolytes. I. Grand canonical ensemble Monte Carlo computations" *J. Chem. Phys.*, **72**, 5935 (1980).

[21] S.A. Rogde and B. Hafskjold, "Equilibrium properties of a 2-2 electrolyte model. Monte Carlo and integral equation results for the restricted primitive model" *Molecular Phys.*, **48**, 1241 (1983).

[22] G.V. Ramanathan and C.P. Woodbury, "Statistical mechanics of electrolytes and polyelectrolytes. I. Symmetric electrolyte solutions", *J. Chem. Phys.*, **77**, 4120 (1982).

[23] C.V. Ramanathan and A.-L. Jensen, "Statistical mechanics of electrolytes and polyelectrolytes. IV. A theory of higher valence electrolytes", *J. Chem. Phys.*, **84**, 3472 (1986).

[24] N.F. Carnahan and K.E. Starling, *J. Chem. Phys.*, **51**, 635 (1969).

[25] H. Falkenhagen, *Theorie der Elektrolyte*, S. Hirzel Verlag, Leipzig, 1971.

[26] M.C. Abramo, C. Caccamo, G. Malescio, G. Pizzimenti and S.A. Rogde, "Equilibrium properties of charged hard spheres of different diameters in the electrolyte solution regime: Monte Carlo and integral equation results", *J. Chem. Phys.*, **80**, 4396 (1984).

[27] D. Laría, H.R. Corti and R. Fernández-Prini, "The cluster theory for electrolyte solutions. Its extensions and limitations", *J. Chem. Soc. Faraday Trans.*, **86**, 1051 (1990).

[28] J. Bagg and G.A. Rechnitz, ≫ Single-ion activity of fluoride in mixed alkali halide solutions ≪, *Analytical Chemistry*, **45**, 1069 (1973).

[29] J.B. Jensen, M. Jaskula and T.S. Sørensen, ≫ Mean activity coefficients in aqueous electrolyte mixtures. I. EMF studies at 25°C on the KCl-KF system ≪, *Acta Chem. Scand.*, **A41**, 461 (1987).

[30] M. Molero, C.W. Outhwaite and L.B. Bhuiyan, ≫ Individual ionic activity coefficients from a symmetric Poisson-Boltzmann theory ≪, *J. Chem. Soc. Faraday Trans.*, **88**, 1541 (1992).

[31] W. Ebeling and K. Scherwinski, ≫ On the estimation of theoretical individual activity coefficients of electrolytes. I. Hard sphere model ≪, *Z. physikal. Chem.* (Leipzig), **264**, 1 (1983).

[32] T.S. Sørensen and K.F. Jensen, ≫ Formation of electric triple layers by interdiffusion of two electrolytes ≪, *J. Chem. Soc. Faraday Trans. 2*, **71**, 1805 (1975).

[33] N.O. Østerberg, J.B. Jensen and T.S. Sørensen, ≫ EMF of concentration cells with liquid-liquid junction established by free diffusion. Part I. ≫ *Acta Chem. Scand.*, **A23**, 721 (1978).

[34] N.O. Østerberg, T.S. Sørensen and L.D. Caspersen, ≫ EMF of concentration cells with liquid-liquid junction established by free diffusion. Part II. ≫ *Acta Chem. Scand.*, **A34**, 523 (1980).

[35] N.O. Østerberg, T.S. Sørensen and J.B. Jensen, ≫ Practical and theoretical aspects concerning the use of salt bridges in electrochemistry ≫ *J. Electroanalytical and Interfacial Chemistry*, **119**, 93 (1981).

[36] R.A. Robinson and R.H. Stokes, *Electrolyte Solutions*, Butterworths, London, 2nd Ed., 1965, Chap. 15.

[37] G.A. Mansoori, N.F. Carnahan, K.E. Starling and T.W. Leland, ≫ Equilibrium thermodynamic properties of the mixture of hard spheres ≪, *J. Chem. Phys.*, **54**, 1523 (1971).

[38] D.A. MacInnes, ≫ The activities of ions in strong electrolytes ≪, *J. Am. Chem. Soc.*, **41**, 1086 (1919).

[39] K.S. Johnson and R.M. Pytkowicz, ≫ Ion association and activity coefficients in multicomponent solutions ≪, in *Activity Coefficients in Electrolyte Solutions, Vol. II*, R.M. Pytkowicz, ed., CRC Press, Boca Raton, Florida, 1979.

[40] T.S. Sørensen, P. Sloth and M. Schrøder, ≫ Simple statistical mechanical models of electrolyte activities for small Bjerrum parameters ≪, *Acta Chemica Scand.*, **A38**, 735 (1984).